Formation control of autonomous vehicles with emotion assessment

Aakash Soni

School of Computer Science and Electronic Engineering

University of Essex

This dissertation is submitted for the degree of

Doctor of Philosophy

University of Essex March 2023

I would like to dedicate this thesis to my loving parents.

Declaration

I hereby declare that except where specific reference is made to the work of others, the contents of this dissertation are original and have not been submitted in whole or in part for consideration for any other degree or qualification in this, or any other university. This dissertation is my own work and contains nothing which is the outcome of work done in collaboration with others, except as specified in the text and Acknowledgements. This dissertation contains fewer than 80,000 words excluding appendices table of contents/figures, abstract, acknowledgements, references, bibliography and footnotes

Aakash Soni

March 2023

Acknowledgements

First and foremost, I would like to express my sincere gratitude and thank my supervisor, Professor Huosheng Hu, for the guidance, encouragement, and advice he has provided throughout my time as his student. I have been fortunate to have a supervisor who cared about my work and responded to my questions and queries promptly. Furthermore, under his supervision, I have had a chance to develop my academic and industrial skills by working on projects and as a tutor. In addition, this training has equipped me with valuable professional and academic skills.

I would like to thank Professor Dongbing Gu, who provided valuable advice and supported my research and thesis directions. I would like to thank Dr. Vishwanathan Mohan for his encouragement and excellent advice during my panel meetings. I would like to thank Dr Ian Daly for his guidance on my research project. Finally, I would also like to thank Mr. Robin Dowling and Mr. Ian Dukes, who supported me with laboratory facilities and technical queries during my PhD research.

I am grateful to all my colleagues and friends, namely Zuyuan Zhu, Qiang Liu, Ruihao Li, Yaser Alothman, Penelope Roberts, Dingtian Yan, and many academic visitors to the Essex robotics laboratory during my PhD research.

Last but not least, I sincerely thank my parents and my brother. They have always loved, supported, and trusted me throughout my studies. Without their support, I would not have made it.

Abstract

Autonomous driving is a major state-of-the-art step that has the potential to transform the mobility of individuals and goods fundamentally. Most developed autonomous ground vehicles (AGVs) aim to sense the surroundings and control the vehicle autonomously with limited or no driver intervention. However, humans are a vital part of such vehicle operations. Therefore, an approach to understanding human emotions and creating trust between humans and machines is necessary. This thesis proposes a novel approach for multiple AGVs, consisting of a formation controller and human emotion assessment for autonomous driving and collaboration. As the interaction between multiple AGVs is essential, the performance of two multi-robot control algorithms is analysed, and a platoon formation controller is proposed. On the other hand, as the interaction between AGVs and humans is equally essential to create trust between humans and AGVs, the human emotion assessment method is proposed and used as feedback to make autonomous decisions for AGVs. A novel simulation platform is developed for navigating multiple AGVs and testing controllers to realise this concept. Further to this simulation tool, a method is proposed to assess human emotion using the affective dimension model and physiological signals such as an electrocardiogram (ECG) and photoplethysmography (PPG). The experiments are carried out to verify that humans' felt arousal and valence levels could be measured and translated to different emotions for autonomous driving operations. A per-subject-based classification accuracy is statistically significant and validates the proposed emotion assessment method. Also, a simulation is conducted to verify AGVs' velocity control effect of different emotions on driving tasks.

Table of contents

List of figures

List of tables

Chapter 1

Introduction

This thesis focuses on developing formation control algorithms for multiple autonomous ground vehicles utilising human emotion assessment. This chapter presents the research motivation, research questions, and thesis outline.

1.1 Motivation

Autonomous Vehicles

A self-driving/autonomous ground vehicles (AGVs) are the next significant innovation in the transport industry. Many automotive companies are now working on five levels of autonomy. Most of these companies are researching developing the fifth level of autonomous cars and are set to launch their cars in the upcoming years. The introduction of fully autonomous vehicles will constitute the most noticeable change to everyday transportation in living memory and is predicted to deliver a wide range of environmental, social, and economic benefits. Moreover, the United Kingdom has launched several projects to develop this technology further and created a Centre for Connected and Autonomous Vehicles (CCAV) [52]. AGVs are at the heart of autonomous driving. Automated driving is a concept that refers to the automation

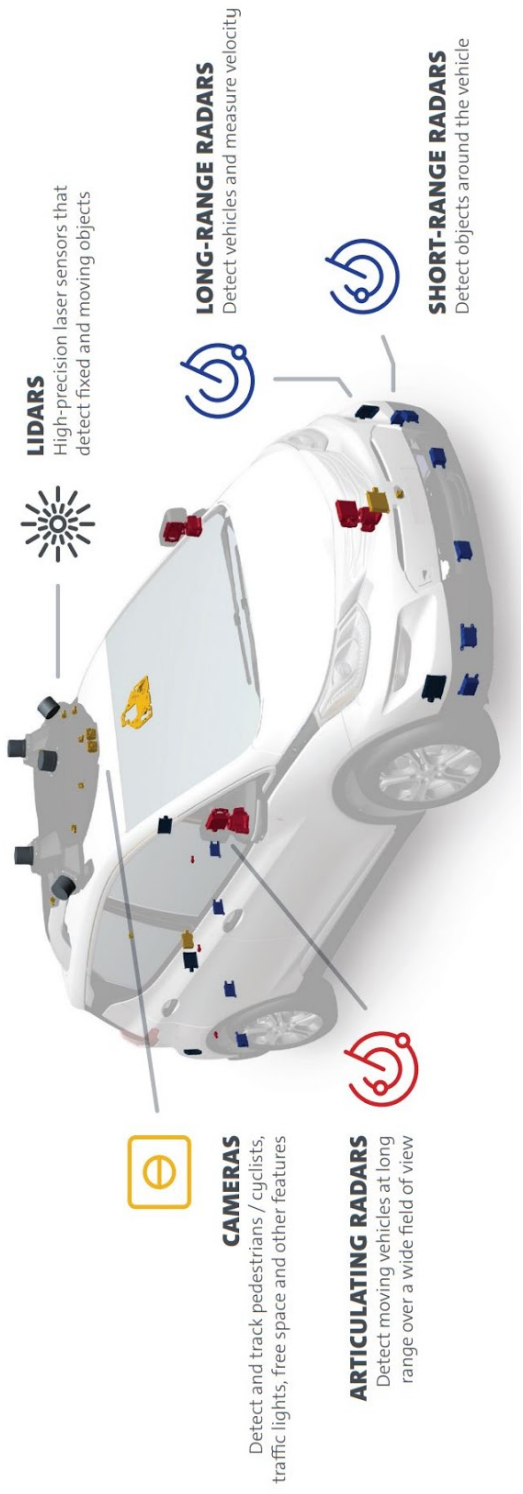

Fig. 1.1 Autonomous Ground Vehicle

of some or all of the human elements of driving with the help of electronic and mechanical devices. AGVs that combine vehicles and humans can operate in a couple of modes, e.g. AGVs with no human control and a human driver taking over from autonomous vehicle control. Its origin can be traced back to the early 20^{th} century, focusing on autonomous speed, lane departure, break, and other aspects of cruise control [127]. Nevertheless, rapid technological advance has only happened during the last decade following the incubation condition of the fourth industrial revolution and the digital revolution [25].

AGVs have three principal sensors, as shown in Fig. 1.1, and they are LIDAR (LIght Detection And Ranging), camera, and RADAR (RAdio Detection And Ranging). These sensors complement each other by offering different capabilities, such as RADAR, which can work in poor weather conditions, often not suitable for LIDAR and cameras. In addition, cameras can capture clear images that are impossible to take through LIDAR and RADAR. LIDAR can provide 360 degrees of high-definition 3D view of the environment, which is difficult to obtain by camera and RADAR. Since all of these sensors have their pros and cons, most vehicle manufacturers utilise a mix of at least two of the three to outweigh their weaknesses. In theory, an AGV system can only be termed an autonomous system when the vehicle's automated system can perform all the dynamic driving tasks in all driving environments [43].

Furthermore, such AGVs can operate in multiple modes, such as fully autonomous mode, as stated in the Society of Automotive Engineers (SAE) levels 4 and 5, a semi-autonomous mode, as stated in SAE levels 0 to 3, and manual mode, which the humans entirely control. The SAE has published standards highlighting levels of automation, explaining what automation process is available at what level in on-road motor vehicles, and includes functional definitions for advanced levels of driving automation and related terms and definitions [64]. As shown in Fig. 1.2, driving automation is divided into six levels. The driving automa-

Fig. 1.2 Taxonomy and Definitions for Terms Related to On-Road Motor Vehicle Automated Driving Systems [64]

tion scope starts with vehicles without this technology, level zero, and ends with entirely autonomous vehicles, level five.

A vehicle platoon formation operation using AGVs can be classified as a part of the multi-robot system. A multi-robot vehicle system is a set of interacting robot vehicles. Interacting with each other means performing tasks using their capabilities and characteristics, leading to solving one common goal. Vehicle platooning is an integral part of traffic management because of several benefits, such as improved safety, fuel efficiency, mileage, the time needed to travel, and reduced road congestion. Vehicles on the road usually follow another vehicle and form a platoon-based formation. A platoon-based formation is simple for the human-operated vehicle and can be seen daily. However, AGVs must stay in the lanes and follow nearby vehicles by maintaining a safe distance and velocity. The platoon formation control aims to confirm that all vehicles move at the same speed while maintaining a desired formation shape or geometry, which is stated by a desired inter-vehicle spacing strategy [75]. Therefore, for AGVs, forming a platoon requires specific algorithms and controllers consisting of longitudinal and lateral control strategies.

Furthermore, for formation control, AGVs need to communicate; therefore, information sharing plays a vital role in the overall operation. This overall operation can be called collaboration within AGVs. Collaboration depends on sensing and information sharing within a vehicular network. The challenge is to make these two operations, i.e., sensing and information sharing, autonomous to achieve the desired control. Therefore, as AGVs are being developed, the next collaboration problem between AGVs needs to be addressed. The solution to these problems will secure the future of AGVs.

Emotions Assessment

As human emotions are highly correlated with the surrounding environment, mental well-being, and physical health, recognising human emotions using physiological signals is an

ever-growing field of research. Today, artificial intelligence and semiconductor technology progress offer ample opportunity to develop powerful computing devices and technologies for healthcare and medical applications. Affective computing is one technology that holds a promising future and can be integrated into everyday applications. It is an interdisciplinary field requiring knowledge of human psychology, biomedical engineering, and computer science. The term affective computing was first coined by Rosalind W. Picard and can enhance computers' abilities to make decisions [130]. In addition, physiological sensors play a vital role in developing affective computing systems. Such sensors include an electrocardiogram (ECG), photoplethysmography (PPG), electroencephalography (EEG), electromyogram (EMG), galvanic skin response (GSR)/electrodermal activity (EDA), skin temperature (SKT), and respiration pattern (RSP) [37]. These sensors are vital in developing portable, reliable, non-intrusive, and computationally efficient medical and healthcare devices [38].

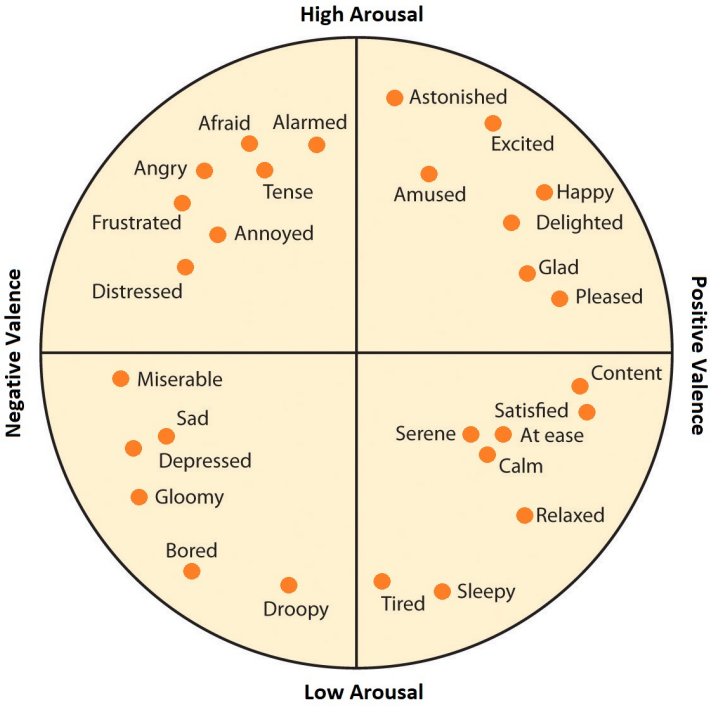

Fig. 1.3 Circumplex Model of Affect, adapted from [143]

The research community widely accepts two methods for emotions assessment, namely discrete emotional models (DEM) and affective dimensional models (ADM) [5]. The DEM method expands its roots back to work carried out by Charles Darwin [28], and the aim is to recognise and label standard emotional states such as joy, sadness, fear, surprise, anger, and disgust [39]. The usefulness of this method relies on how well the arbitrary state is defined and must be distinguishable from other emotions. On the other hand, the ADM method is based on work carried out by Wilhelm Wundt [137], later adopted by James Russell, where the affective state consists of two parameters or dimensions, arousal and valence, as shown in Fig. 1.3 [143]. In ADM, arousal measures the emotional stimulation and intensity of the physiological activation and varies between high and low. Valence measures pleasantness or pleasure for the experienced emotion, ranging from pleasant (positive) to unpleasant (negative). These two variables form a 2D space. Other dimensional models includes vector model [14], positive activation - negative activation (PANA) model [168], plutchik's model [132], and Pleasure-arousal-dominance (PAD) emotional state model [109]. Moreover, several methods are developed and validated in various settings to recognise human emotions, such as speech emotions [83, 161], facial emotions [81], text-based emotions [3], and physiological sensor-based emotions [37, 38, 154].

Overall, AGVs can provide numerous benefits, such as better traffic management, increased safety, reduced emissions, and enhanced transportation networks. Formation control for AGVs enables many applications, including security patrols, search and rescue, everyday transport networks, and factory automation. For example, a group of autonomous vehicles in military missions must maintain a specific formation for area coverage and reconnaissance. In automated highway systems, the throughput of the transportation network can be significantly increased if vehicles can form platoons at the desired velocity while maintaining a specified distance between them. In factory automation, formation control of AGVs can help with the collaborative transport of rigid objects and manipulation of deformable objects, objects of

variable shape. Formation control research also aids in the understanding of some biological and social phenomena, such as insect swarms and bird flocking [24]. Emotion assessment of passengers driving AGVs can also enable many applications, including passengers' reaction to autonomous decisions, enabling various in-vehicle ambient conditions using emotion recognition, and providing a safe transition to AGVs from traditional vehicles by considering humans in the loop. Therefore, after clearly understanding AGVs, platoon formation, and emotions assessment, a method needs to be developed to integrate all these concepts to provide a convenient, pleasant, and, more importantly, trustworthy experience for humans interacting with such vehicles.

1.2 Research Questions

Based on the motivation stated in the previous section, this thesis proposes an approach to how human emotions can be utilised for autonomous driving. The thesis provides a comprehensive insight into developing a controller for multiple AGVs and the controller's performance by conducting simulation experiments. Moreover, the development steps of designing a robot simulator are discussed. A method for human emotion recognition and the implementation of this method for autonomous driving is also provided. The research is carried out by answering the following four questions.

1. What controllers exist for the multiple AGVs configurations? Can new controllers be devised that go beyond those already existing?

Three approaches are available for developing controllers for AGVs operating on roads. They are the leader-follower approach, the behaviour-based approach, and the virtual structure approach. These approaches could be divided further, as shown in Fig. 2.1. Each of these approaches has its advantages and disadvantages. Further to these approaches, two types of controllers could be developed, centralised and decentralised. A centralised controller

heavily relies on communication. Thus, the whole multi-robot system could break down in the case of communication loss. Whereas decentralised controller does not require access to the entire global state, and all control computation is done locally. Therefore, a decentralised controller is best suited for developing a controller for multiple AGVs navigation.

2. How to evaluate the performance of such a controller?

Once a controller is developed, it is best to test it using a simulation. Performing real-world experiments with teams of robots is a challenging task due to cost and complexity. On the other hand, a simulation can emulate reality and provide an inexpensive and less time-consuming development process compared to real-world robot testing. Furthermore, a controller could be transferred to real robots once satisfactory results are obtained through simulation. However, not all simulators can offer the benefit of transferring the code used for simulation to real robots. Therefore, the careful selection of a simulator plays a vital role.

3. What methods exist for detecting human emotions? Can new methods be devised that go beyond those already existing?

The research community widely adopts two approaches for emotion assessment, the discrete emotions model (DEM) and the affective dimensional model (ADM). Several studies have been published targeting several human responses, such as speech, face, text, and physiological signals. The advantage of emotion detection using physiological signals is that they are unconscious responses of the human body and very difficult to conceal compared to physical signals such as facial and speech emotions, as they are easy to control and hide. For example, the effect of emotions on a person's heart and collecting relative changes to heartbeat rhythms can provide insight into the relationship between the cardiac cycle and felt emotions. Moreover, the resultant approach should be able to be used by human drivers conveniently.

4. How can the evaluated human emotions be used in multiple AGV control?

Once an emotion is recognised, a subsequent control automation task must be performed based on the identified emotion. A closed-loop controller must be developed to attain this capability, which can take emotions as a tuning parameter or feedback to vehicle automation. For example, the driving automation tasks for passengers with positive emotions such as relaxed, happy or excited should be different from passengers experiencing negative emotions such as sadness, anger or annoyance. Different control tasks can be slowing down or stopping AGVs, maintaining the dedicated velocity of the AGVs, taking control of the AGVs if driven by the passenger, and providing a personalised ambient environment.

1.3 Thesis Outline

This thesis is organised into eight chapters. Chapter 1 is an overview of the research. Chapter 2 is the background of the research work. Chapter 3 presents the proposed approach and methodologies. Chapters 4, 5, 6, and 7 are the main research work conducted in this research. Finally, Chapter 8 concludes the thesis.

Regarding research questions (RQ), the first part of RQ1 is answered from the literature in Chapter 2. The second part is answered in chapters 4 and 5. An RQ2 discusses the development of a simulation tool which is addressed in Chapters 4, 5, and 7. The first part of RQ3 is answered from the literature in Chapter 2, and the second part is answered in Chapter 6. Finally, the RQ4 is discussed in both Chapters 2 and 7. The details of the individual chapters are outlined here:

- Chapter 2 presents a literature review related to this research. An introduction to control techniques of multiple AGVs, emotion assessment methods and their use cases in autonomous driving are discussed. Three approaches for developing algorithms of multiple AGVs are covered in this section: leader-follower, behaviour-based, and virtual structure approaches.

- Chapter 3 presents the proposed approach and research methodology. The overall system diagram of how emotions can be employed in AGVs is presented. Finally, the problems are addressed to carry out this research.

- Chapter 4 proposes an algorithm utilising model predictive control for path planning. An introduction to model predictive control and its framework are presented in this chapter. Finally, a robot navigation algorithm for one and multiple robots are discussed, and their simulation results are stated.

- Chapter 5 discusses the development of a multi-robot simulator. This chapter briefly introduces the robot operating system (ROS) and Gazebo simulator and the development of simulation environments and mobile robots. Several robots are simulated in this environment, and their results are discussed. As well as this chapter presents an algorithm for leader-follower navigation.

- Chapter 6 presents a novel approach to deriving human emotions using physiological signals. Data from electrocardiogram (ECG) and photoplethysmography (PPG) sensors are considered for training machine learning models. A support vector machine, neural network classifiers, and long short-term memory are employed for binary classification, and their results are discussed.

- Chapter 7 presents an approach to integrate human emotion assessment with autonomous driving operations. This chapter provides an understanding of emotions, why human feels different emotions, and their impact on driving tasks. A controller that can take human emotion as a control parameter is considered and simulated on single and multiple AGVs.

- Chapter 8 summarises the research work conducted in this thesis, including significant research achievements and some brief ideas for future work. The conference and journal papers published and planned to be published during this research are listed.

Chapter 2

Literature Search and State of the Art

This chapter presents literature on formation control approaches, emotion assessment methods, and the use of emotions in AGVs control. Section 2.1 to Section 2.4 provides a literature review of three types of methods used for AGVs formation control. Section 2.5 introduces different emotion assessment approaches and reviews emotion assessment methods. Section 2.6 presents literature on how emotion assessment can be applied in autonomous driving. Finally, Section 2.7 summarises the chapter.

2.1 Formation Control

A formation control is a coordinated control for a fleet of AGVs to follow a predefined trajectory while maintaining a desired spatial pattern. Formation control can be divided into three principal approaches. These approaches are the leader-follower approach, the virtual structure approach, and the behaviour-based approach. Moreover, some of these approaches can be further divided into sub-approaches, as shown in Fig. 2.1.

Some concepts frequently used in formation control are multi-robot systems, communication topologies, graph theory, and consensus. A consensus control theory is used to study the interaction between a group of dynamic agents. The graph theory is commonly used

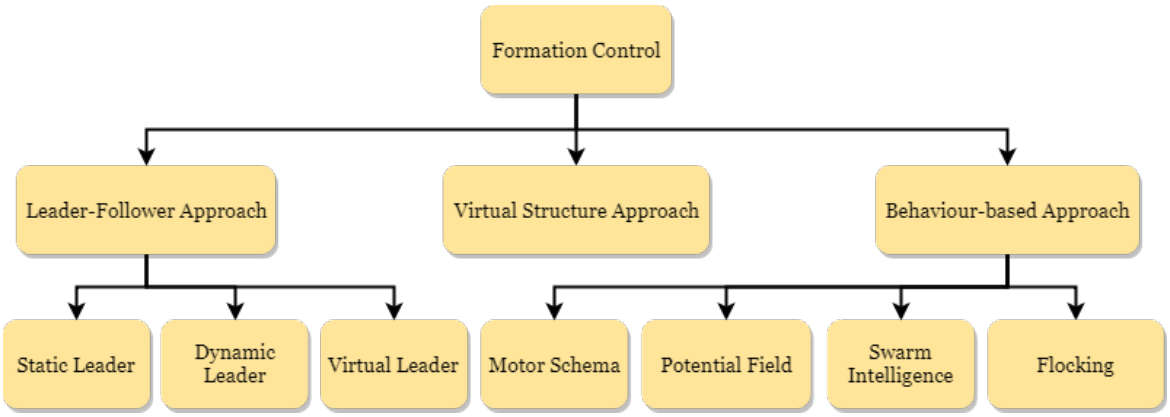

Fig. 2.1 Formation Control Approaches

to analyse consensus control strategies, whereas the communication topologies indicate a potential interaction between neighbouring agents and are described by the graph.

2.1.1 Multi-Robot Systems

It has been proven that multiple robots cooperating can solve complex tasks that are difficult to accomplish by a single robot. The basic idea behind such a system is to divide a bigger problem into a sub-problem and let individual robots solve this problem by interacting with each other such as maintaining a platoon formation. Some of the benefits of a multi-robot system include [125, 184]:

- Multiple robots can concurrently work on the task to achieve it faster.
- Robots can be heterogeneous in their capabilities to provide a cost-effective solution to achieve a task where each robot handles specific components matching its capabilities.
- Multiple robots can effectively deal with a task inherently distributed over a wide area.
- Using multiple robots for achieving a task provides fault tolerance, as the presence of multiple robots capable of similar processes can be used to compensate when any of them fails.

When AGVs start to interact with each other, a controller should be devised to handle such interactions. One of the goals for this controller can be forming a platoon formation. As discussed in chapter 1, forming a platoon requires specific algorithms and controllers consisting of longitudinal and lateral control strategies. Therefore, when evaluating such a controller in simulation, the performance of these two control strategies should be investigated.

There can be a variable number of robots within a multi-robot system. Therefore, a system with two or more robots can be defined as a multi-robot system. For example, a group of five robots for a platoon formation using AGVs should be sufficient for a single platoon. However, another platoon can be formed for another group of five AGVs, resulting in a multi-platoon system. The reason behind choosing five AGVs within a single platoon is that large platoons and real-world traffic conditions make a formation maintenance goal a complex problem.

2.1.2 Autonomy Levels

SAE has defined different levels of automation and guides which level of autonomy contains what type of autonomy features.

- Level 0 is the starting point, with no advance support. This is how an average modern car would look, lacking gadgets that could improve a driver's safety and efficiency. The steering, braking, and accelerating controls should all be under the driver's constant watch.

- Level 1 is the next level of autonomous driving. It supports lane centring or adaptive cruise control. A car with lane centring provides steering support, whereas a car with adaptive cruise control provides acceleration and brake support. Only one support is available at the time at this level.

- Level 2 further enhances the previous level of autonomy. This level provides support for lane centring and adaptive cruise control. Therefore, it supports both steering as well as braking/acceleration at the same time. However, the driver must supervise these support features at all times.

- Level 3 broadens the automation level. From this level, the driver is not driving when supports at this level are activated. However, when features request the driver to drive, the driver must drive. For example, one highlighted feature at this level is traffic jam assistance, where a vehicle would gently keep a safe distance from another vehicle in a traffic jam scenario.

- Level 4 further extends the autonomy where a vehicle handles all driving responsibilities, whether the driver is present or not. The features at this level can drive a vehicle under limited conditions and require a driver to take control of the vehicle if conditions are not met. For example, an autonomous taxi is one potential application at this level which may not have a steering wheel or acceleration/brake pedals.

- Level 5 is a fully autonomous driving mode in which a vehicle can control a complex driving task in any road conditions, weather, and traffic scenarios. This is where most companies are doing their current research and engineering work.

2.1.3 Topology

Information sharing with other robots is crucial in the multi-robot system to attain formation control. Therefore, topologies are implemented in vehicle platooning to address the information-sharing problem. These topologies are responsible for the information exchange flow, which describes how the vehicles in a platoon exchange information with each other. There are different types of communication topologies [182] to choose from, and some of them are shown below;

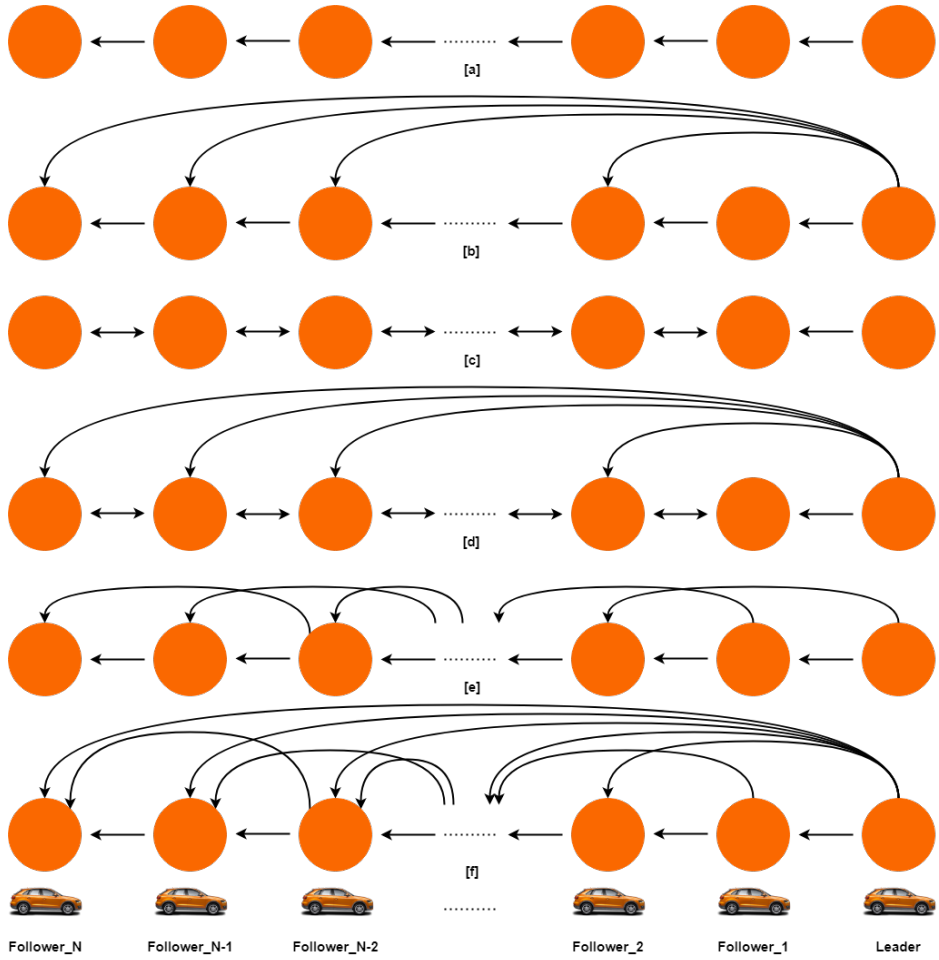

Fig. 2.2 Topology

Several leader-follower topologies are presented in Fig. 2.2. Here, topology A is the predecessor-following (PF) topology. Topology B is the predecessor–leader following (PLF) topology, and topology C is the bidirectional (BD) topology. Topology D is the bidirectional-leader (BDL) topology, topology E is the two-predecessor following (TPF) topology, and topology F is the two-predecessor–leader following (TPFL) topology. Note that these topologies are for single-platoon formation. However, several scenarios can occur during platoon operation, such as the interaction between multiple platoons or loss of communication under existing topology. Therefore, dynamic or switching topologies should be considered for platoon stability and mobility. Here, dynamic or switching topology means that the topology of platoon formation switches into a different topology over time.

2.1.4 Algebraic Graph Theory

Graph theory is used in the multi-robot formation control for the information exchange between autonomous robots to perform the formation's stability analysis and achieve consensus. The topologies discussed previously are modelled as a graph where robots can be represented as graph nodes, and intersections such as sensing and communication can be represented as edges. Here, two fundamental graph theories are presented, directed graph or digraph and undirected graph.

A digraph is called strongly connected if there is a directed path from every node to every other node. A digraph g is defined as pair (V,E), where V denotes the set of nodes and $E \subseteq VxV$ denotes the set of ordered pairs of the nodes, called edges. It is assumed that there is no self-edge, i.e., $(i,i) \notin E$ for any $i \in V$. The set of neighbours of $i \in V$ is defined as a set $N_i := j \in V : (i,j) \in E$. A directed path of g is an edge sequence of the form $(v_{i_1}, v_{i_2}), (v_{i_2}, v_{i_3}), ..., (v_{i_{k-1}}, v_{i_k})$. If $(i,j) \in E$, j is called a parent of i and i is called a child of j. A tree is a directed graph where a node, called the root, has no parent, and the other nodes have exactly one parent. A spanning tree of a directed graph is a directed tree containing every node of the graph.

Given a directed graph $g = (V,E)$, where w_{ij} is a real number associated with (i,j) for $i, j \in V$ and assume that $w_{ij} > 0$ if $(i,j) \in E$ and $w_{ij} = 0$, otherwise. The Laplacian matrix $L = [l_{ij}] \in \mathbb{R}^{|v|x|v|}$ of g is defined as:

$$l_{ij} = \begin{cases} \sum_{k \in N_i} w_{ik}, & \text{if } i = j, \\ -w_{ij}, & \text{if } i \neq j. \end{cases} \tag{2.1}$$

An undirected graph is connected if a path exists between any distinct pair of nodes. Let g be a directed graph such that $(i,j) \in E$ if and only if $(j,i) \in E$ and $w_{ij} = w_{ji}$ for all $(i,j) \in E$. Then, g is said to be undirected. The Laplacian matrix L of g is symmetric and positive semi-definite. If g is connected, the second smallest eigenvalue of L is positive. Furthermore,

the Laplacian matrix L can be defined as, $L = D - A$. Here, D is the degree matrix and A is the adjacency matrix.

2.1.5 Consensus

In multi-robot systems, reaching a consensus is one of the essential requirements where AGVs can reach an agreement to form a formation by sharing information locally with their neighbour vehicles. Generally, convergence to a common value is called consensus, which depends on communication between AGVs. Therefore, analysing the emergence of consensus behaviour resulting from local interactions among mobile agents who share information only with their neighbours according to some designed distributed protocols can help evaluate controllers. Furthermore, a consensus is helpful in several ways, such as:

- Alignment (Pointing in the same direction)
- Synchronisation (Agreeing on the same time)
- Distributed Estimation (Agreeing on the estimation/measurement of the distributed quantity)
- Rendezvous (Meeting at a common point)

2.2 Leader-Follower Approach

In the leader-follower approach, a leader is assigned to the multi-robot formation, and the remaining robots are the followers. In this approach, a leader follows their desired trajectory while follower robots track the position of the leader. This approach has three kinds of leaders: static, dynamic, and virtual. The advantage of this approach is the reduced tracking errors which can be analysed using standard control techniques [26]. Another benefit is that only the leader is responsible for planning trajectories, and followers must follow the

coordinates of the leader; therefore, it results in a simple controller. However, in terms of disadvantages, a leader's fault can penalise the whole formation, and feedback from followers to a leader is generally not applied in this approach.

The leader-follower control is a widely adopted formation approach. In this approach, a leader robot can be implemented in three ways: a static leader, where the leader robot does not change; a virtual leader, where a software leader is employed; and a dynamic leader, where leadership changes depending on the situation. Furthermore, a communication topology responsible for the information exchange between robots plays a vital role in the leader-follower approach. For the controller design, most of the literature discusses longitudinal control. However, lateral control is equally essential for navigation autonomous vehicles in a structured environment. Once the formation is attained, the stability analysis of the formation is carried out using string stability analysis. In the leader-follower approach, a consensus is said to be reached on each sum of a position vector and an inter-vehicle separation vector, and the information flow is itself a directed spanning tree [138].

2.2.1 Leader-follower Formation Controller

A leader-follower formation tracking control of the autonomous vehicles was achieved on a straight path proving that recursive implementation of a cascaded system-inspired controller leads to a spanning-tree communication topology [102]. In this article, the authors recommended working on switching communication topologies to measure the performance of the formation-tracking controller. In another paper, a leader-follower semi-centralised approach was employed for the formation control of the robots using the Hungarian method [166]. In this study, during the first phase, robots selected a leader and moved following the leader. During the second phase, a formation was given a centre, and robots moved referring to the centre, establishing a formation around the centre, such as square, circle and triangle formations.

Several controllers were developed for the formation control of multiple vehicles targeting a leader-follower tracking problem, such as a feedback linearisation controller for formation maintenance, an adaptive controller to achieve ideal control due to inaccurate relative distance, and a robust adaptive controller to cope with the external interference [96]. This study confirmed the system's stability through the Lyapunov method. Moreover, a virtual leader was employed for the distributed formation control of multiple nonholonomic wheeled mobile robots [128]. Here, the global position of the virtual leader was not supplied to each follower robot, but followers were able to exchange information with their neighbour robots. In this study, a distributed kinematic controller was proposed to achieve consensus, and an adaptive dynamic controller was designed to maintain the stability of the kinematic error system. Another publication proposed a decentralised leader-follower tracking agreement controller, which used relative velocity and position measurement of the actual robot concerning a leader robot [105]. Here, a virtual reference vehicle was used for the reference trajectory generation, and resultant angular and linear velocities were communicated to the leader robot. Moreover, Lyapunov's direct method was employed to establish global asymptotic stability.

An active vision-based adaptive leader-follower formation control was achieved without communication [23]. In this study, a follower robot was tracking the features of a leader robot through a camera, and two controllers were developed: a formation controller to maintain formation and a camera controller to provide visual measurements. Furthermore, a vision-based leader-follower formation control was achieved by developing a neural-dynamic optimisation-based nonlinear model predictive control (MPC) [99]. In this study, a camera on the follower robot was employed to track the features and measure the leader robot's state and velocity. Finally, a vision-based localisation and leader-follower formation control was studied for the nonholonomic mobile robots [106]. This work derived a necessary condition for observability, and an extended Kalman filter was employed to estimate inter-robot distance.

Another publication used a GQ(λ) algorithm, a gradient-based off-policy temporal-difference learning algorithm [104], to achieve leader-follower formation control. This work implemented a static line follower where a leader robot moved without requiring advanced path planning and map recognition. In contrast, follower robots tried to learn to follow the robot directly in front of them. In the leader-follower approach, controlling the throttle and brake of the follower vehicles is mandatory to regulate the follower vehicle's speed and position concerning the leader vehicle. An actor-critic algorithm with three layers of neural networks was developed using longitudinal vehicle control to learn the follower vehicle's near-optimal throttle and brake control policy. In this work, the vehicle's speed and distance were input to the network, whereas output was the desired action, throttle or break[183]. In this study, the authors recommended doing experiments on actual vehicles.

A platoon formation control can be viewed as a leader-follower approach. It has attracted several research studies and confirmed its application to practical on-road traffic scenarios by developing robust controllers. One publication presented the platoon formation framework and divided this framework into four components, node dynamics, information flow topology, a distributed controller, and formation geometry, as shown in Fig. 2.3 [97]. In this framework, node dynamics describe the behaviour of an individual platoon vehicle, and information flow topology defines the information exchange between each vehicle inside the platoon. The distributed controller implements the feedback control via neighbouring vehicle's information, and formation geometry maintains desired inter-vehicle distance in a platoon.

2.2.2 Second-order Dynamics

A second-order consensus of multiple inertial agents was achieved for a leader-follower network in the presence of communication loss and delays. In this work, a necessary and sufficient condition was given and proved that if damping and stiffness gains are chosen appropriately, the exponential consensus can be achieved [22]. Furthermore, a second-order

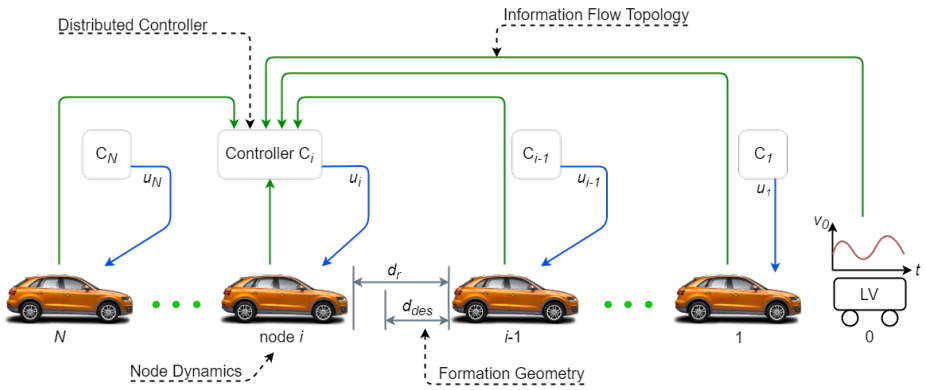

Fig. 2.3 Framework

feedback-based control protocol was developed to form a platoon formation under the non-lane-discipline road to show that the proposed controller can reach a consensus state under sufficient convergence time [98]. Here, convergence means that the longitudinal gap can converge to the desired distance, the lateral gap can converge to zero, and the velocity can converge to the desired speed. Finally, in this paper, network topology was evaluated under different initial states by putting vehicles at different positions, and the stability of the platoon was analysed using the Lyapunov technique.

Once the platoon formation is attained, it is vital to keep track of the performance of the formation. A string stability analysis is used to study or maintain this formation. Therefore, it is important to evaluate the platoon formation's behaviour. A string stability analysis is a process of attenuating the disturbance along the vehicle string or platoon. It is evaluated by considering the amplification of signals such as the distance error, the velocity, the acceleration, or the control effort in the vehicle string as the vehicle index increases [121]. Moreover, the CAV technology relies on wireless communication between autonomous vehicles. Therefore, there might be a case when communication is delayed, or the communication link introduces a time-varying delay over the vehicular network. Thus, the resultant effects might affect the stability of the platoon formation. [170].

A theoretical study demonstrated a distributed control protocol to achieve platoon formation in the presence of heterogeneous time-varying delay by achieving a second-order

consensus where string stability was achieved using a Lyapunov–Razumikhin theorem [30]. The resultant architecture provided guaranteed stability to the platoon in the presence of disturbances. An experimental study applied a previously designed control protocol in [30] to the three-vehicle platoon. Here, convergence to the desired spacing policy and robustness with time-varying communication topology was achieved under two scenarios, vehicle joining or leaving a platoon and loss of communication links [29]. In this study, velocity and acceleration fluctuation were attenuated downstream of the string of vehicles by the proposed algorithm to accomplish string-stability requirements.

The effects of wireless communication on string stability were studied for cooperative adaptive cruise control (CACC) using several parameters. One study presented the modelling and string stability analysis method for vehicle platooning by considering parameters like time-varying transmission intervals and delays [122]. In contrast, a subsequent study discussed the design trade-off between the specification for the vehicle following controller, network performance, and string stability performance criteria by considering parameters like sampling, constant network delay, and zero-order hold (ZOH) for string stability of the platoon [121].

A distributed consensus-based reconfigurable control approach for vehicle platooning was proposed considering heterogeneous vehicles and time-varying delays [145]. In this study, the Lyapunov–Razumikhin theorem was used to attain string stability, and a proposed controller was tested using the dynamics of heterogeneous vehicles. In this paper, the convergence analysis was performed to check the performance of platoon maintenance and transient manoeuvres. In another publication, a study was conducted analysing the influence of switching topology on the stability of a platoon of heterogeneous vehicles moving in a rigid formation[19]. In this study, the Krasovskii-based method proved more effective against communication delay than the Razumikhin-based approach.

Moreover, local and improved second-order consensus control algorithms were applied to a cooperative car-following model where a local algorithm provided stability and an improved algorithm used local traffic information and downstream traffic information to smooth the traffic perturbation [66]. This study recommended working on a third-order system by adding actuator lags and sensing delay. In another theoretical study, a consensus control was applied to multi-platoon cooperative driving with consideration of the realistic inter-vehicle communication using IEEE 802.11p standard [67]. The proposed consensus algorithm considered the position and velocity data, and acceleration was determined by the state difference between the vehicle and its neighbouring vehicles. However, to achieve an equilibrium state, the authors recommended working on getting acceleration data, which means achieving a third-order consensus.

2.2.3 Third-order Dynamics

A distributed control algorithm was developed to achieve a third-order consensus of a vehicular platoon network in the presence of time-varying heterogeneous delays [10]. In this work, acceleration errors due to time delay were considered to improve control reactivity, and the Lyapunov–Krasovskii function was constructed for the stability analysis. Another paper presented a controller for emergency braking for collision avoidance in a platoon. In this third-order dynamical model, a centralised control methodology of the heterogeneous platoon method was investigated [21]. Lyapunov–Razumikhin and Lyapunov–Krasovskii theorems were applied to construct a common Lyapunov function for a constant time headway strategy. Moreover, a third-order distributed protocol for heterogeneous vehicle platooning under time-varying delays and switching topologies were presented [144]. Here, the stability of the closed-loop vehicular network was achieved using the Lyapunov–Krasovskii theorem and stability under a switched topology was achieved using the Lyapunov–Razumikhin theorem.

A virtual leader scheme was considered for multiple vehicle platoons to guarantee inter-platoon internal stability and string stability in the presence of communication and parasitic delays [20]. This study assumed that each leader in the inter-platoon network communicates with preceding and subsequent leaders; therefore, the resulting topology was bidirectional virtual leader-following. Furthermore, stability analysis was performed by decoupling the closed-loop dynamics.

2.2.4 Platoon Management

A vehicle platoon can result in multiple formation operations, such as several platoons working in the same environment; therefore, multi-platoon management, such as inter-platoon and intra-platoon management, is necessary. A leader-follower approach was employed to address multi-platoon management. Furthermore, several algorithms were proposed to tackle inter-platoon position management, intra-platoon position management, platoon joining manoeuvres management, and extra spacing for secure manoeuvring [46]. Another article developed a platoon management protocol for autonomous vehicles to perform basic manoeuvres such as merge, split, and lane change [6]. In addition, some basic platoon scenarios were addressed in this study, such as leader leave, follower leave, and vehicle entry. Finally, information sharing was achieved through single-hop message broadcasting and a finite-state machine approach.

Moreover, considering the longitude control of the autonomous vehicles, a vehicle controller was proposed for platoon management in a simulation study [45]. This study analysed the effects of acceleration, inter-platoon speed, inter-platoon distance, and space errors. Another study proposed a distributed controller for the multi-lane heterogeneous vehicles [116]. This controller was based on Laplacian control consisting of a lateral controller for staying in the lane and a longitudinal controller for desired inter-vehicle

distance. This graph-based controller was able to adapt to the shape of the curvilinear road shape.

As autonomous vehicles emerge on the road, they must interact with other human-operated vehicles. Therefore, the interaction between autonomous vehicles and the presence of human-operated vehicles on roads needs to be studied. One publication studied this interaction by applying second-order consensus control to a vehicle platoon in a single-lane roadway [68]. This study proposed a unified multiclass model for a heterogeneous platoon that analyses the system's steady-state errors and transient-state performance. Furthermore, a controller was developed to obtain string stability in vehicle platoon using feedback linearisation and further extended to attain merging of a two-string of vehicles using time-gap and velocity profiles. Here, input to the controller was given by time-gap and velocity profiles. Moreover, a string stability analysis was studied for velocity and time-gap tracking errors. Fig. 2.4 shows the operation of the autonomous vehicle platoon.

Fig. 2.4 Autonomous Vehicle Platoon [164]

2.3 Behaviour-based Approach

In the behaviour-based approach, each robot shows several behaviours based on sensory inputs such as obstacle avoidance, goal-seeking, and formation-keeping, where absolute

control is derived from the weighting of the relative importance of each behaviour. This approach has four main methods: motor scheme, potential field, swarm intelligence and flocking. This approach can be defined as a structured network of such interacting behaviours where the behaviour coordinator derives the final action of each robot. The behaviour coordinator multiplies the output of each behaviour by its relative weight, then sums and normalises the results. One advantage of this approach is that it can operate in the unknown and dynamic environment because it is a parallel, real-time, and distributed method, requiring less information sharing [26]. Another advantage is that each behaviour has its physical meaning, and the formation feedback can be incorporated into group dynamics by coupling the outputs of each behaviour. On the other hand, this method has some disadvantages, such as the need to derive a mathematical model of group dynamics, study the convergence of specific formations, and guarantee the stability of the whole formation [88].

Behavioural control is used to achieve coordinated control of a multi-robot system in an unknown or dynamic environment. The behaviour-based approach serves best when the real world cannot be accurately modelled or characterised. This approach provides the autonomy to the system to navigate in complex or cluttered environments by avoiding offline path planning and using sensors to obtain instantaneous information about the environment. Furthermore, the environment for autonomous vehicles is uncertain, unpredictable, noisy, and dynamic. Therefore, a behaviour-based architecture is an answer to overcoming these difficulties by enabling real-time processing, relying heavily on sensing without constructing potentially erroneous global world models [7].

Behaviour-based robots are highly autonomous, mechanically imprecise, equipped with few computational resources, improve through learning, are programmed with software reuse, and integrated into the environment [12]. The basic principles of behaviour-based control can be described as follows [108]:

- Behaviours are implemented as control laws, either in software or hardware, as a processing element, or as a procedure.
- Each behaviour can take inputs from the robot's sensors and other modules in the system and send outputs to the robot's effectors and other modules.
- Many behaviours may independently receive input from the same sensors and output action commands to the same actuators.
- Behaviours are encoded to be relatively simple and incrementally added to the system.
- Behaviours are executed concurrently, not sequentially, to exploit parallelism and speed of computation and the interaction dynamics among behaviours and between behaviours and the environment.

In order to enable formation behaviour in a multi-robot system, each robot should maintain a certain distance and angle from other robots. For line or platoon formation, each robot should be able to move forward and backwards and turn left and right to maintain desired velocity and position. The consensus in the behaviour-based approach is said to be achieved on each deviation vector between the actual vehicle location and the desired vehicle location, and the information flow forms a bi-directional ring topology [138].

A hierarchical architecture consisting of a behaviour module, velocity tuning module, and supervisory module was proposed for the multi-robot formation control [33]. The behaviour module was responsible for the formation-keeping and obstacle-avoidance tasks and was implemented using a fuzzy logic technique. The supervisory module was implemented using a fuzzy neural network to derive the final output from the formation-keeping and obstacle-avoidance tasks. The velocity module was responsible for tuning and handled by the fuzzy inference system. Moreover, the behaviour-based approach for the formation control of a swarm robot was proposed using a fuzzy logic controller [57]. In this study, obstacle avoidance and formation-keeping behaviours were implemented.

2.3.1 Motor Schema-based Control

Motor schemas for mobile robots are sequences of actions that accomplish a goal-directed behaviour. Rather than representing the simplest elementary actions available to the robot, such as a simple command to a robot actuator, schemas and motion primitives represent a higher-level abstraction of robot actions, such as avoiding obstacles, avoiding the robot, maintaining formation, and moving to goal. These schemas and motion primitives define control policies encoded with only a few parameters and serve as the robot's basis set or movement vocabulary. Such primitives are sufficient for generating the robot's entire repertoire of motions via the combination of schemas or primitives.

Several formation shapes such as line, column, diamond, and wedge were considered by implementing several motor schemas such as move-to-goal, avoid-static obstacle, avoid-robot, and maintain-formation [8]. These schemas were used to implement the overall behaviour of the robot to move to a goal location while avoiding obstacles and collisions with other robots and remaining in the formation. In this study, a comparison between three formation position determination techniques, unit-centre-references, leader-referenced, and neighbour-referenced, was carried out. The advantages and disadvantages were discussed regarding these three techniques. In another study, a distributed layered formation control framework to guide the robots in an unknown environment by avoiding obstacles and collisions between robots was developed [86]. In this study, a leader-follower approach for formation control and a behaviour-based approach for obstacle avoidance was implemented, and dynamic role-switching of the leader was proposed.

The formation of the swarm of robots was considered where two significant formation control problems, efficient initial formation and formation control while avoiding obstacles, were solved [171]. For initial formation control, a classification-based target-searching algorithm was proposed. Here, formation control while avoiding obstacles was attained by implementing five behaviours: moving to the goal, avoiding obstacles, wall-following,

avoiding robots, and formation-keeping. Another article proposed a decentralised behaviour-based formation control and obstacle avoidance algorithm for multiple robots in which information exchange was considered only between neighbouring robots [89]. In this study, collision avoidance was obtained by determining the avoidance angle using the distance between obstacles. The formation generation behaviour was obtained by selecting the leader robot and determining the location in the formation using the locations of other mobile robots and the formation matrix.

2.3.2 Artificial Potential Field

In the artificial potential field (APF) method, the mobile robots have two fields generated by the goal and obstacles in search spaces. These two fields are the repulsive force field generated by obstacles and the attractive force field generated by goals. These forces are more decisive close to the obstacles or goal and have a more negligible effect at a distance. In this method, the goal location gains an attractive force, while the obstacles produce a repulsive force on robots. The resultant forces of the fields on the robots are used to determine the robots' motion and speed and the direction of travel while avoiding a collision.

APF is proved to be a good algorithm for obstacle avoidance and is employed for the formation problem. In a simulation-based study, an algorithm was developed for formation control and obstacle avoidance using second-order consensus control and a modified APF method where both fixed and switching topology were considered [180]. Another paper employed an APF approach for the cooperative merging manoeuvre using a longitudinal control scheme [149]. In this study, a single controller was able to perform different tasks, such as vehicle following, gap closing, obstacle avoidance, and platoon merging.

Formation generation through virtual nodes was proposed, where a robot converges to virtual nodes under the velocity matching to attain formation. In this study, distributed formation control algorithms were proposed to guarantee the stability of the formation

using a Lyapunov approach meaning that robots converge to a desired position under the velocity matching, thus maintaining the formation. This paper proposed four algorithms for formation control: formation connection control algorithm, collision avoidance algorithm, obstacle avoidance algorithm, and target tracking algorithm. In formation connection control, attractive force fields are created to drive free robots to move towards their desired positions. For collision avoidance, a local repulsive force field was created. For obstacle avoidance, the rotational force field was combined with the repulsive force field surrounding the obstacle to drive the robot to escape obstacles without collisions. Finally, for target tracking, a leader robot is selected based on the minimum distance from a target, and then the leader leads the formation to track the moving target.

An adaptive approach for formation control of a swarm of multi-robots was proposed using a potential field method and artificial neural networks (ANN) [40]. This study considered three potential fields: obstacle field, swarm robots field, and target field. Here, an artificial neural network was implemented to optimise the parameters of the potential field method. Furthermore, another study proposed a distributed hybrid control architecture based on APF and MPC for the vehicle merge and platoon split operations[62]. First, an AFP model was established to describe the mutual effect and collaboration between a vehicle and its surrounding environment in this method. Then, an MPC controller incorporating APF was presented to synchronise the path planning and motion control.

A two-stage formation tracking controller was proposed for mobile robots with limited sensing ranges by incorporating bump functions with potential functions and using the backstepping technique [32]. Here, the robots' heading and velocity were used as a control input for position tracking and collision avoidance during the first stage. Next, the robot's angular velocity was used as a control input to stabilise the error between the actual robot heading and its immediate value at the origin.

2.3.3 Flocking

Flocking describes the behaviour of a group of flying birds, fish schooling, or insect swarming behaviour. Flocking control mainly includes three behaviours: collision avoidance, also known as separation, velocity matching, also known as alignment, and flock centring, also known as cohesion [140]. Here, velocity matching is a vector quantity referring to the combination of heading and speed. Collision avoidance is a separation behaviour to avoid overcrowding and collision with each other, whereas flock centring makes robots near the centre of the flock or nearby flockmates.

The flocking problem could be viewed as a subcase of the formation control problem, requiring robots to move together along some path in the aggregate, but with only minimal requirements for paths taken by specific robots [124]. However, formations are stricter than flocking, requiring robots to maintain certain relative positions as they move through the environment. Therefore, this section considers flocking and formation control for multiple mobile robot systems.

One paper established a connection between formation control and flocking behaviour for multiple nonholonomic kinematic agents using algebraic graph theory and Lyapunov stability analysis [31]. Here, it was shown that when inter-agent formation objectives cannot occur simultaneously in the state-space, then, under certain assumptions, the agents' velocity vectors and orientations converge to a common value at a steady state under the same control strategy that would lead to a feasible formation. Furthermore, using LaSalle's invariance principle, it was proved that agents converge to the desired configuration, and all agents have a common orientation.

Inspired by the flocking behaviour, an algorithm for nonholonomic vehicles was derived to realise the application of flocking control in structured environments such as roads and highways [59]. In this paper, a virtual vehicle was employed to linearise the nonholonomic car model, and LaSalle's invariance principles were utilised to prove the convergence of

the entire system. Furthermore, simulation results showed that multiple cars were able to achieve steady formation. In another publication, a distributed formation control algorithm was proposed for multiple wheeled mobile robots in a free space environment [94]. This work used LaSalle's invariance principles for the stability analysis. Moreover, simulation results showed that the proposed method could achieve the desired shape of the formation while keeping the same velocity and heading angle.

A single control architecture was derived for the formation control of mobile robots consisting of three controllers: path planning, flocking, and formation controllers [165]. In this work, flocking provided asymptotic stability for formation control, and a synchronising velocity vector of individual vehicles achieved formation shape. In another publication, considering the problem of decentralised flocking and global formation building of the group of wheeled robots, a randomised decentralised navigation algorithm was presented where autonomous vehicles move in the same direction with the same speed, thus forming a formation [146]. Here, each robot did not know a priori its position in the desired configuration, and the robots attained consensus on their positions via local information exchange. In this paper, a consensus for formation building was achieved through variables of speed, heading, and mass centre of the formation.

2.3.4 Swarm Intelligence

Swarm robotics refers to applying swarm intelligence techniques where a desired collective behaviour emerges from the local interactions of robots with one another and with their environment. Swarm intelligence has great potential for implementation in vehicular traffic of the CAVs due to their ability to control a group of robots. There are several algorithms inspired by swarm intelligence. References in Table 2.1 include comprehensive detail on the original algorithms and their survey papers. Note that modified, hybrid, and advanced versions of these basic algorithms are used in many fields besides mobile robotics.

Table 2.1 Algorithms Details and their Survey Papers.

Algorithms	Algorithm Details	Survey Papers
Particle Swarm Optimization (PSO)	[76, 153]	[150, 133]
Ant Colony Optimization (ACO)	[35]	[17]
Artificial Bees Colony Optimization (ABCO)	[70, 71]	[72]
Artificial Fish Swarm Algorithm (AFSA)	[179]	[117]
Bacteria Foraging Optimization (BFO)	[126]	[136]
Glowworm Swarm Optimization (GSO)	[84]	[73]
Firefly Algorithm (FA)	[174]	[163]
Bat Algorithm (BA)	[175]	[18]
Grey Wolf Optimizer (GWO)	[112]	[44]

Exploration and Exploitation

Balancing the exploration and exploitation process is a requirement that depends on the algorithms' parameters to achieve good performance from the algorithms. Exploration is the process of exploring the search space efficiently on a global scale, whereas exploration can generate a diverse solution far from the current solution [176, 1]. The advantage of exploration is achieving global optimality and avoiding getting trapped in a local mode. The disadvantage of exploration is the slow convergence, which is computationally expensive because many new solutions can be far from global optimality. On the other hand, exploitation is a local search process and uses local information; therefore, a new solution generated by the exploitation is better than the existing ones. The advantage of exploitation is the high convergence rate—however, at the cost of getting trapped in a local optimum. Therefore, more exploration and a few exploitation results in a slow convergence, and more exploitation and a few exploration results in a fast convergence, but chances of finding true global optimality are low [176]. Thus, this balance depends on algorithm parameters setting and tuning, as shown in Table 2.2.

Table 2.2 Parameters for Optimising the Balance between Exploration and Exploitation

Algorithms	Algorithm Parameters
PSO	Inertia Weight, w
ACO	Pheromone evaporation rate (Good at exploring)
ABCO	Distance between food source (Good at exploring)
AFSA	Visual and step
BFO	Run length
GSO	Euclidean Distance
FA	Attractiveness (Good at exploring)
BA	Frequency, loudness and pulse emission rates
GWO	a and A

Swarm Intelligence and Formation Control

The piece of literature on the implementation of swarm intelligence-based algorithms in robot formation control is limited. However, PSO is one of the first algorithms implemented compared to other swarm intelligence-based algorithms. Therefore, a formation and co-ordination task was carried out using PSO where ground robots were simulated for the forest fire scenario [129]. The simulation results showed that it was possible to get good strategic positions for a multi-robot system's operation using PSO with adequate parameters. Moreover, cooperative PSO and distributed receding horizon control (RHC) scheme were incorporated for multi-robot formation control in which robots were able to track a reference trajectory while maintaining formation [92].

Another publication proposed a distributed MPC scheme incorporating cooperative PSO for multi-robot formation control problem [93]. In this study, the Nash equilibrium strategy was considered, and robots could track the reference path while maintaining the triangle formation. Furthermore, a hybrid approach of control parametrisation and time discretisation (CPTD) and PSO was proposed for the formation reconfiguration of multiple wheeled robots [69]. This study tested a group of three ground robots for the proposed algorithm.

The research was conducted on intelligent vehicle navigation problems for path planning and vehicle guiding to the target position [56]. This work employed a vehicle dynamic method

and PSO to test behaviour coordination problems such as lane-keeping, lane-changing and overtaking. Moreover, a cooperative driving and vehicle platooning problem was addressed using PSO by proposing algorithms for platoon reorganisation and platoon control [100]. In this article, vehicles can accelerate to join the preceding platoon or decelerate to depart from the current platoon.

A distributed and dynamic graph-based formation control approach was presented for vehicles to join, leave, or change lanes without affecting the stability of the convoy. Here, PSO was implemented to optimise the parameters of the control law (lane-keeping and obstacle avoidance) and to reduce the overall formation control errors [107]. This paper used a vision sensor for lane-keeping, and LIDAR was used for obstacle avoidance. In another study, a consensus algorithm and PSO were employed to maintain formation and explore the unknown static environment [53]. A consensus algorithm was based on graph theory, and positions were shared to achieve consensus.

ACO was used to address the reformation problem in the multi-agent system in which a recursion algorithm was proposed to reduce the distance travelled by each agent during the reformation process [173]. Moreover, ACO was implemented for the formation control of swarm robots by implementing ants and pheromone level as software agents [120, 119, 172]. Here, the first agent calculates the location of the conceptual barycentre of the formation and all the locations for the robots to occupy. Then, the second agent physically drives the robots to the locations to compose the formation.

In a comparative study, formation control and obstacle avoidance problems were studied using BFO and PSO. BFO resulted in good formation performance with low computation time, and PSO produced optimal trajectory but avoided the formation [142]. Furthermore, BA was used for the formation reconfiguration of multi-robot systems. Then, the CPTD method was applied to convert the time-optimal formation reconfiguration problem into a parameter optimisation problem [95]. Here, BA was used to get the control law. Finally, in

this study, a comparison was made between three different methods: BA-CPTD, CPTD, and line-of-sight, in which BA-CPTD was able to derive a better result.

In another study, inspired by swarm intelligence, a decentralised platooning concept was proposed for CAV platooning, where a spring-mass-damper system was considered for platoon formation and evolution [9]. This study achieved platoon formation via three zones: attractive, alignment, and repulsion zone.

2.4 Virtual Structure Approach

In the virtual structure approach, a rigid virtual structure represents a form of agents. Then, the virtual rigid structure's desired motion is then given, and the agents' motion is derived from the given structure. Finally, a tracking controller for each agent is derived to track the agents. The formation is maintained by minimising the error between the virtual structure and the current agent position. The desired trajectory is not assigned to the single agent in this approach, but the formation team shares it. In terms of advantages, this approach easily prescribes the coordinated behaviour for the whole group [26]. However, this approach is centralised; therefore, a single point of failure can crash the whole system. Furthermore, heavy communication and computation burden is concentrated on the centralised location, which may degrade the overall system performance[139].

A virtual structure approach is targeted to address the problem of maintenance of a geometric configuration during movement in cooperative robotics. As per [160], a virtual structure is a collection of elements, e.g., robots, which maintain a (semi) rigid geometric relationship to each other and a frame of reference. Therefore, the merit of the virtual structure approach can be described as follows [160]:

- Capability of achieving high-precision control.
- Inherently fault-tolerant during the failure of robots by maintaining formation.

- No need to elect leader robot.
- Reconfigurable for different kinds of virtual structures with no modification.
- Can be implemented in a distributed fashion with no increase in communications from a centralised implementation.
- No explicit functional decomposition.

Inspired by the above-mentioned centralised method, a decentralised virtual structure approach was proposed to achieve the following characteristics [7]:

- A decentralised framework for a large number of agents/robots and for a strict limitation on inter-vehicle communication.
- Integration of formation feedback in the framework to improve group robustness.
- Ability to prescribe a group manoeuvre directly in the framework.
- A framework to guarantee high precision for maintaining formation during a manoeuvre.

In this decentralised approach, each robot in the formation instantiates a local copy of the coordination vector in the virtual structure framework. The local instantiation of the coordination vector in each robot is then synchronised by communication with its neighbours using a bidirectional ring topology. Regarding consensus in a decentralised virtual structure approach, it is said to be reached on each instantiation of the virtual structure states, and the information flow forms a bidirectional ring topology [138].

2.4.1 Virtual Structure Controllers

A vehicle convoy is formed when multiple CAVs collaborate over multiple lanes by maintaining a pre-designed formation. A virtual structure approach was adopted by separating the

convoy control problem into a high-level virtual structure control problem and a low-level vehicle control problem to control this convoy.[135]. The MPC controller was developed to generate reference trajectories by considering longitudinal and lateral offsets. Furthermore, a nonlinear MPC controller was implemented for autonomous driving by integrating lane-keeping and collision-avoidance behaviours. Another publication proposed the architecture of adaptable virtual structure formation control by developing a formation tracking controller for the nonholonomic mobile robots to track the time-varying formation configurations [103]. In this work, two controllers were derived, a tracking controller to achieve stable tracking control performance during the transitions between two formation configurations and a formation controller to generate online formation references and make robots converge to a given formation pose.

A stabilising control method was proposed using the flexible virtual structure approach that ensured the non-collision among the agents in formation and preserved the desired shape configuration [41]. This work used three control laws to perform multi-robot navigation: a formation-keeping and inter-robot collision avoidance law, an attractive control law to guarantee the convergence to the desired final configuration, and an obstacle avoidance law. Moreover, a controller was developed to solve the problem of formation control of multiple wheeled mobile robots by guaranteeing that the derivative of the Lyapunov candidate is a negative definite, meaning that the controller is robust against disturbances [16]. Finally, this work achieved a triangular formation on a circular track using three robots.

A formation control strategy was proposed for nonholonomic intelligent vehicles based on the virtual structures approach and consensus technique [34]. Here, formation control was achieved by employing target and formation tracking strategies. A target tracking strategy was responsible for tracking the target points of the virtual structure, and a formation control strategy was responsible for tracking the trajectory by collecting velocity and pose messages.

The developed controller improved the convergence speed and increased the system's stability by employing the leader-following consensus protocol.

2.5 Emotion Assessment Methods

Over the years, emotions have been identified in several ways. Earlier, emotion assessment was based on self-assessment reports where participants reported their feeling using pen and paper. Afterwards, machine-based assessment took over traditional techniques by measuring various biological parameters. Finally, some researchers combine these techniques to increase the reliability of the obtained results. Currently, the focus is shifted towards automatic emotion assessment that can be realised using various methods, as discussed previously, such as speech emotions, facial/vision-based emotions, text-based emotions, and physiological sensor-based emotions.

Vision-based Emotions

The facial/vision-based emotion recognition method analyses facial expressions to identify a person's emotional state. This method generally comprises three steps, detection of face, detection of facial expression, and classification of emotional state from given facial expression. In this method, emotion assessment is based on facial landmark positions such as movement of the eye, lips and nose. Moreover, facial emotion recognition can be performed using static images and video. In static images, handcrafted features are extracted, and classification is performed to identify the emotion. In the video, information on spatiotemporal features is analysed to classify emotions [81].

Speech-based Emotions

Speech-based emotions recognition method analyses speech signals to identify a person's emotional state. This method comprises four steps, speech to text conversion, feature extraction, feature selection, and classification of those features to identify emotions. In this method, emotion assessment is based on local and global features of given speech signals that can be analysed using four classes, prosodic features, spectral features, voice quality features, and Teager Energy Operator-based features [167]. In this method, global features are based on statistical feature extraction, whereas local features represent temporal dynamics in given prosody.

Text-based Emotions

The text-based emotion recognition method analyses text content to identify a person's emotional state. This method comprises five steps, content acquisition, data preprocessing, feature extraction, feature selection, and classification to recognise emotions. Here, feature extraction analysis can be performed using five methods: lexical analysis, syntactic analysis, semantic analysis, disclosure integration, and pragmatic analysis [87]. The most common approaches for identifying text-based emotions are keyword-based, rule-based, machine learning-based, and deep learning-based.

Physiological Sensor-based Emotions

The physiological sensor-based emotion recognition method analyses biomedical signals to identify a person's emotional state. This method comprises five steps, signal acquisition, signal preprocessing, feature extraction, feature selection, and classification to recognise emotions. Here, signal acquisition can be from one or more such sensors as ECG, PPG, EEG, EMG, GSR/EDA, SKT, and RSP. Here, properties from these signals are studied at different emotions, which results in a feature extraction method. Furthermore, PPG and

ECG sensors are widely available in the consumer market, and their awareness is widespread among customers. Moreover, these sensors are easy to integrate with wearable devices and provide easy access to data. For these reasons, ECG and PPG sensors are considered for emotion assessment during autonomous operations.

2.5.1 Electrocardiogram (ECG)

ECG is a powerful diagnostic tool in medicine used to assess the heart's functionality. Obtaining physiological signals from ECG is a conventional method for non-invasive interpretation of the heart's electrical activity in real time. The ECG signal is recorded by attaching electrodes to the body's surface using a standard 12-lead ECG system. These currents stimulate the cardiac muscle and cause the contractions and relaxations of the heart. The electrical signals propagate through the electrodes to the ECG device to record the characteristic of waves. Different waves reflect the activity of different heart areas, generating the respective flowing electrical currents.

In practice, ECG signals are recorded as a difference of electric potentials at the two points inside of the heart, on its surface or a surface of the human body. The potential difference corresponds to the voltage recorded between two points where the measurements were taken. This voltage is the amplitude of the ECG signal recorded in the two-pole (two-electrode) system. Such a two-electrode system applied to recording the ECG signal is called an ECG lead. In this two-pole ECG recording system, one electrode is an active measurement electrode, while the second is the reference one. The changes during a time of voltage variation between the ECG recording electrodes depict a course of ECG signal.

The ECG signal is quasi-periodic, and each beat is composed of three waves: P-wave, QRS Complex and T-wave. Fig. 2.5 shows a systematic representation of a normal ECG signal and its various waves. Here, the P-wave represents atrial depolarisation, T-wave represents ventricular repolarisation, the first deflection in the complex, if it is negative, is

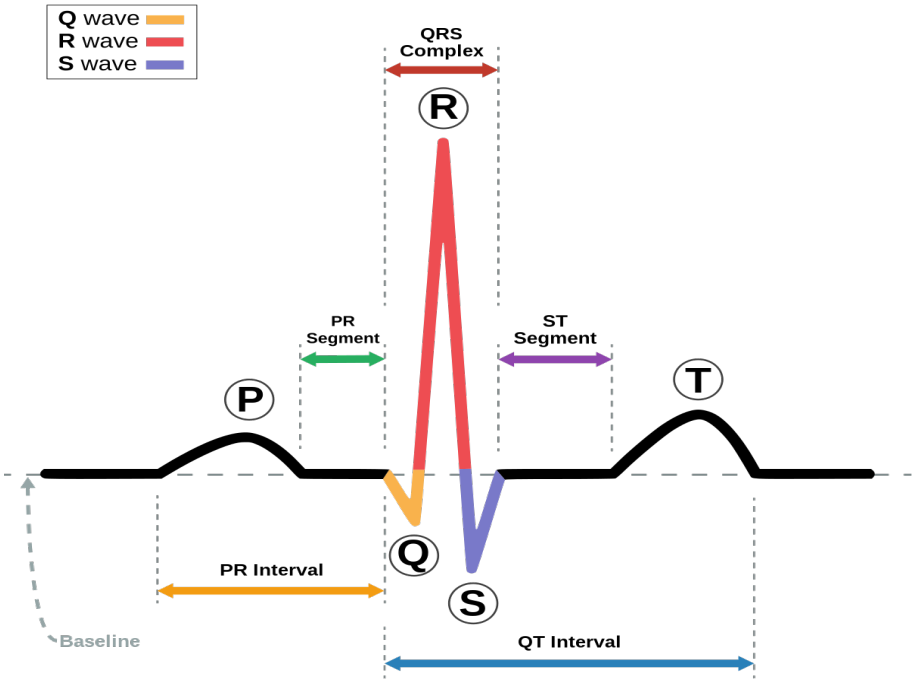

Fig. 2.5 ECG Signal [169]

called a Q-wave, the first positive deflection in the complex is called R-wave, a negative deflection after R-wave is called S-eave and U-wave represent repolarisation of the Purkinje fibres.

2.5.2 Photoplethysmography (PPG)

PPG is regularly used in clinical diagnostics to monitor heart-induced changes in blood volume in micro-vascular beds at peripheral body locations such as the finger, nose, earlobe and toe. The pulsating element of a PPG signal is associated with modifications in the quantity of blood within the arteries and is synchronous with a heartbeat. In contrast, the non-pulsating element depends on the blood volume, breathing, sympathetic nervous system, and thermoregulation. The maximum pulsatile component of reflected light occurs approximately between 510nm and 590nm. Because of this wavelength, green (565nm) or yellow (590nm)

light is generally used for reflective PPG sensors. Moreover, the red (680nm) or near-infrared (810nm) light is generally used for transmissive PPG devices, with the infrared light having the deepest penetration [159].

The PPG signal is measured from the vascular blood flow measurement sensor. It is originally used to detect arterial oxygen saturation and HR for cardiac arrhythmia diagnosis. The working principle of the PPG sensor is based on the emission of infrared light by an LED which penetrates the skin and blood vessels. The detector captures this light to measure the bloodstream, as shown in Fig. 2.6. The results of the PPG signal depend primarily on the flow of blood and oxygen to the capillary vessels in each heartbeat. In theory, PPG has two types of signals: alternating current (AC) and direct current (DC) signals. Here, the AC signal is generated by the heartbeat affecting the blood volume when light passes through the arteries. The DC signal is generated by the constant absorption of light passing through the tissue.

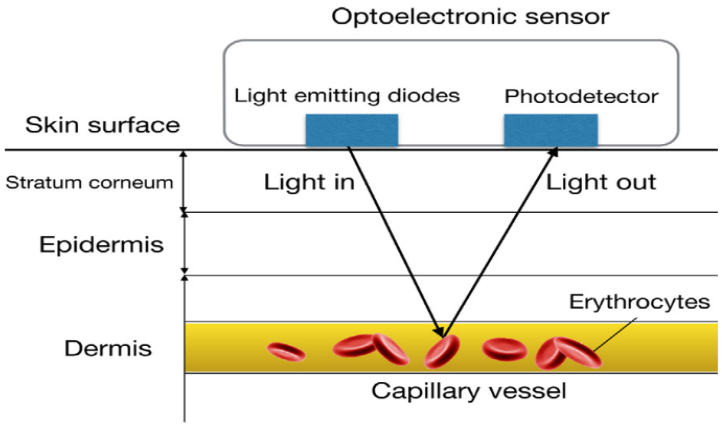

Fig. 2.6 PPG Sensor Working Principle [181]

There are two functioning principles for photoplethysmography sensors: the transmission or reflection of light through or by a specific part of the body [114]. Fig. 2.7 shows the two types of working principles of PPG: the transmission operation (Fig. 2.7(a)), in which the emission module and the photodetector are located on opposite sides, which is widely used in

clinical diagnostics; and by reflection (Fig. 2.7(b)), in which the emission module is located on the same side as the photodetector which is suitable for wearable products.

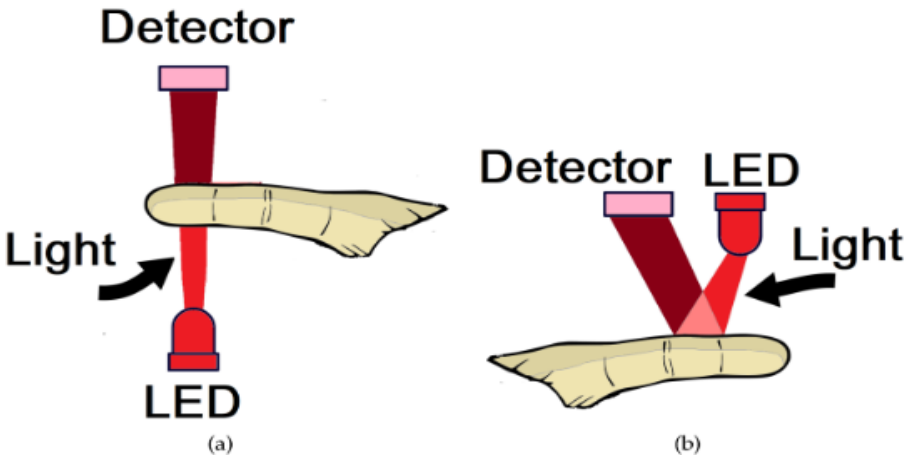

Fig. 2.7 Transmissive and Reflective PPG [114]

Fig. 2.8 shows a PPG signal and several components such as systolic point, diastolic point and dicrotic notch. The systolic point results from the direct pressure wave travelling from the left ventricle to the body's periphery. The diastolic point (or inflection) results from reflections of the pressure wave by arteries of the lower body. A dicrotic notch is usually seen in the catacrotic phase of subjects with healthy compliant arteries, and an IBI is an inter-beat interval.

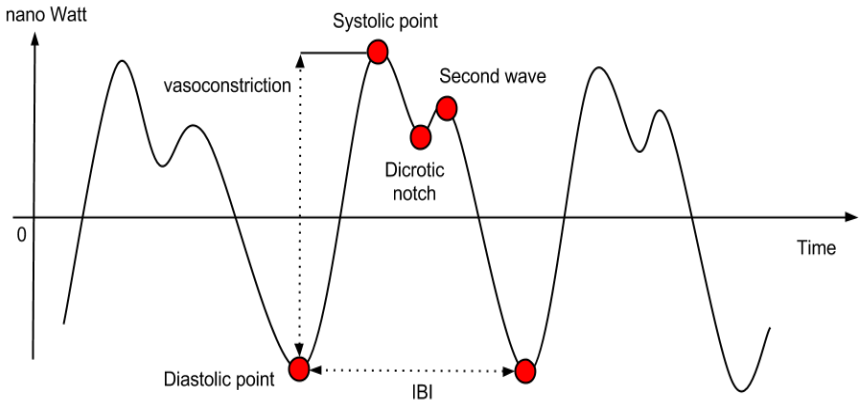

Fig. 2.8 PPG Signal [11]

2.5.3 Emotion Assessment Using ECG and PPG Sensors

Since emotion recognition is an extensive research area with many published studies, this research focuses on physiological sensor-based emotions assessment literature covering ADM and DEM methods. For example, five emotional states (happiness, disgust, fear, sadness, and neutral) can typically be accessed using heart rate variability (HRV) features for DEM classifications [115]. Here, the HRV features were derived from the ECG signals, indicating the heartbeat variation within a specific time frame. In their work, video clips were played to induce different emotions, and three electrodes were used to acquire the ECG signal. Regarding performance, the maximum average classification rates for the k-nearest neighbour (KNN) and linear discriminant analysis (LDA) were 69.75% and 67.81%, respectively. Another study used ECG, SKT, and EDA's bio-signals to recognise discrete emotions such as sadness, anger, stress, and surprise [78]. Here, features like heartbeat interval, HRV, skin conduction response (SCR) amplitude, and temperature variations were extracted from a short segment of bio-signals. Using the SVM classifier and DEM method, they have achieved a correct classification rate of 78.4% for the three emotions categories and 61.8% for the four emotions categories.

Many researchers use nonlinear analysis in bio-signal processing, and features such as approximate entropy, largest Lyapunov exponent, correlation dimension, Hurst component and nonlinear prediction error have been studied. These features convey information related to properties such as similarity, predictability, reliability and sensitivity of the signal. For example, the Hurst exponent analyses the smoothness of a time series and is based on self-similarity and correlation properties. It also evaluates the presence or absence of long-range dependence and its degree on a time series. Therefore, a nonlinear approach was proposed, and six emotional states (happiness, sadness, fear, disgust, surprise and neutral) were measured using audio-video stimuli [148]. Here, a nonlinear Hurst feature was calculated using Re-scaled Range Statistics (RRS) and Finite Variance Scaling (FVS)

methods, and new Hurst features were proposed by combining Higher Order Statistic (HOS) method with RRS and FVS. These features were then classified using four classifiers, Bayesian Classifier, Regression Tree, K-nearest neighbour (KNN) and Fuzzy K-nearest neighbour (FKNN). Regarding performance, the Hurst computed using FVS and HOS provided better results using the FKNN classifier.

Another publication developed an automated approach in emotion recognition based on several biosignals such as EMG, ECG, RSP, and EDA [74]. Here, four emotional states (high stress, low stress, disappointment, and euphoria) were estimated using a support vector machine (SVM) and adaptive neuro-fuzzy inference system (ANFIS). Regarding performance, SVM performed slightly better than ANFIS classifier. Another paper targeted five emotions (sad, angry, happy, fearful, and relaxed) induced by video stimulus using the HRV feature of the ECG signal [54]. Here, the HRV signal was analysed in both the time and frequency domain, and three statistical parameters were considered, Kurtosis coefficient, entropy and skewness value. Moreover, principle component analysis (PCA) was used to compress the extracted feature, and an SVM classifier was employed to distinguish emotional states. Regarding performance, the accuracy result for the classification of two emotional states was higher than the classification of five.

PPG signals have been employed for emotion recognition using the ADM method [91]. Here, a one-dimensional convolutional neural network (1D CNN) was used to extract features, and a database for emotion analysis using physiological signals (DEAP) [82] was used to validate the method. By splitting the PPG signal into a single pulse signal, this proposed method achieved 75.3% classification accuracy for valence and 76.2% accuracy for arousal. In another study, an end-to-end approach was employed by replacing handcrafted features to predict levels of arousal and valence from physiological signals [77]. Here, raw ECG and EDA signals were used to recognise dimensional emotion using convolutional neural networks (CNN) and recurrent neural networks (RNN). This approach proved that the

proposed system could learn intermediate data representations related to affective behaviours and outperform the handcrafted features method.

Some researchers used EMG, EDA, skin temperature, blood volume pulse, ECG, and respiration signals for developing their emotion detection method [55]. They extracted seven features to train two separate neural network classifiers for arousal and valence. Regarding performance, 96.6% correct classification for arousal and 89.9% for valence was achieved by allowing a bandwidth of 20% for the output to be counted as correct. Another study employed multi bio-signals to recognise six emotional states: joy, happiness, fear, anger, despair, and sadness [177]. This work used EEG, ECG, PPG, GSR, and RR signals for 15 different types of feature extraction. An artificial neural network (ANN) classifier was employed to recognise emotion patterns for classification. Regarding performance, the classification rates of each emotion are joy (86%), happiness (91%), fear (79%), anger (87%), despair (76%), and sadness (94%).

Many researchers have used multi-modal bio-signal for emotion detection. However, using several signals is not convenient from the user's perspective as this would interfere with an individual's daily activities, and processing multiple signals is computationally expansive. Therefore, using only a PPG sensor, an automatic discrete emotion recognition method was developed using music videos that targeted several emotion elicitations such as love, hate, and fun [51]. The DEAP dataset [82] and a support vector machine (SVM) classifier were employed in this study. Here, Poincare's section theory was used to demonstrate the type of attractor and recognise the shape characteristics of the original signal trajectory. This method achieved average classification rates (training/test) of 99.14% / 91.11%, 99.26% / 90%, and 97.78% / 88.89% for discriminating love, hate, and fun from the other classes, respectively.

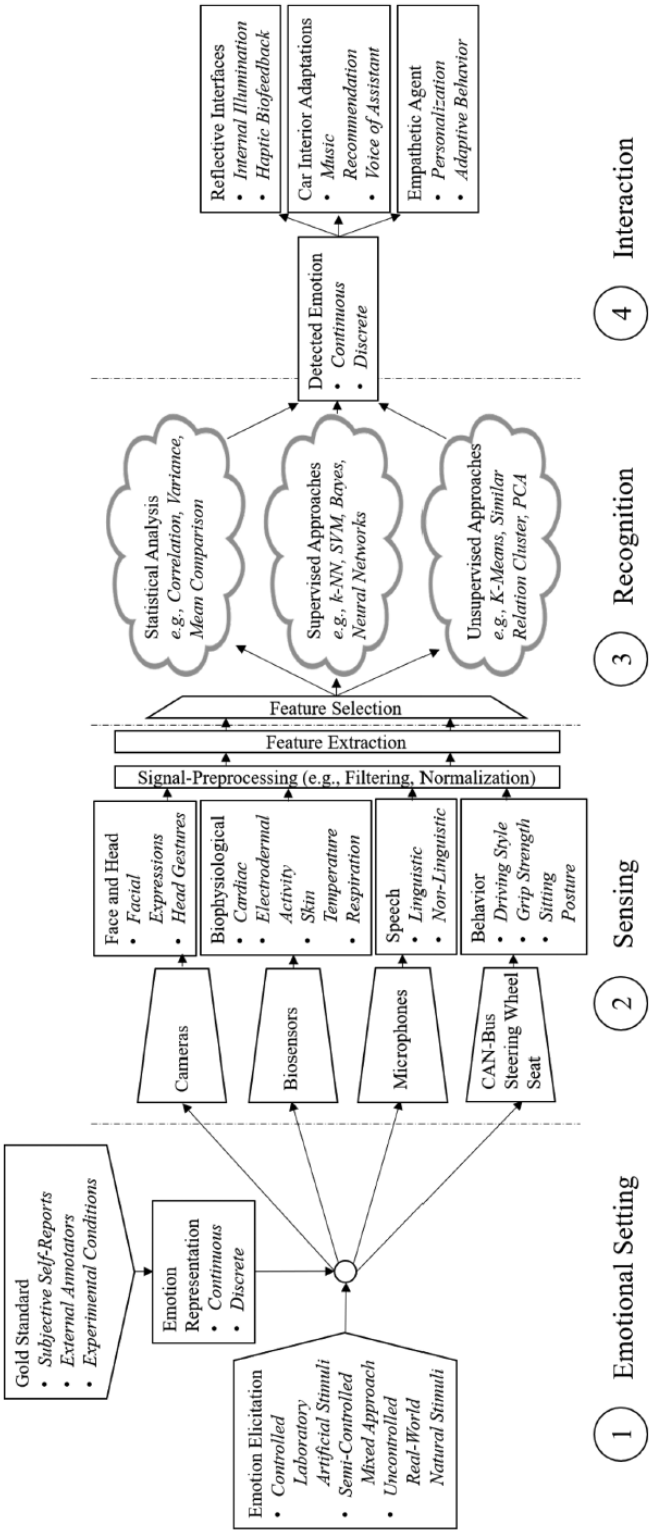

Fig. 2.9 Emotion Assessment in AGVs [178]

2.6 Emotion Assessment in Autonomous Driving

Recently, emotion assessment in autonomous driving has been gaining popularity. Driving is one of the major tasks faced by humans in their daily routines. The impact of emotion on driving can affect road safety and human health, such as driving during anger or stress emotions. SAE's driving automation levels provide an understanding of which levels perform what automation tasks. However, current results show that AGVs are imperfect, and companies are still working on the fifth level of autonomy [162]. Moreover, employing emotion assessment in AGVs can help make the system safer. This method can be employed within current automation levels, or Level 6 can be created.

Several studies mention using emotion assessment approaches for the autonomous driving scenario. Fig. 2.9 provides an overview of the main stages of emotion assessment in drivers. Stages 1 to 3 are widely used techniques in assessing human emotions, whereas stage 4 is a novel step to employ these results in AGVs. In stage 1, emotions are elicited in participants/drivers by artificial or natural stimuli or mixed stimuli, and responses are collected by self-reports, external annotators, and experimental conditions. This stage forms the base of how a person feels about particular stimuli or situations. In stage 2, sensors are used to capture different emotions and relative changes in the driver's behaviour and biological properties. This sensor data is then used to extract meaningful features corresponding to specific emotions. In stage 3, machine learning approaches are generally employed to recognise emotions. Finally, the interaction between the driver and AGV is enabled based on detected emotions in stage 4. An interaction between a driver and AGV can be of multiple functions. On a multimedia side, AGVs can offer better music recommendations, tune the voice assistant, and illuminate the car interior based on the identified emotion. On the control side, AGVs can steer the vehicle by maintaining a speed during positive emotions and reducing speed during negative emotions.

One study assessed the emotional state of drivers based on facial analysis and vital signs acquired from a camera, galvanic skin response (GSR) and photoplethysmography (PPG) [110]. The participants were shown video clips containing eight different emotions to evoke emotions. The results concluded that facial analysis, combined with physiological sensors, can be used to evaluate the driver's emotional state. Another study proposed a calibration function for autonomous driving algorithms using emotion assessment [155]. In this study, facial emotions were considered available from a public dataset containing images with various facial expressions. Classification results were obtained using a neural network on each dataset. Moreover, 11 driving situations were tried to assess participants' emotions with different calibration values.

Study in [101] proposed the use of an explainable intelligence technique in understanding some of the tasks involved in the development of AGVs using the detection of driver's emotions and the distraction of drivers. Here, a deep neural network takes images of drivers and predicts their moods and activity. EEG sensors are widely used in emotion assessment research. One study [4] used such a sensor to develop a wearable headband for measuring stress-related brain activity during driving to access how autonomous driving algorithms impact EEG brain activity. This research used a driving simulator, and participants were told to experience three algorithms, one manual controller and two autonomous controllers. The results found that manual driving revealed the highest stress on drivers compared to autonomous driving.

A change in autonomous control function in AGV driving based on the driver's circumstances and emotions can provide insight into developing a better autonomous controller. Therefore, one research proposed a new human–machine interaction for driver-assisted driving control while considering the driver's situation and emotions [90]. Four scenarios were simulated, and emotions were assessed using PPG and GSR sensors. The results concluded that bio-signals could be implemented for AGVs' speed control. Furthermore, one study

used a public dataset and 14-channel EEG sensors to develop an emotion assessment method for autonomous driving operations and drive monitoring [63]. Here, frequency and power density data were used to cluster and identify a subject's emotional state when exposed to a particular stimulus. In this study, K Nearest Neighbours (KNN) algorithm was employed, which achieved a classification accuracy of 96% for arousal and valence.

One study investigated the effect of happiness and anger on grip strength applied to the steering wheel, focusing on human-computer interaction in cars [118]. The driver's emotions were collected using a driving simulator in this study. Moreover, the steering wheel was designed using in-built fibre that measured deformation caused by the driver's force applied to the steering wheel. The results concluded that grip strength was increased during happy emotions and decreased during angry emotions. When the AGVs reach operational limits, drivers must take over the vehicle immediately. Therefore, one research examined the effect of emotional valence and arousal on takeover performance in conditionally automated driving [36]. This study involved participants driving using a driver simulator while exposed to several emotions, and a takeover warning was issued during each emotion. The result found that positive valence led to better takeover quality, and high arousal did not yield an advantage in takeover time.

2.7 Summary

Chapter 2 reviewed three areas: formation control techniques for AGVs, emotion assessment techniques, and the role of emotion assessment in AGVs. First, three formation control methods were discussed and their advantages and disadvantages. Then, controllers covering leader-follower, behaviour-based, and virtual structure approaches were discussed. Afterwards, a review of the emotion assessment method was presented, covering both ADM and DEM models. Finally, the implementation of emotion assessment in AGV's operation was presented.

After clearly understanding the state-of-the-art techniques, the research questions mentioned in chapter 1 can be addressed in the following way. First, literature on formation control techniques will be applied to answer research questions 1 and 2. It is found that a simulator development is necessary to test the controller for multiple AGVs. Furthermore, the development of a controller will be based on techniques discussed in the literature. Research question 3 will be answered using literature on emotion assessment methods. Both ADM and DEM models are applicable in the emotion assessment method, and several sensors can be employed to collect physiological data from a human. The focus should be on how easily this data can be collected, and the resultant method should be fast and continuous to provide results. Finally, research question 4 will be answered using the literature available on applying emotion assessment in AGVs. It should be noted that limited literature is found in this growing area, and no one has developed a simulator that can simulate multiple AGVs employing different emotions. The five levels of autonomy primarily consider sensors and actuators and control based on information obtained by these sensors. Human is an essential element of this technology; therefore, human information can also play an important part in achieving safe autonomous control by considering human-in-the-loop.

Chapter 3

The Problems Addressed, Proposed Approach and Research Method

This research aims to develop formation control algorithms and an approach to assess human emotions via wearable devices for autonomous vehicles. The research results will be applicable in on-road autonomous vehicles, mobile robots within warehouses, and for education and research purposes. The main problem addressed here is using identified emotion in the AGV control task. As stated in Chapter 1, this research is divided into four research questions to address this problem. Furthermore, this chapter explains the major research paradigms, approaches and methods used to carry out this research and addresses the problems which should be solved. Finally, a summary is provided of this chapter.

3.1 Research Paradigms

A research paradigm is a conceptual framework that provides a community of scientists with an appropriate model for investigating problems and finding solutions. A paradigm can be defined as 'the entire constellation of beliefs, values, techniques, and so on shared by a given [scientific] community members' [85]. Three major questions can help define

Table 3.1 Major Research Paradigms [131]

	Positivism	**Postpositivism**	**Interpretivism**
Ontological stance	'Realism'	'Critical realism'	'Relativist'
	Belief in a tangible, social reality. This reality exists independently of those 'creating' the reality. A social reality can exist just as a natural reality exists.	Belief in social reality but acceptance that knowing this reality will always be inhibited by imperfections in detecting its nature. The imperfections are the result of human fallibility.	Belief in multiple, constructed realities that cannot exist outside the social contexts that create them. Realities vary in nature and are time and context-bound.
Epistemological stance	Objectivist/ dualist	Modified dualist/ objectivist	Transactional/ subjectivist
	Investigator and investigated are independent of each other.	Acceptance that independence is not possible but objectivity is seen as the goal and demonstrated by external verification.	The results of the investigation are a product of interaction between the subject and the investigator. What can be known is a result of the interaction.
Methodological stance	Experimental/ manipulative	Modified experimental/ manipulative	Empathetic interaction
	Hypothesis testing, variables identified before the investigation. Empirical testing is conducted in order to establish the 'truth' of the proposition.	Hypothesis testing but more emphasis placed on context.	Investigator interacts with the object of the investigation. Each construction of reality is investigated in its own right and is interpreted by the investigator.
	Predominantly quantitative.	Quantitative and qualitative.	Qualitative.
	Analysis by variables.	Analysis by variables.	Analysis by case.
Purpose	Prediction/control/ explanation	Prediction/control/ explanation	Understanding/ reconstruction
	Framing of general laws.	Generalisations.	Transfer of findings.

a research paradigm: ontological question, epistemological question, and methodological question. 'Ontology' is the nature of reality; 'epistemology' is the philosophy of how we can know that reality; and 'methodology' is the practice of how we approach knowing that reality. Three major research paradigms include positivism, postpositivism and interpretivism. Table 3.1 provides an overview of the contrasting basic beliefs of each of the three paradigms.

3.1.1 Positivism

Unlike the 19^{th} century's prevalent theological and metaphysical ideologies, social positivism was developed to study social phenomena as an empirical science. Positive knowledge was identifying phenomena' causal rules derived straight from observation. Typically, positivist research starts with a hypothesis experimentally verified through planned experiments. The positivist method emphasises describing how things happen to foresee what will happen next and have influence over what occurs. Quantitative methodology is used in positivist research.

3.1.2 Postpositivism

Postpositivism was as much a reaction to positivism's failings as it was to a shift in natural science's emerging changes in fundamental axioms. Although the process has changed from that of the early positivists, postpositivists still primarily use experimentation and hypothesis testing as their methods of inquiry. The postpositivism method is somewhat identical to the positivist method. The most significant difference is the idea of falsification, which involves denying the existence of a phenomenon that had been a positive result of research. Quantitative and qualitative methodologies are used in positivist research.

3.1.3 Interpretivism

Interpretivism is used as a covering term for several approaches to research with a major focus on empirical interpretivism and critical theory. The former focuses on studying social

phenomena in natural settings, whereas the latter conducts ideologically motivated research by analysing contemporary ideas and social structures. The research procedure may have produced some of the data that was collected. The data will be influenced by the occasion and setting of its collection. The interpretivism method believes that any study endeavour will change the studied subject. Qualitative methodology is used in interpretivism research.

This research study adapts the postpositivism approach. This strategy backs the idea of methodological pluralism and the notion that the research question should guide the methodology. In this research, the quantitative approach includes studying the controller's behaviour and statistical analysis. At the same time, the qualitative approach includes using participants' observation data to derive their emotions.

3.2 Proposed Approaches and Methodologies

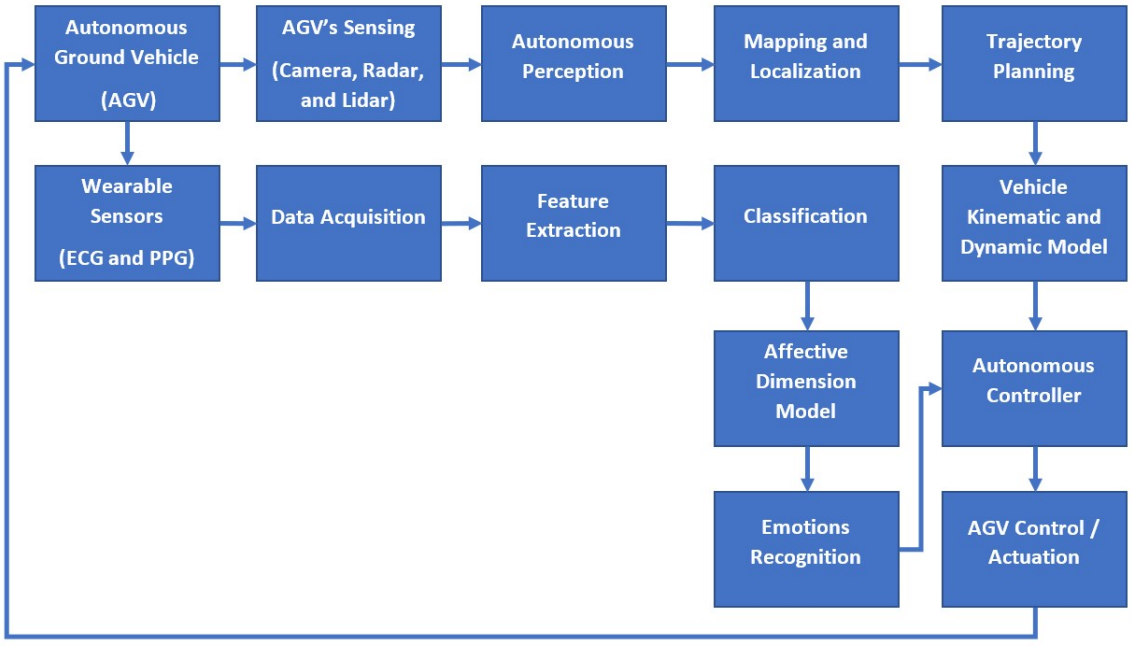

Fig. 3.1 Autonomous Navigation with Human-in-the-Loop

Figure 3.1 shows the closed-loop system of how emotions can be utilised with the AGV controller. Each of these blocks of Figure 3.1 are explained below:

- **Autonomous Ground Vehicles** is equipped with various sensors and actuators. As a result, AGVs can perform some or all of the operations autonomously without requiring human input. Chapter 1 provides details of such vehicles.
- **AGV's Sensing** block includes several sensors such as Camera, RADAR, and LIDAR. Chapter 1 provides information on the operation of such sensors.
- **Autonomous Perception** senses environment using sensor. This block aims to collect environmental information to process this data to understand the world around the AGV.
- **Mapping and localisation** help build a map and localise AGV in that map simultaneously. This block helps AGV steer through an unfamiliar environment while simultaneously identifying its location.
- **Trajectory Planning** is the real-time planning of AGV's move from one feasible state to the next, satisfying the car's kinematic limits based on its dynamics and as constrained by the navigation mode.
- **Vehicle Kinematic and Dynamic Control** block deals with the motion. Vehicle kinematics does not consider forces that cause motion, while vehicle dynamics considers the motions that result from forces.
- **Autonomous Controller** block takes several inputs from AGVs, and wearable sensors and issues control commands to the AGV.
- **Wearable Sensor** includes mainly ECG and PPG sensors. These sensors are worn by passengers inside the AGV and can be placed at body locations such as the wrist and chest. Chapter 1 provides more information on such sensors.
- **Data Acquisition** block is responsible for capturing raw data from wearable sensors such as ECG and PPG.

- **Feature Extraction** step processes raw data from ECG and PPG data and extracts features as explained in chapter 6.
- **Classification** block uses a trained classifier on extracted features and classifies valence and arousal levels.
- **Affective Dimension Model** helps translate predicted valence and arousal values into specific emotions based on the circumplex model of affect.
- **Emotions Recognition** block confirms identified emotion of a human, which is then taken as a control parameter for an autonomous controller.
- **AGV Control / Actuation** block controls the AGV based on control instruction produced by the autonomous controller block. For example, this can include velocity control, steering control, and in-vehicle multimedia control.

Fig. 3.1 provided high-level information on the operation of each block. The approaches adopted in this thesis to answer the research questions include:

3.2.1 Simulator Development

Testing controllers on actual robots and developing real-world scenarios within a laboratory or outdoor environment is a time-consuming process. Therefore, a simulator is required to be able to simulate multiple AGVs and to study the performance of controllers. A simulation environment is developed using ROS and Gazebo to test developed algorithms and to address research question 2. ROS is a popular framework amongst research communities and has become the standard for robotics research. At first, a simulation world with roads and junctions is developed. Then, a differential drive mobile robot is developed and simulated. The proposed simulator offers the ability to modify the world map such as more junctions and roads can be added, and multiple mobile robots can be simulated.

3.2.2 Controller Development

Two types of controllers are developed and tested to address the first research question. They are traditional rule-based controllers and model predictive controllers. Each of these controllers is implemented for multiple AGVs navigation. To develop a rule-based controller, a laser sensor is considered, and platoon formation is realised via the distance sensed by this sensor. Also, a rule-based controller provides good insight into developing multiple AGV controllers. On the other hand, MPC is helpful because of its ability to predict future information and use them to optimise control actions. Furthermore, MPC offers a choice to set constraints that can stabilise the overall system, such as AGV. Here, the simulator helps track AGV's movement and evaluate the controller's performance.

3.2.3 Emotion Assessment Method

The effect of emotions on a person's heart and collecting relative changes to heartbeat rhythms can provide insight into the relationship between the cardiac cycle and felt emotions. Here, ECG and PPG sensor data are considered to extract heart rate signals. After having these signals, novel features such as signal morphology, instantaneous frequency, and spectral entropy are extracted to assess human emotions using an affective dimensional model to answer the third research question. Here, three classifiers, support vector machine, neural networks, and long short-term memory (LSTM), are used to obtain the classification accuracy of the proposed approach. After obtaining the classifiers' accuracy, a statistical significance test is employed to verify the results.

3.2.4 Integrating Emotions with AGVs

The text-based emotion assessment method is unsuitable in the autonomous driving scenario since passengers do not generate such data during driving operations. Furthermore, the speech-based emotion method is challenging to implement since passengers may not speak

during driving. On the other hand, facial/vision-based and physiological sensor-based emotion recognition approaches can be applied to autonomous driving operations because it is relatively easy to collect data continuously via camera and physiological sensors during driving operations. Furthermore, the advantage of emotion detection using physiological signals is that they are unconscious responses of the human body and very difficult to conceal compared to physical signals such as facial and speech emotions, as they are easy to control and hide. Here, output from the emotion recognition method is taken as feedback for the AGV controller to answer the fourth research question.

3.3 The Problem Addressed

To implement the approaches described above, the following methodologies have been adopted in this thesis:

The Problems in Simulation

The developed algorithms and controllers require a simulation platform to evaluate the performance of AGVs and their algorithms. A simulator is a valuable tool to test robot hardware configuration, software integration, and interaction with other robots and the environment. Furthermore, simulation provides an idea of the robots' behaviours on implemented algorithms and is crucial to rapidly reproducing experiments.

Model Validation Problems

In a simulation, the validation process produces a better model and proves the model's credibility. In this research, the simulation models, such as robot vehicles and world environment, mimics an accurate representation of the actual system being studied. For example, this

research uses RVIZ to visualise the robot's joints, how they move/rotate, their connections to each other, and their interaction in the environment with other such robots.

Controller Development Problems

Two types of controllers are developed to form a platoon formation. One controller uses a laser sensor based on a rule-based approach, while the second utilises MPC. In addition, longitudinal and lateral control is studied. The longitudinal controller regulates the AGV's cruise velocity, while the lateral controller steers the AGV's wheels for path tracking.

Data collection Problems

A public dataset is considered containing physiological data and annotations for developing emotion assessment methods. Various datasets are available for emotion assessment research. For a given emotion stimuli, annotation can be discrete or continuous. Continuous annotations benefit from recording changing emotional responses compared with discrete annotations. Most of the datasets have discrete annotations. This study considers continuous annotation.

Feature Extraction Problems

An emotion assessment using physiological signals is purely based on feature extraction related to different felt emotions. Several features can be extracted from the ECG and PPG signals. The morphological features, spectral entropy, and instantaneous frequency of the ECG/PPG signals are considered to train classifiers.

Statistical Significance Test Problems

After obtaining classifier accuracy, it is essential to validate results using statistical methods. One such tool is called the null-hypothesis significance test. The results are statistically

significant for p-values less than 0.05 ($p \leq 0.05$). A $p \leq 0.05$ indicates strong evidence against the null hypothesis. Therefore, a p-value test is considered for classifier accuracy.

Autonomous Control with Human-in-the-Loop

Adaptive control bridges the gap between autonomous control schemes and emotion assessment. It updates control parameters based on identified emotions and delivers safe autonomous driving operations. The output from an emotion assessment classifier is used as a tuning parameter of a controller to update autonomous control.

Experimental Verification

The development of emotions-aware AGVs benefits the passengers and enhances the trust between machines and humans. This research endeavour is potentially fruitful with a strong science base and wide real-world applications. Experiments are carried out in simulation in order to validate the proposed approaches. The results provide a better understanding of the feasibility and performance of the proposed solutions and how autonomous control can be improved by using human emotions as feedback.

3.4 Summary

This chapter provided an overview of the research community's major research paradigms. Positivism adopts a scientific and quantitative method, while interpretivism adopts a qualitative approach. This research identified postpositivism as a preferred method, using both quantitative and qualitative methods. Then, a block diagram of the whole approach is provided, and each block is explained. After that, four approaches are discussed to help answer four research questions. Finally, the problems are identified to carry out this research, and each of these problems is explained to justify the methodology used for this research.

Chapter 4

MPC for Efficient Control of Multiple Vehicles

This chapter introduces model predictive control (MPC), controller design, and simulation results. First, Section 4.1 introduces the main components of MPC. Then, Section 4.2 discusses a general MPC framework. Next, Section 4.3 discusses controller development and implementation on single and multiple mobile robots are discussed in Section 4.4. Finally, Section 4.5 presents a summary of this chapter.

4.1 Introduction

This chapter describes a simulation of a multi-AGV navigation scenario in a warehouse environment. A 2D robot model and simulation world are presented to achieve this result. At first, one AGV is simulated, and its result is analysed. Then, multiple AGVs are simulated. Using AGVs in a warehouse can have multiple applications, such as transporting rigid objects and manipulating deformable objects, objects of variable shape. Using AGVs in the warehouse also results in finishing tasks in minimum time, thus minimising power consumption. Therefore, MPC is employed to simulate multiple robots.

MPC, also known as dynamic matrix control, receding horizon control, dynamic linear programming, and rolling horizon planning, is a popular controller used in the process industry and automation. An MPC is an approach to control design rather than a specific algorithm. An MPC has seven main components, prediction, receding horizon, modelling, performance index, degrees of freedom, constraint handling, and multivariable. The key to implementing MPC is a clear understanding of these components.

4.1.1 Prediction

Prediction plays an essential role in developing such a controller. One should think through all the likely consequences and possibilities before planning an activity; otherwise, the outcome of a controller may be far from the desired outcome. This parameter cannot be seen as a tuning parameter. It is better to always predict beyond the safe braking system; otherwise, avoiding a crash cannot be guaranteed. As a rule of thumb, a prediction horizon value should always be larger than the settling time of a car. For example, if a developed controller can only predict 20 meters ahead while driving at 60 mph, a sharp corner will inevitably cause a car crash. When deciding a value of the prediction horizon, it is better to consider different weather effects (snow, fog, and rain), other vehicles, pedestrians, and speed limit changes.

4.1.2 Receding horizon

In the receding horizon step, prediction values and decision-making are continuously updated to take account of the most recent target and measurement data. In other words, the prediction horizon is always relative to the current position and thus recedes away from the viewer as the viewer moves forward. Therefore, the horizon (the actual prediction distance) stays the same. Thus, in MPC, the continuous update of prediction and decision-making to take account of the most recent target and measurement data introduces feedback. In other words,

measurement is a core part of a feedback loop, and decisions based on measurement are the second core component.

4.1.3 Modelling

A core part of MPC is prediction. In order to automate prediction, a model is required for modelling system behaviours. For model design, it is better to start by taking basic requirements such as the model should be easy to form prediction and ideally linear, easy to identify model parameters, and provides accurate predictions. In MPC, the role of the model is to compute system output prediction; therefore, if the model provides accurate enough predictions, it is considered fit for purpose. In practice, predictions can be 10-15% out in the steady state and still be highly effective as they capture key dynamic changes during transients. In addition, continuous feedback will correct minor modelling errors.

4.1.4 Performance Index

In order to automate an MPC, a performance index should be defined to decide which input trajectory is best for vehicle navigation, for example. Simpler definitions are better as they lead to better-conditioned and More straightforward optimisations. As the optimisation is carried out online, with corresponding risks, the performance index should only have increased complexity where the benefits are clear. Typically quadratic performance indices give well-conditioned optimisation with a unique minimum and generally smooth behaviours. If a model is of low quality, it does not expect a highly defined performance index and vice versa. Handling the trade-off between optimal and robust performance is also essential, as high-performance demands are not cost-free. High performance implies high risks, less robustness, and the inability to deal with uncertainty. On the other hand, low performance with a high-fidelity model implies low risks, likely to be safe, and robust to uncertainty.

4.1.5 Degree of freedom

The degree of freedom describes the complexity of the input predictions. Consequently, this issue is closely related to performance indices. It is possible to utilise a high degree of freedom with a highly demanding performance index if the model is good. Moreover, the result of any corresponding optimisation would be essentially meaningless. The degree of freedom is linked to prediction accuracy. If one cannot predict accuracy, there is no point in having many degrees of freedom. Time-varying targets need a high number of degrees of freedom, and advanced target information can only be used well with high numbers of a degree of freedom.

4.1.6 Constraint Handling

One significant advantage of predictive control is that it embeds constraints into strategy development. The proposed input trajectory is optimal while satisfying constraints. The systematic embedding of constraint information is critical to effective and robust closed-loop behaviour. The constraints are embedded into the planning. For example, MPC will not propose an input flow that allows the car to over speed. This acceleration constraint may result in a slightly slower acceleration rise during transients, but it will be safe. In addition, MPC will be aware that the input is limited to 100% and thus will not allow earlier input choices that make the system not stabilise after that. In general, embedding constraints such as awareness of curbs while driving and the speed limit for a car will ensure that the proposed input strategies are continuously optimised and the tuning changes, if needed, for different operating points. A simple, well-tuned, unconstrained law may be very effective in a small range but dangerous if used over a more comprehensive operating range.

4.1.7 Multivariable

One key observation of MPC is the ability to handle multivariable/interaction. Often, changing one input changes all the outputs, and an effective control law has to consider all inputs and outputs simultaneously. One advantage of MPC is that the framework automatically takes account of such interaction.

4.2 MPC Framework

Fig. 4.1 shows a block diagram of a nonlinear MPC system.

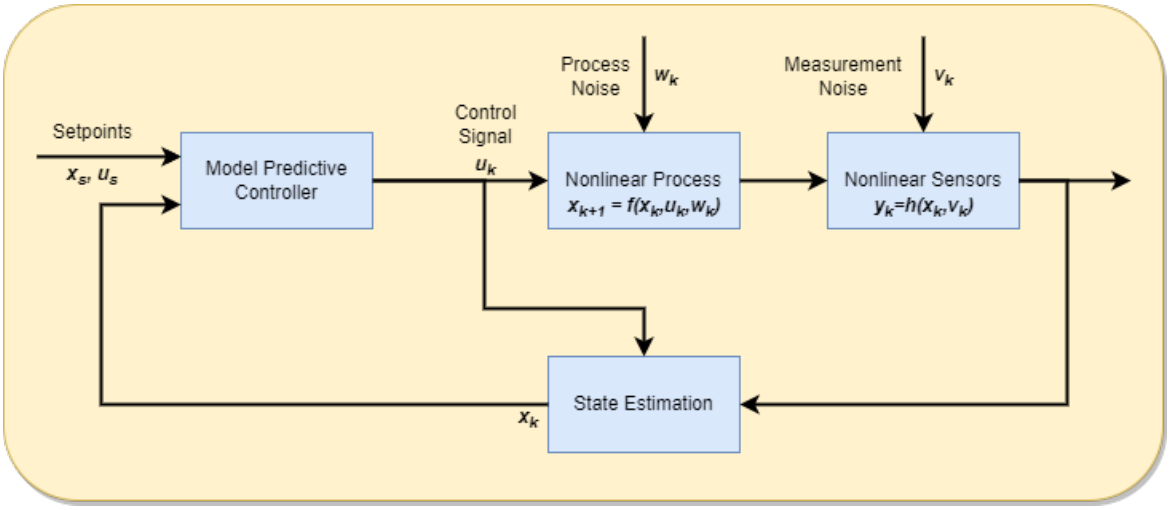

Fig. 4.1 Non-Linear MPC Block Diagram

MPC usually solves an optimisation problem online by minimising the cost function depending on the state and plant input. This step is repetitive and happens at every update time of the control system. A plant's current state is used as the initial state, and the optimisation is performed based on the predicted state of the system, which is based on the system mode. A control input sequence is a solution to the optimal control problem. Hence, an input subset of this sequence is applied to the plant. The process is then repeated at constant time intervals.

A nonlinear nominal discrete-time control system can be generally expressed as follows:

$$x_{t+1} = f(x_t, u_t) \tag{4.1}$$

where $x_t \in R^n$ and $u_t \in R^m$ are the dimensional state and dimensional control vector, respectively. The function f is assumed to be continuous. System (4.1) is subject to constraint, particularly $x(t) \in X, u(t) \in U, \forall t \in \mathbb{Z}^+$.

Let $H \in \mathbb{Z}^+$ be the prediction horizon. Then, the problem of steering the system to the origin as a finite-time optimal control problem with the cost function $C : \mathbb{R}^n \times \mathbb{R}^{H\times m} \to \mathbb{R}^+$ as

$$J(x(t), U(t)) = \sum_{k=t}^{t+H-1} l(x(k), u(k)), \tag{4.2}$$

where $U_t = [u_t, ..., u_{t+N-1}]$ is the sequence of N future input to be optimised, and $x_k, \forall k \in [t, ..., t+N]$ is the resulting state trajectory. Ultimately, $l : \mathbb{R}^n \times \mathbb{R}^m \to \mathbb{R}^+ \in C^1$ is the stage gain. From the previous definition in 4.2, at each sampling time, the optimisation problem can be solved as,

$$\begin{aligned}
\underset{U(k)}{min} \quad & J(x(k), U(k)) \\
s.t. \quad & x(k+1) = f(x(k), u(k)) \quad k = t, ..., t+H-1 \\
& u(k) \in U \quad k = t, ..., t+H-1 \\
& x(k) \in X \quad k = t, ..., t+H-1 \\
& x(k) = x(t)
\end{aligned}$$

Then, apply $u(k)$ to the system and repeat the optimisation with new measured states. Summarising, a standard MPC scheme works as follows:

1. obtain measurements/estimates of the states of the system

2. calculate an optimal input minimising the desired cost function over the prediction horizon using the system model for prediction

3. implement the first part of the optimal input until the next recalculation instant

4. continue with 2.

4.3 Controller

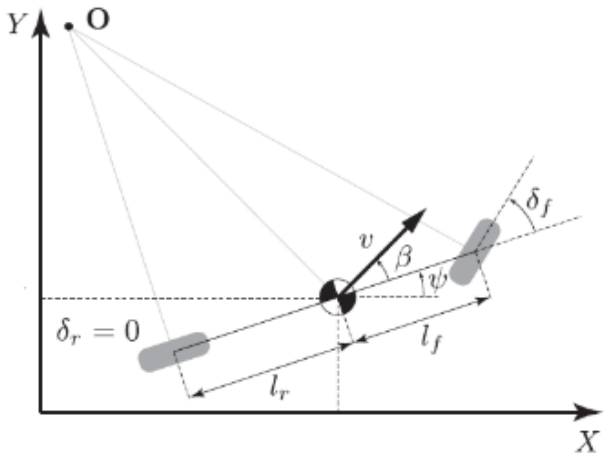

Fig. 4.2 Bicycle Model

The kinematic model of the bicycle model vehicle, as shown in Fig. 4.2 includes x and y positions, orientation angle, velocity, cross-track error, and ψ error. They are given by,

$$x_{t+1} = x_t + v_t cos(\psi_t) dt \tag{4.3}$$

$$y_{t+1} = y_t + v_t sin(\psi_t) dt \tag{4.4}$$

$$\psi_{t+1} = \psi_t + \frac{v_t}{L_f} \delta_t dt \tag{4.5}$$

$$v_{t+1} = v_t + a_t dt \tag{4.6}$$

$$cte_{t+1} = f(x_t) - y_t + v_t sin(e\psi_t) dt \tag{4.7}$$

$$e\psi_{t+1} = \psi_t - \psi des_t + \frac{v_t}{L_f} \delta_t dt \tag{4.8}$$

Here, x, y, and ψ are the position and orientation of the mobile robot, v is the velocity, cte is a cross-track error (the difference between the trajectory defined by the waypoints and the current mobile robot position y in the coordinate space of the mobile robot), and the $e\psi$ is an orientation error.

The constraints are the steering angle and throttle, which are bounded by the following limits,

$$\delta \in [-25^\circ, 25^\circ] \tag{4.9}$$

$$a \in [-1, 1] \tag{4.10}$$

The cost function is the summation of the squares of the cross-track error, orientation error, difference between current and reference velocity, actuation, the difference between sequential actuation, and the difference between acceleration.

$$cost = \sum_{t=1}^{N} (cte_t - cte_{ref})^2 + (e\psi_t - e\psi_{ref})^2 + (v_t - v_{ref})^2 + \delta_t^2 + (\delta_t - \delta_{t-1})^2 + (a_t - a_{t-1})^2 \tag{4.11}$$

An IPOPT (Interior Point OPTimiser) software is used for nonlinear optimisation. It is designed to find a local solution of mathematical optimisation problems.

4.4 Simulation

A Stage simulator is employed for simulating multiple AGVs. This simulator provides a virtual world populated by mobile robots and sensors. Its graphical interface is designed using OpenGL, which provides the advantage of graphics processor (GPU) hardware, being fast and easy to use. The Stage is realistic for many purposes, yielding a helpful balance between fidelity and abstraction [157].

4.4.1 Single Robot Simulation

After deriving the kinematic model and cost function, a simulation study on one robot is carried out using a Stage simulator. The Stage simulator provides several sensors and actuator models. It is designed to handle multi-robot systems by providing simple and computationally cheap models. Fig. 4.3 shows the RQT graph for one robot simulation consisting of five nodes: MPC node, move base node, stage ROS node, AMCL node, and map server node. Here, the MPC node issues linear and angular velocity commands to the Stage simulator for the mobile robot. The move base node provides navigation goals in the simulation world. The stage ROS node is the simulation environment itself. An AMCL node keeps track of the pose of the robot. Finally, a map server node offers map data.

Fig. 4.4 shows a robot's multiple coordinate frames that maintain the relationship between coordinate frames in a tree structure buffered in time. A tf library handles this. The tf library was designed to provide a standard way to keep track of coordinate frames and transform data within an entire system such that individual component users can be confident that the data

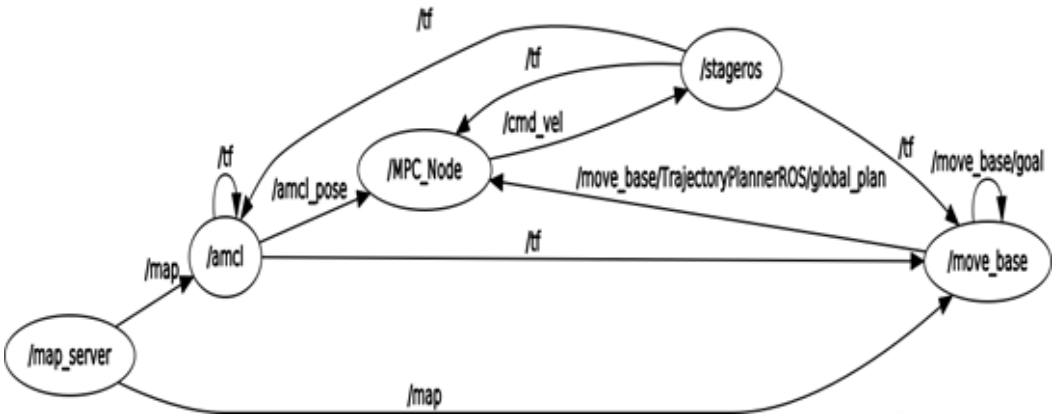

Fig. 4.3 RQT Graph for One Robot

is in the coordinate frame that they want without requiring knowledge of all the coordinate frames in the system [47].

After checking the correctness of the RQT graph and transform frames (Tf), a simulation is carried out in the Stage environment. Fig. 4.5 and Fig. 4.6 show the simulation of single robot navigation. Fig. 4.5 represents the RVIZ window of a single robot simulation. The red line shows the trajectory of the mobile robot. A similar simulation is shown in fig. 4.6, the Stage simulator. In this picture, a mobile robot can be seen. The Stage provides a graphical view of the simulation, whereas RVIZ provides detailed information on robot operations, such as trajectory in this case.

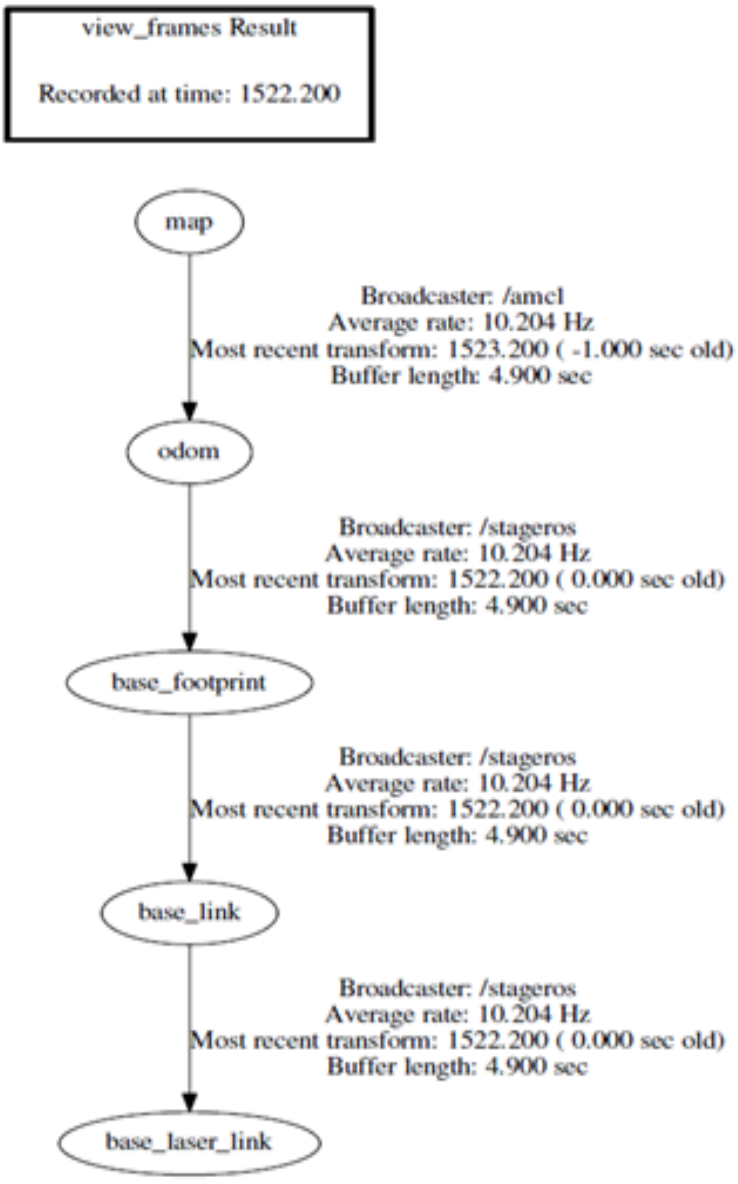

Fig. 4.4 Tf frame for one robot

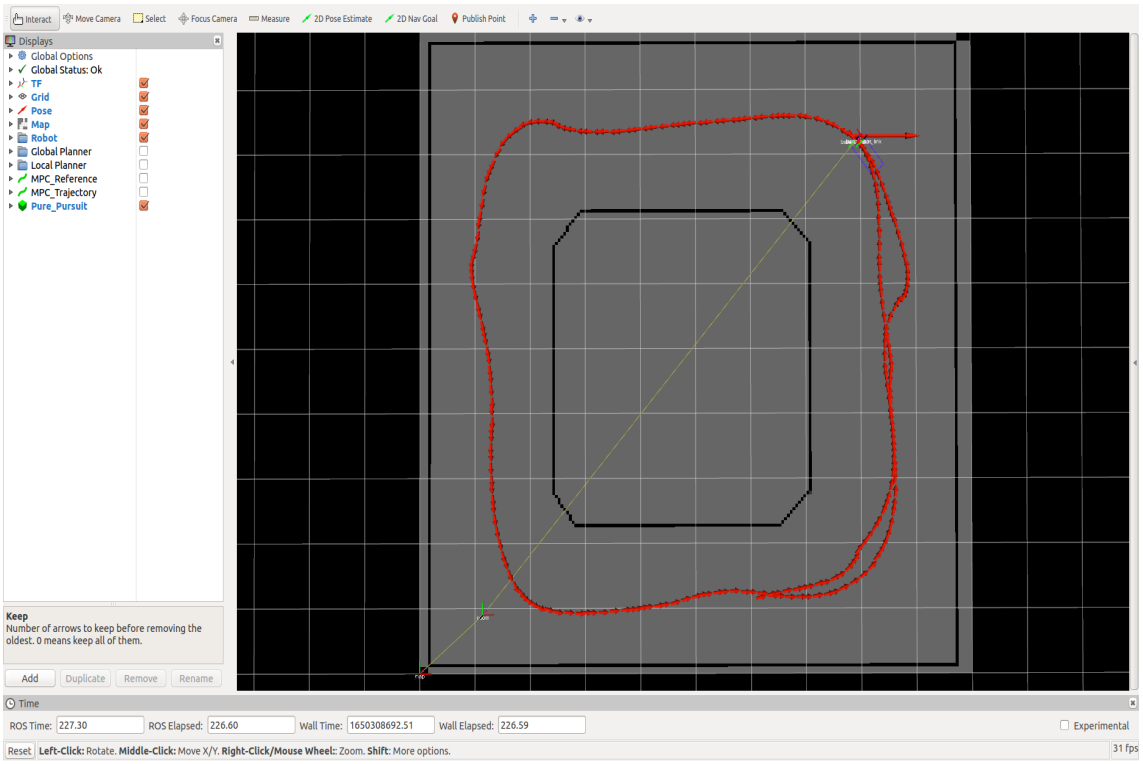

Fig. 4.5 Simulation of Single AGV - RVIZ

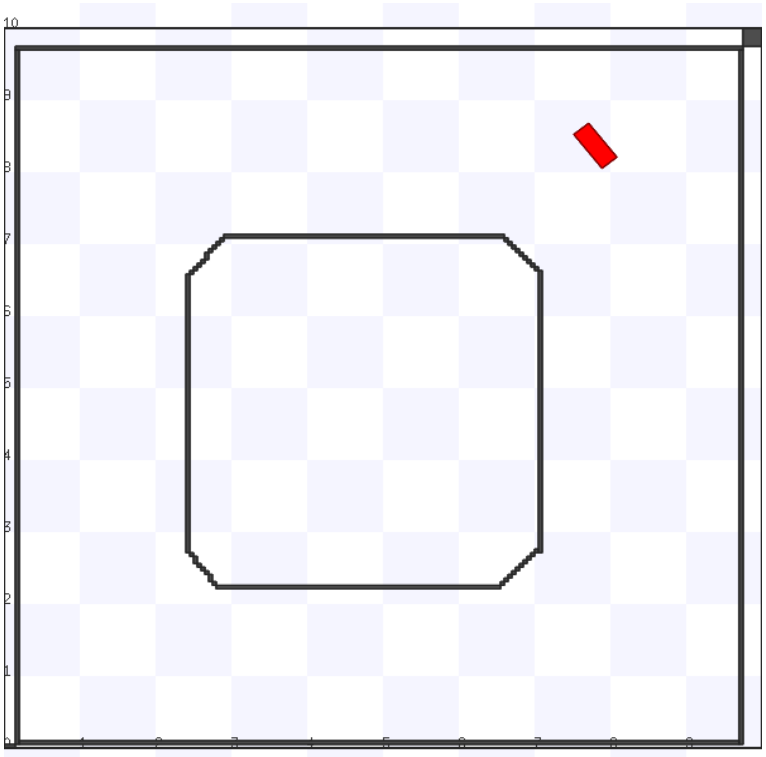

Fig. 4.6 Simulation of Single AGV - Stage

4.4.2 Multi-Robot Simulation

A simulation study on two robots is carried out using a Stage simulator. Fig. 4.7 shows the RQT graph for two robot simulations. Here, the map server node and stage ROS node remains the same as both robots are in the same environment and share the same map. All other nodes are created twice for robots, such as two MPC nodes are created for individual robots. MPC node issues linear and angular velocity commands to Stage simulator for a mobile robot. A move base and AMCL node are created for both robots.

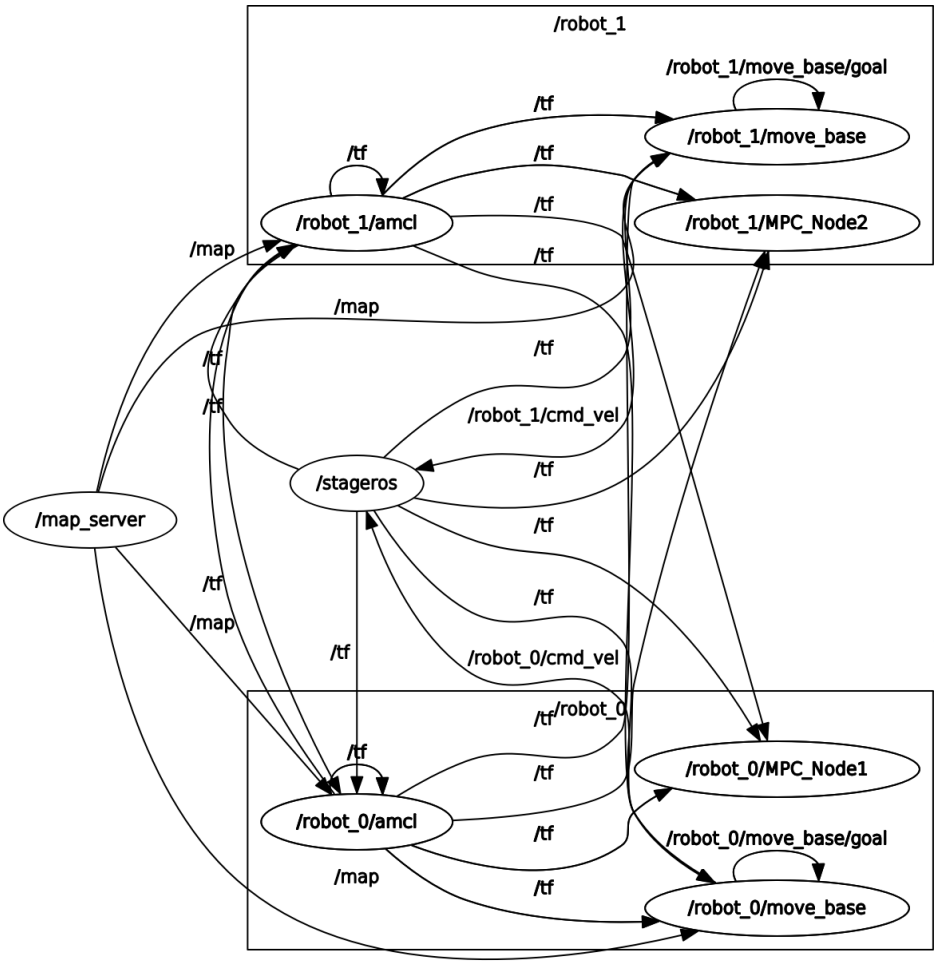

Fig. 4.7 RQT Graph for Two Robots

Fig. 4.8 shows the multiple coordinate frames of two robots which maintain the relationship between coordinate frames in a tree structure. Here, it can be seen that both robots share the same map as they are being simulated in the same environment.

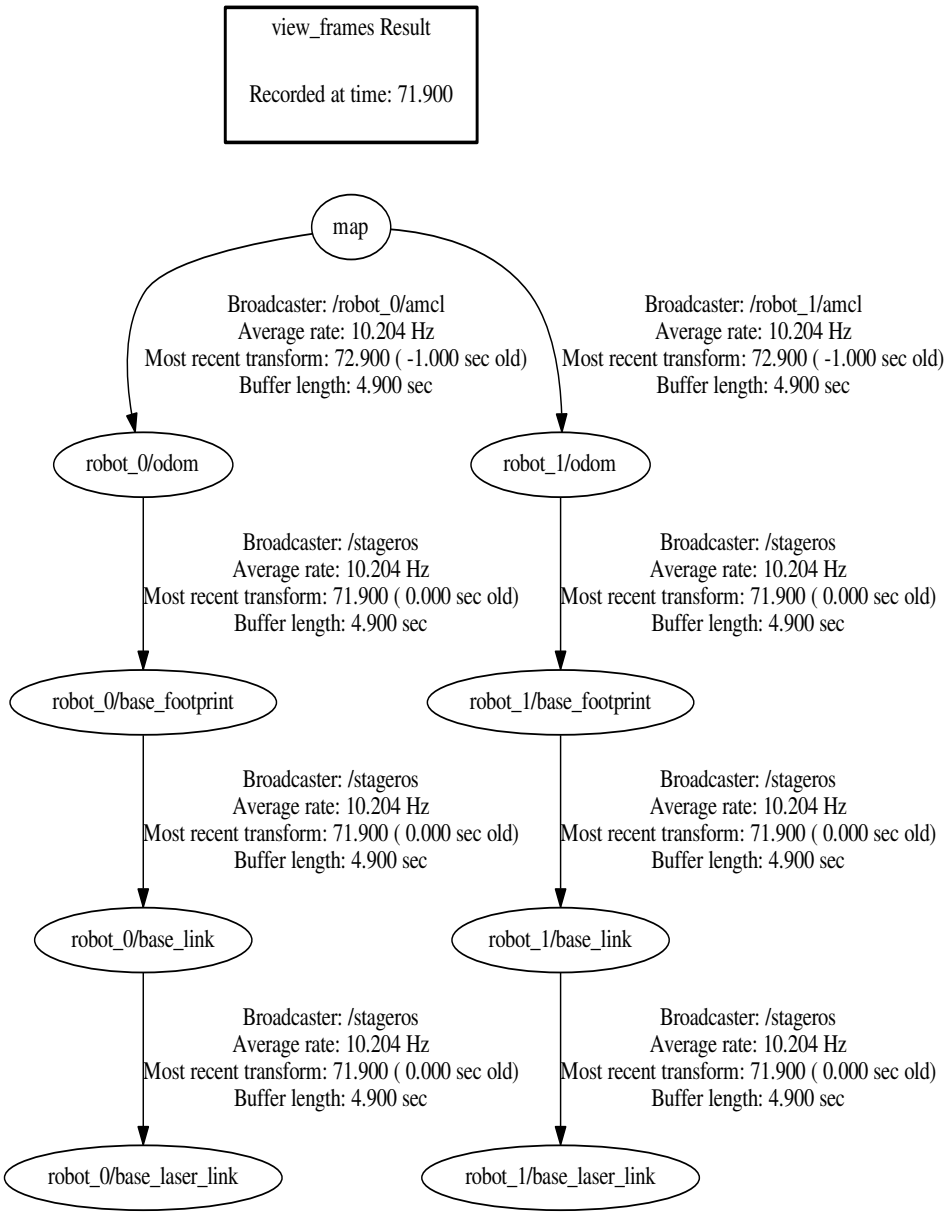

Fig. 4.8 Tf Frame for Two Robots

After checking the correctness of the RQT graph and transform frames (Tf), a simulation was carried out for two robots in a Stage environment. Fig. 4.9 and Fig. 4.10 show the simulation of multi-robot navigation. Fig. 4.10 represents the RVIZ window of multi-robot simulation. The red line shows the trajectory of the one mobile robot while the blue line for the other robot. A similar simulation is shown in Fig. 4.9, a Stage simulator with two mobile robots.

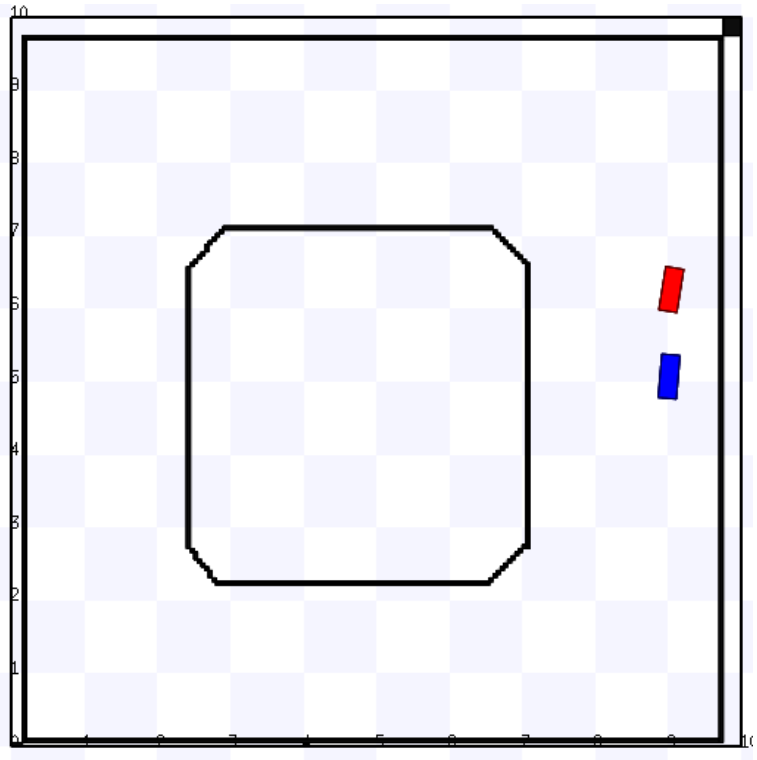

Fig. 4.9 Simulation of Two AGVs - Stage

Like the previous approach, five robots were deployed inside the simulation world, and their trajectory was captured as shown in Fig. 4.11 and Fig. 4.12. However, for this simulation, the RQT graph and Tf frames of five AGVs are not generated as they result in a large image that cannot be displayed here.

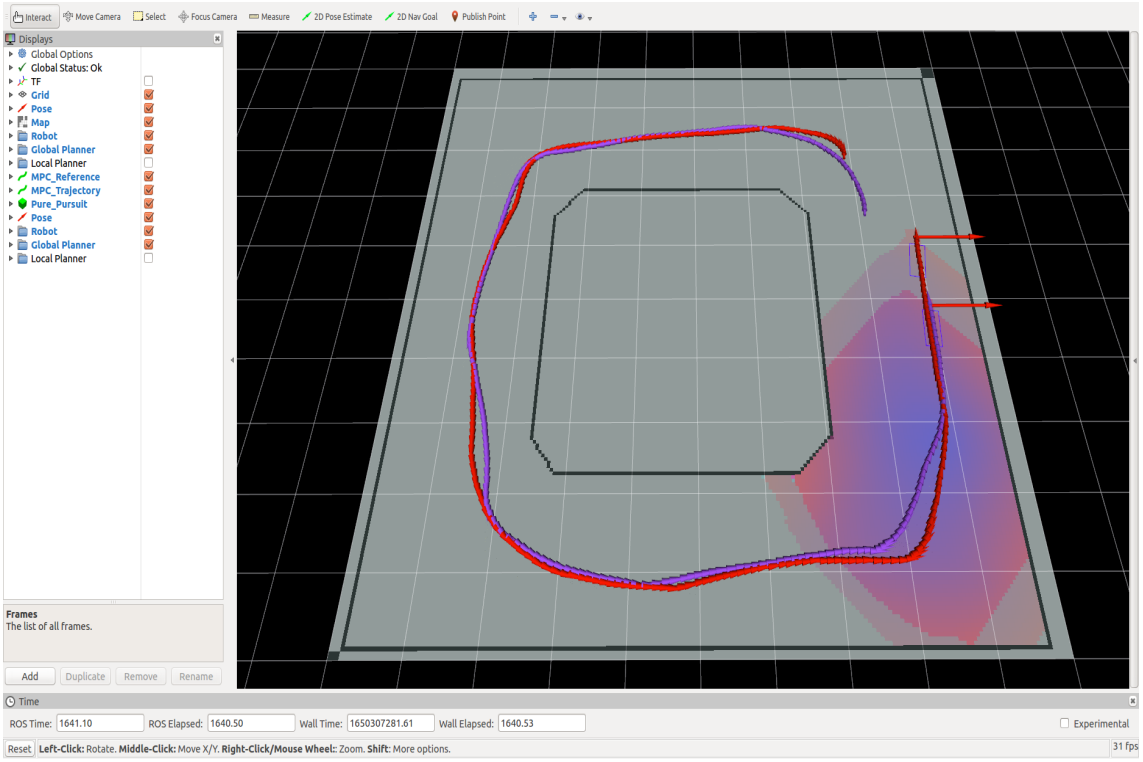

Fig. 4.10 Simulation of Two AGVs - RVIZ

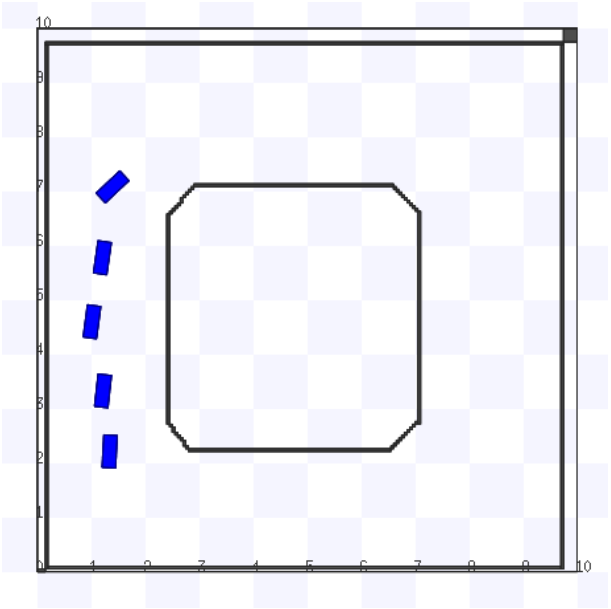

Fig. 4.11 Simulation of Five AGVs - Stage

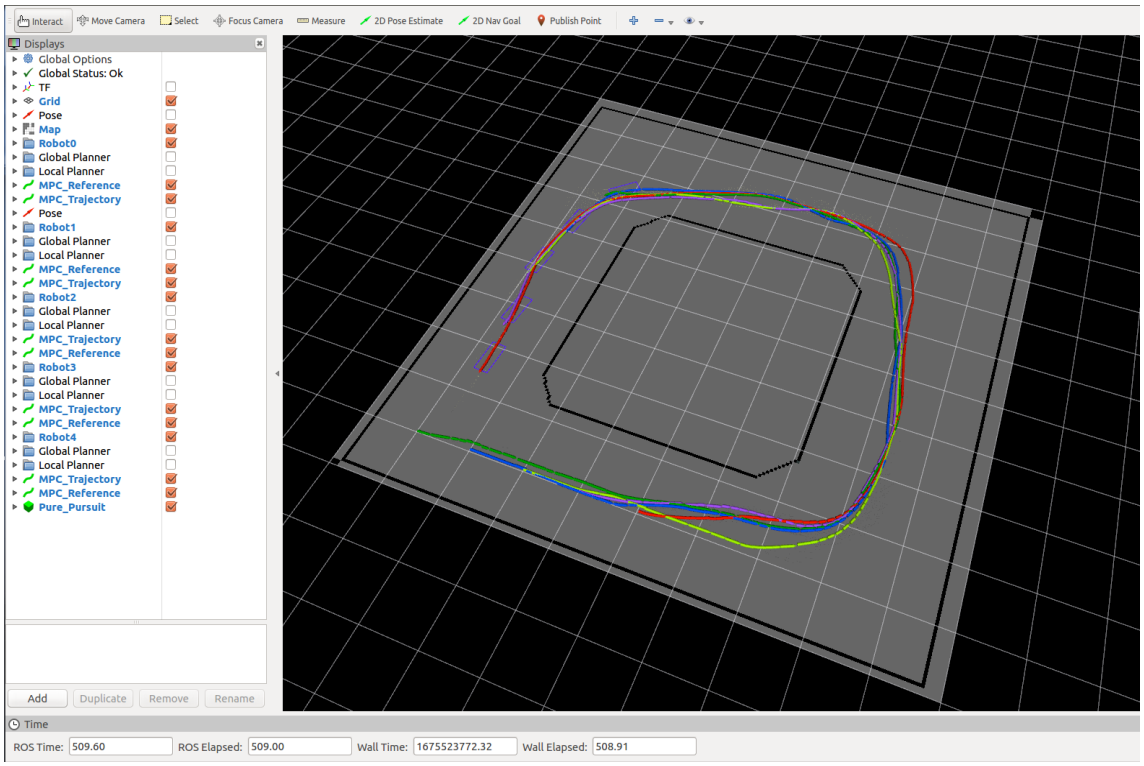

Fig. 4.12 Simulation of Five AGVs - RVIZ

4.5 Summary

A single-robot and multi-robot navigation strategy is presented using nonlinear MPC and simulated under a Stage environment. The controller provides good results as robots can move around the environment and reach the goal destination. Furthermore, the application of AGVs in a warehouse environment can benefit humans as these robots perform task-oriented jobs alongside them.

The purpose of the Stage simulator is to provide simple, computationally cheap models for a given simulation scenario. However, the Stage simulator cannot emulate any device with great fidelity. The simulated objects should have friction, mass, and various attributes to achieve high realism in simulations. Furthermore, a simulator should allow the assembling multiple shapes and different joints to make a simulated robot. Moreover, the end user should

be able to build and simulate diverse robotic platforms. A Stage cannot offer this advantage. Therefore, a 3D simulator is employed in the next chapter.

Chapter 5

Simulating On-road Multi-robot Vehicle System

This chapter discusses development work on a multi-robot simulator. Section 5.1 introduces this chapter and explains the need for developing such a tool. Section 5.2 guides through the overall package description and shows the simulation of multiple robots. Section 5.3 provides information on the leader-follower algorithm, and its implementation is discussed in Section 5.4. Finally, Section 5.5 presents a summary of this chapter.

5.1 Introduction

This chapter describes a simulation of a multi-AGV navigation scenario on a single-lane public road. A 3D robot model and simulation world are created to achieve this result. At first, several robots are simulated navigating autonomously using laser sensors perception. In the second scenario, a simulation of a self-organising platoon consisting of five AGVs is considered in which laser sensors are used to navigate AGVs and maintain platoon formation. Since AGVs are simulated using a laser sensor, the time of the day would not affect the performance of measuring distance. Moreover, a laser sensor measures the time at which

light is emitted to the surface of the objects and reflected back to it to determine distance. Therefore, laser sensors have higher accuracy, wide range, and greater transmission speed for efficient measurement.

Several packages [58, 158, 27, 60] were considered before finalising ROS and Gazebo platform. ROS is an open-source system well adopted by the research community, whereas Gazebo is also an open-source simulator and can accurately and efficiently simulate populations of robots in complex indoor and outdoor environments. The developed simulator can emulate reality and provide a cost-effective and less time-consuming development process than real robots' testing. Several theoretical and real-world robot experiments are performed for the leader-follower formation problem, and several simulators are developed for multi-robot applications. Several papers have addressed multi-robot navigation problem through physical and numerical simulation, whereas few studies targets formation control problem using only sensors and physical simulation, as discussed in the literature. The significance of this work is the combination of the above-discussed works.

5.2 Package Description

The architecture of the multi-robot simulator includes three parts: a gazebo version-7 simulator, application-specific robot controllers, and ROS kinetic middleware. This architecture is flexible, meaning that a user can develop or edit the existing world, different algorithms can be analysed, and new robots can be developed and deployed. Fig. 5.1 shows the system overview.

5.2.1 ROS

Several robotics frameworks have been developed, but ROS has proved reliable and popular among research communities and has become the standard for robotics research and develop-

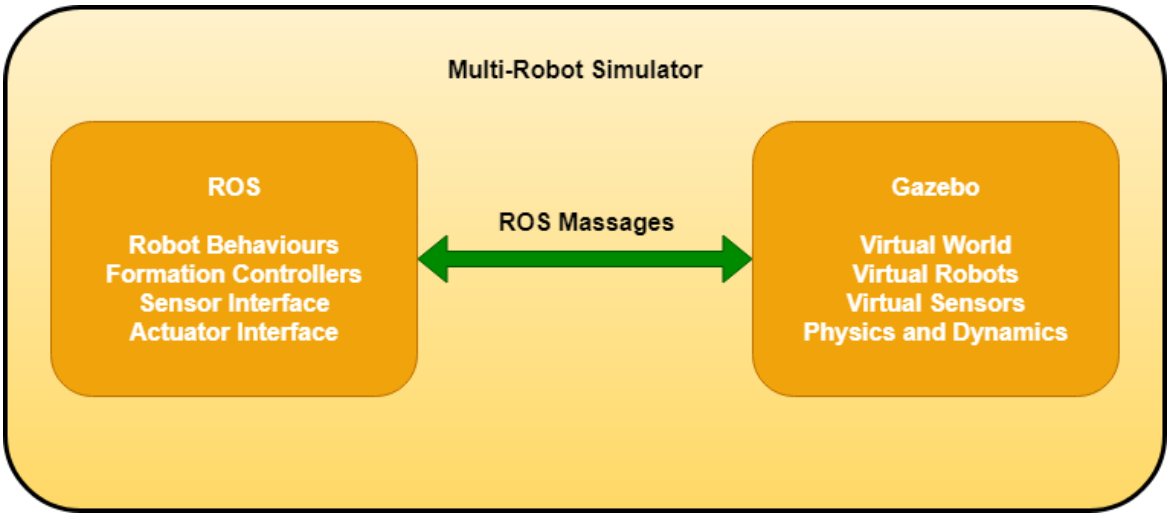

Fig. 5.1 Multi-robot Simulator Architecture

ment. ROS's primary goal is to support code reuse in robotics research. However, it should be noted that ROS is not a real-time framework but can be integrated with real-time code.

The primary services provided by ROS are hardware abstraction, low-level device control, implementation of commonly used functionalities, message-passing between processes, and package management. It also provides tools and libraries for obtaining, building, writing, and running code across multiple computers. Furthermore, ROS offers modularity that uncouples the control software from the robot body's drivers, allowing the use of precisely the same control software in simulations and actual robot experiments. The goal of the ROS framework can be described as:

- Sharing: Ability to share processes by grouping them into packages and stacks
- Collaboration: ROS supports a federated system of code repositories that enable collaboration to be distributed
- Thin: Code written for ROS can be used with other robot software frameworks
- ROS-agnostic libraries: The preferred development model is to write libraries with clean functional interfaces

- Language independence: Ability to use Python, C++, Java, Matlab and LISP programming languages
- Easy testing: Built-in test framework called rostest makes it easy to bring up and tear down test fixtures
- Scaling: Ability to handle large run-time systems and large development processes

ROS is a platform for developing and running robotic applications and consists of some core components: ROS Master, node, service, topic, and message. The ROS Master manages all the nodes and provides naming and registration services to the rest of the nodes in the ROS system. The Master coordinates the communication of all the nodes and tracks publishers and subscribers to topics and services. All the nodes talks and swap messages peer-to-peer after locating each other through the Master. The Master also provides the Parameter Server that allows data to be stored and retrieved during run time.

The node is a process that performs the computation of messages. Nodes are combined into a graph and usually communicate with one another using streaming topics and the parameter server. A node can be regarded as a single module of the ROS system, and each node can represent a device or processing component of the robot system. For example, one node controls a laser range finder, and one node controls the robot's wheel motors, one node performs localisation, one node performs path planning, one node provides a graphical view of the system, and so on.

Messages are the data transferred between nodes in the form of topics. A message can be any data structure, including standard primitive types like integer, floating point, Boolean, string, and array. In addition, messages can include arbitrarily nested structures and arrays like C structs.

A topic is a type of bus over which different nodes exchange messages via a transport system with publish/subscribe semantics. This information is organised as a data structure

and can have different data types. Topics can be identified by their name and their type. In addition, each topic has a name used to identify where the messages are subscribed to and published. Topics are intended for unidirectional streaming communication.

The publish/subscribe model feature is a very convenient communication, but it is also many-to-many and one-way transport which does not work for the request/reply interactions of a distributed system. The solution of the ROS is to create services defined by a name and a pair of message structures: one for the request and one for the reply. Although ROS services are only for computations and quick actions, they offer an excellent complement to topics. Topics are used for unidirectional data streams, and services are used for a client/server architecture.

5.2.2 Gazebo

A gazebo is an open-source 3D dynamic simulator with the ability to accurately and efficiently simulate populations of robots in complex indoor and outdoor environments while offering a higher degree of fidelity, a suite of sensors, and interfaces for both users and programs. This effective, scalable, and simple tool can test robotics algorithms, design robots, and perform regression testing with realistic scenarios.

Gazebo supports four physics engines, ODE, Bullet, Simbody, and DART, making Gazebo capable of rigid-body dynamics simulation. Out of these four physics engines, one engine must be defined within the world model description. Moreover, Gazebo offers a rich library of models such as robots, sensors, actuators, and arbitrary objects. Gazebo maintains a simple API and the necessary hooks for interaction with client programs for these models. The third-party libraries that handle the physics simulation and visualisation are a layer below this API.

A complete environment is a collection of models and sensors. The ground and buildings represent stationary models, while robots and other objects are dynamic. Sensors remain

separate from the dynamic simulation since they only collect or emit data if it is an active sensor. Gazebo contains following essential components:

- Models: Any object that maintains physical representation is a model and can be anything from simple geometry to a complex robot.
- Bodies: Bodies are the basic building block of the model. Their physical representation is derived from many geometric shapes, such as boxes, spheres, cylinders, planes, and lines.
- Joints: Joints provide the mechanism to connect bodies together to form kinematic and dynamic relationships.
- Interfaces: Program can access and control models via an interface. Commands sent over an interface can instruct a model to move joints, change the configuration of associated sensors, or request sensor data.
- Sensors: A sensor in Gazebo is an abstract device without any physical representation. It is only activated when incorporated into a model.

5.2.3 Robot Development

A robot model is developed for simulation using the Unified Robot Description Format (URDF), an XML format for representing a robot model. Here, XML format describes the robot's joints, visualisation, appearance, and various controllers' integration and parameters. Fig. 5.2 shows the developed robot in RVIZ (ROS Visualisation) software. This URDF file is then converted into the XACRO (XML Macros) format. The benefit of using XACRO is that it produces a more readable and shorter version of XML files. Furthermore, RVIZ is a 3D visualiser for displaying sensor data and state information from ROS. RVIZ also provides a chance to visualise the robot's joints, how they move/rotate, and their connections.

This robot has a differential steering locomotion system meaning that the robot's movement changes by varying the speed of the two rear wheels individually. In addition, a caster wheel is placed in the front, which balances and supports the robot's movement. The wheels are controlled by the plugin called libgazebo_ros_diff.so, and their parameters are application dependent and need to be defined in the XACRO file. The robot design is inspired by the EMoRo Robot[1] developed by Inovatic ICT. The frames of this robot can be seen in Fig. 5.3. This frame image is modified to fit on one page.

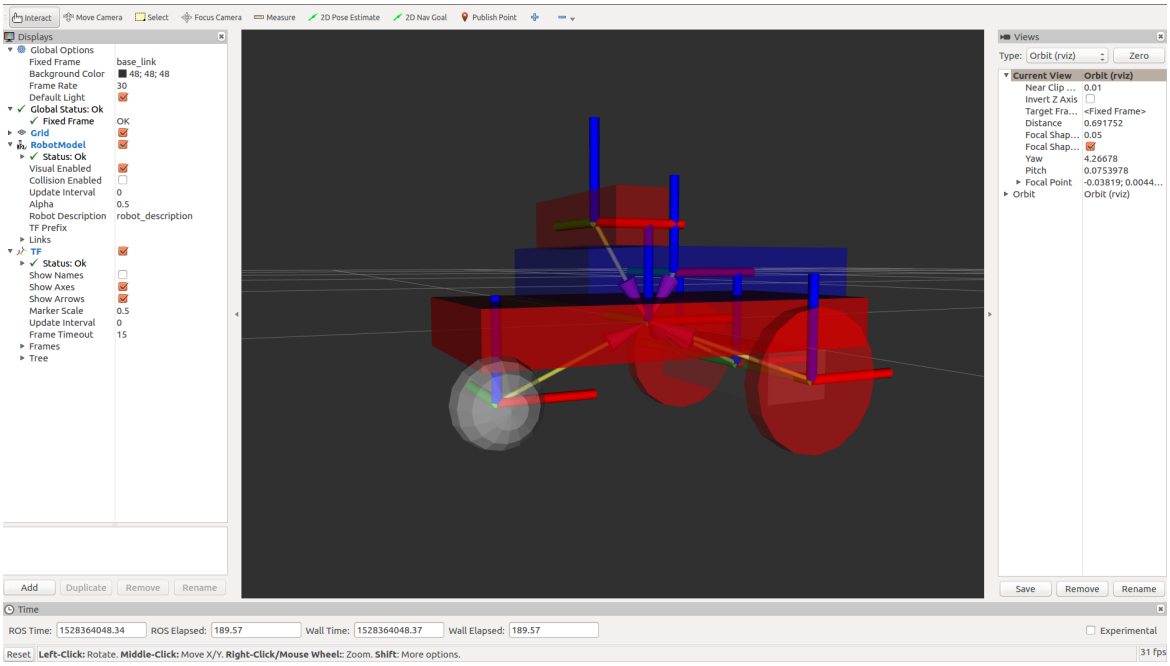

Fig. 5.2 Robot Development

5.2.4 Laser Sensor

A laser sensor plugin used in this experiment is called libgazebo_ros_laser.so and is based on the hokuyo UTM-30LX sensor. For a leader robot, the scanning range for this sensor is set between [-90°, 90°] or 720 samples, and the measurement range is set between [0.30m, 3.0m]. On the other hand, for follower robots, the scanning range is [-11.5°, 11.5°] or 720

[1] http://www.emoro.eu/

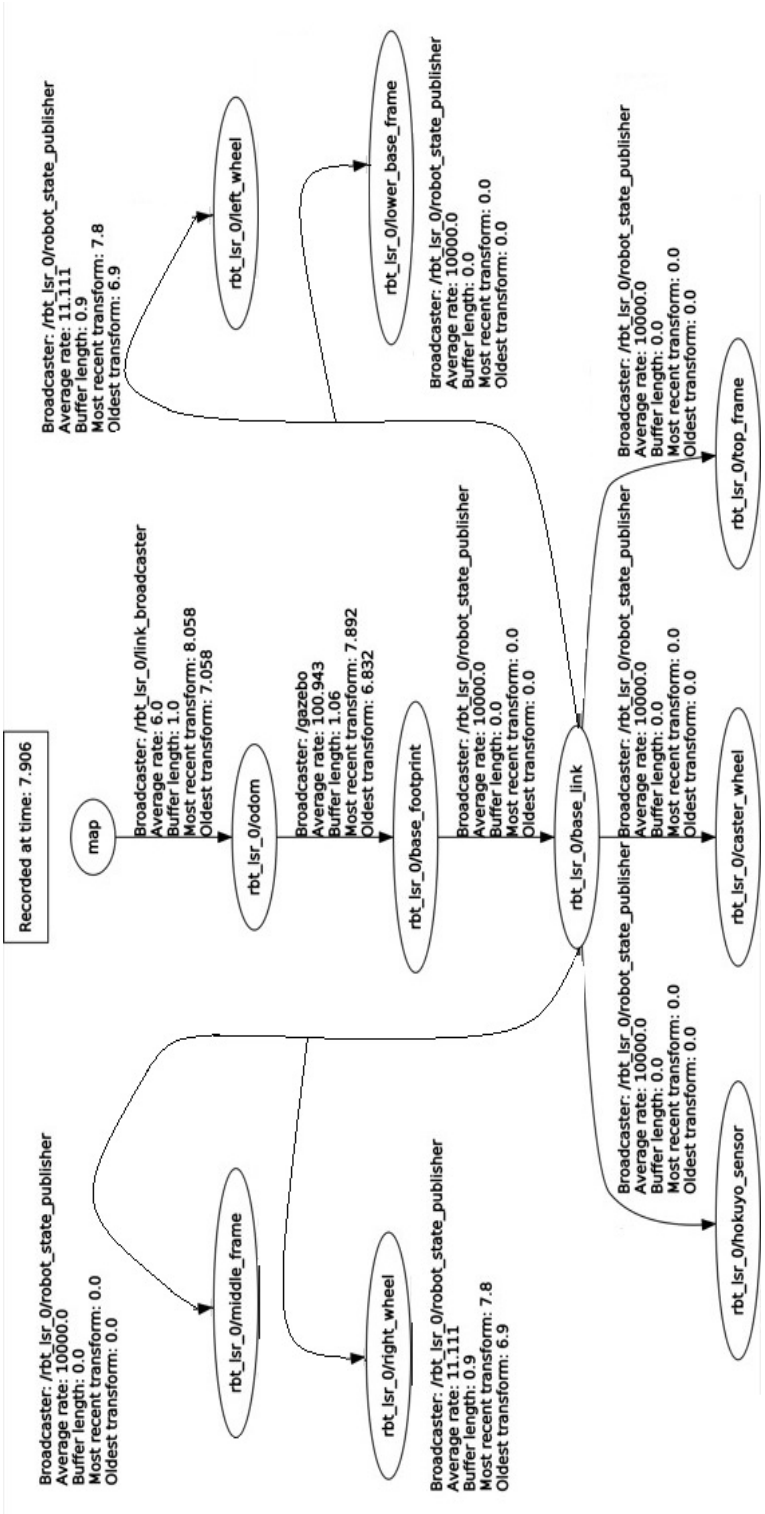

Fig. 5.3 Robot Frames

samples, and the measurement range is [0.30m, 1.0m]. The reason behind setting a lower scanning range for follower robots than the leader robot is that they only measure the range between the preceding robot and the robot itself. Furthermore, setting a lower measurement range for follower robots ensures that the distance between the leader and follower does not exceed more than one meter.

5.2.5 Differential Drive Controller

In this experiment, a differential drive controller is used to control the two rear wheels of the robot. This controller accepts the velocity command and is sent on the two wheels of a differential drive wheelbase. The controller extracts the x component of the linear velocity and the z components of angular velocity. A differential drive mobile robot's kinematics are shown in Fig. 5.4. A differential drive robot requires two parameters to move around in the simulation environment: velocity V and heading/angular velocity θ. In this figure, V_r and V_l are the velocity of the right and left wheel, respectively, L is the distance between the centre of the wheels, θ is the angular velocity of the robot, and r is the radius of the wheel.

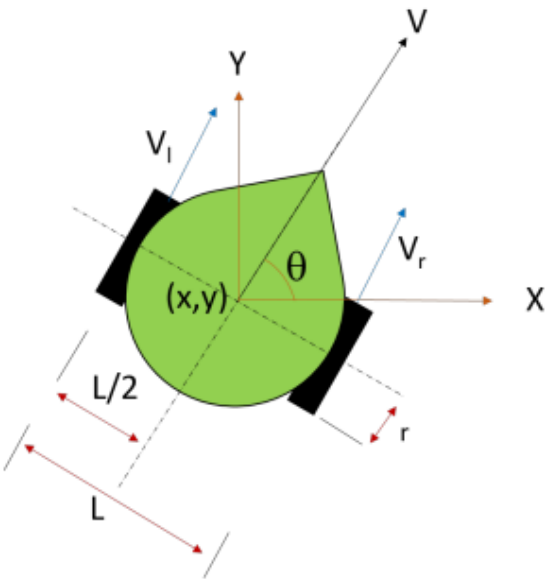

Fig. 5.4 Differential Drive Robot Kinematic

Here, the overall velocity of the robot is the average velocity of the individual wheel velocity and derived as,

$$V = \frac{V_r + V_l}{2} \tag{5.1}$$

To prove this equation further, consider the rate of change of position of mobile robot in x-direction is $x = Vcos(\theta)$, in y-direction is $y = Vsin(\theta)$, and the angular velocity of the robot is $\theta = \omega = \frac{V_r - V_l}{L}$. Now substituting the linear velocity V from equation 3.1 in position of the robot x and y gives,

$$x = \frac{V_l + V_r}{2} cos(\theta) \tag{5.2}$$

$$y = \frac{V_l + V_r}{2} sin(\theta) \tag{5.3}$$

The velocity V of the mobile robot in a fixed reference coordinate system is given by $V = \sqrt{x^2 + y^2}$. Therefore, from equation 3.2 and 3.3, V is,

$$V = \sqrt{(\frac{V_l + V_r}{2} cos(\theta)) + (\frac{V_l + V_r}{2} sin(\theta))} = \frac{V_r + V_l}{2} \tag{5.4}$$

The individual velocity of left and right wheel can be obtained by using equation 3.1 and angular velocity.

$$V_r = (V + \frac{L}{2}\omega) \tag{5.5}$$

$$V_l = (V - \frac{L}{2}\omega) \tag{5.6}$$

The V_t and V_l can be used to generate the output of x, y and θ and provide the mobile robot's actual position and orientation. For driving a mobile robot in a specific direction, the

error between desired and actual angles is given by $e = \theta_d - \theta$. This error is regulated by the PID controller such that,

$$PID(e) = K_P e(t) + K_I \int_0^t e(\tau) d\tau + K_D \dot{e}(t) \tag{5.7}$$

5.2.6 World Development

A simulation world is used to analyse the robots' movement. The world created for this study includes several features, such as double lanes, two-way traffic lanes, and intersections. Furthermore, this world is reconfigurable, depending on the test requirement. After developing the world, ten robots were deployed in the environment, as shown in Fig. 5.5. This work makes the simulation world as simple as possible using resources available through models within Gazebo. Moreover, numerous models are available in the Gazebo model library and can be added to this world, including buildings, signposts, barriers, and trees.

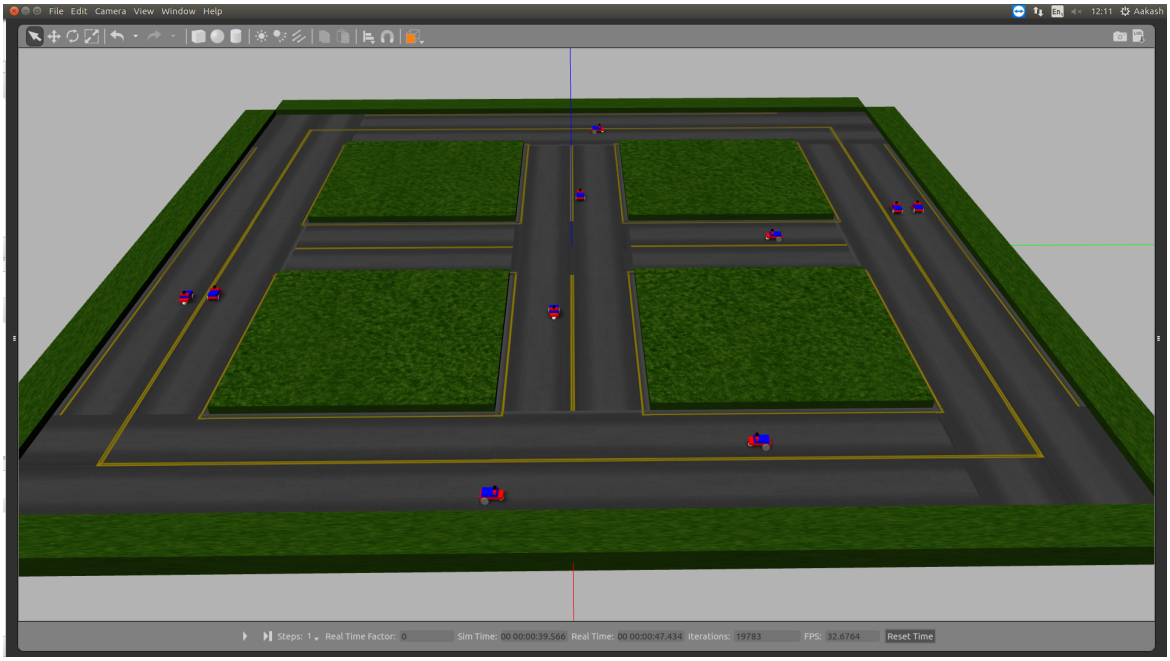

Fig. 5.5 Simulation World

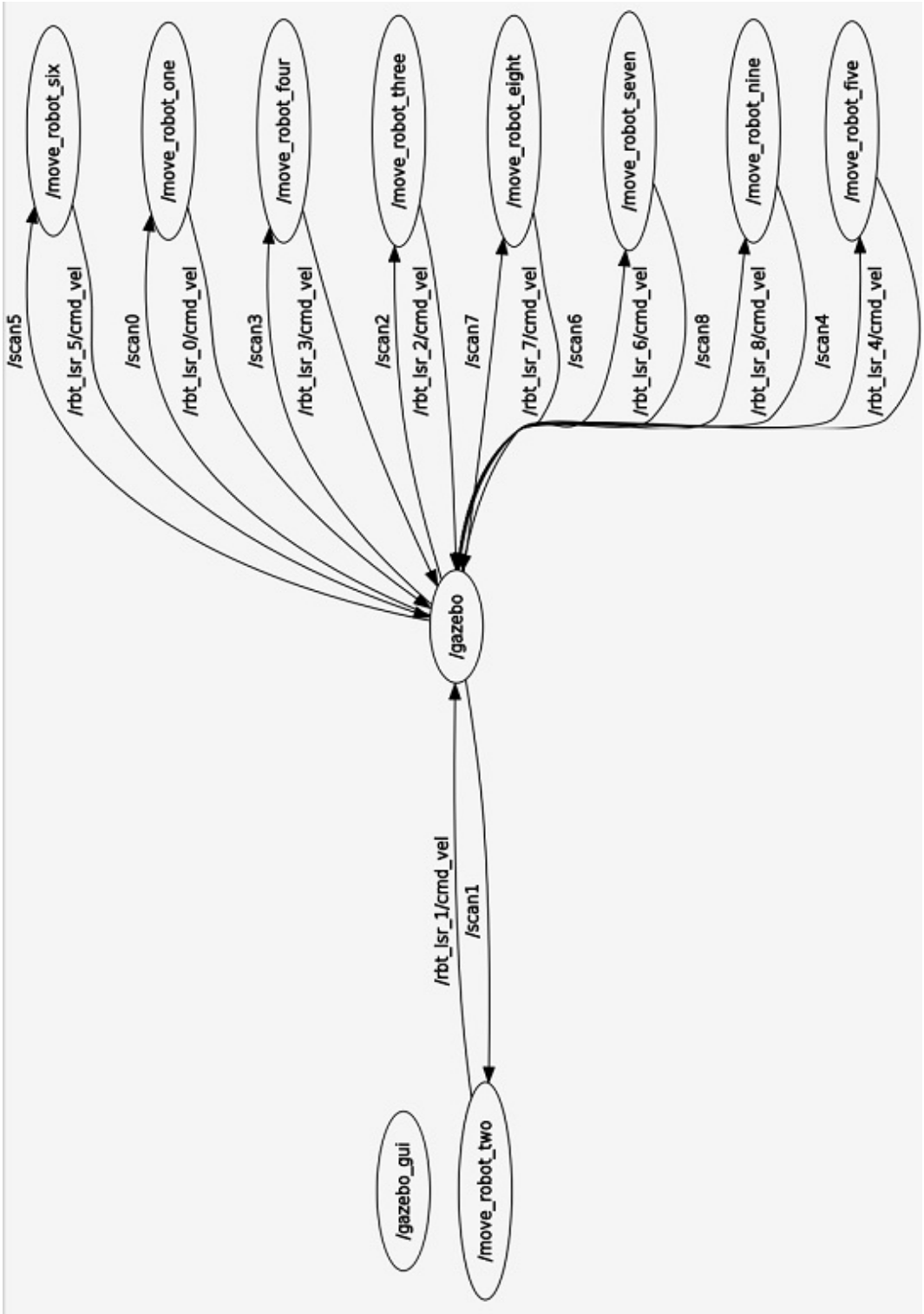

Fig. 5.6 RQT Graph of Multi-Robot Simulation

5.2.7 Multi-robot Simulation Results

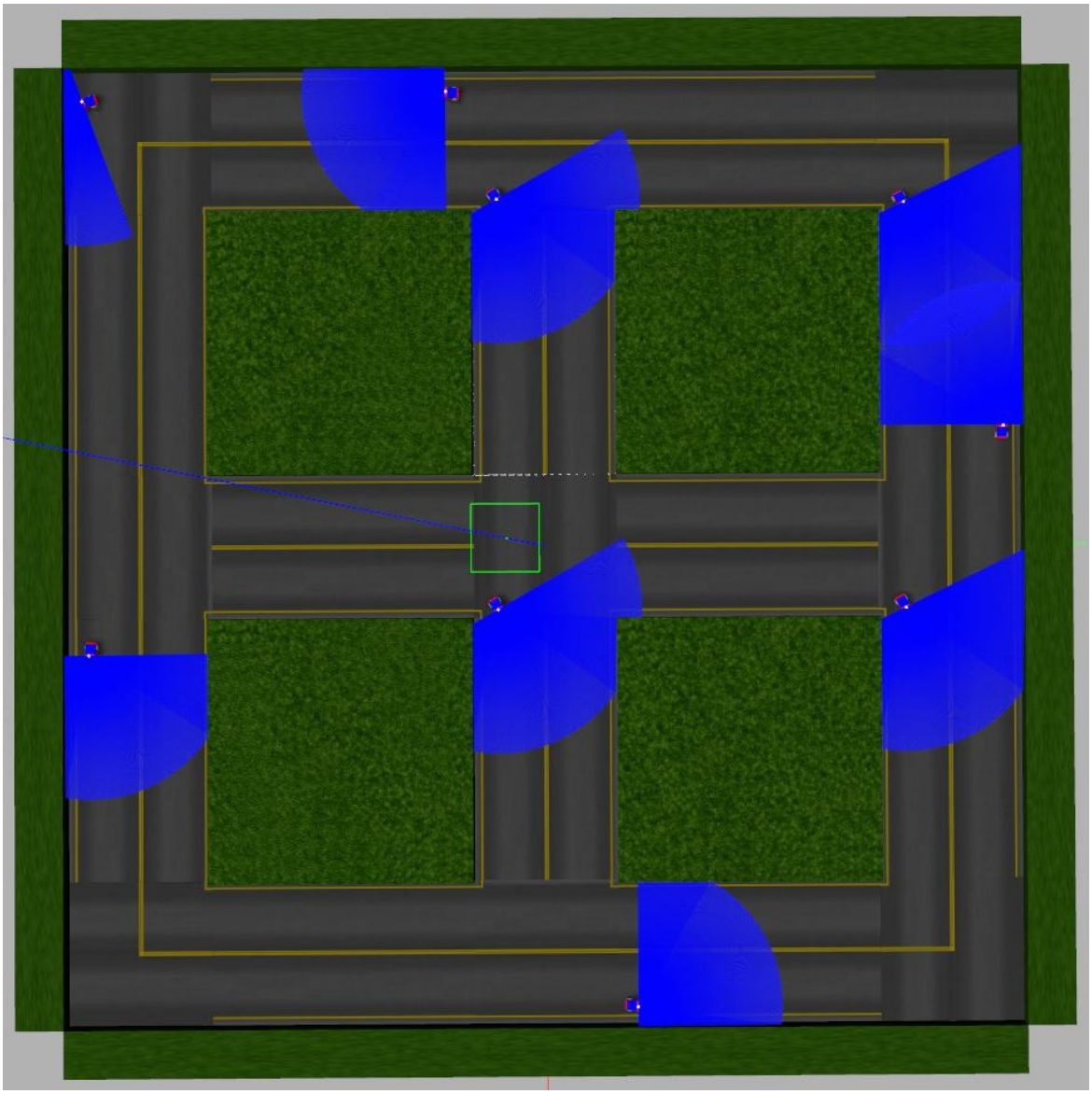

Fig. 5.7 Multi-robot Simulation

After developing simulation worlds and launching several robots, a simple controller is developed to navigate these robots using a laser sensor. Fig. 5.6 shows the RQT graph of the simulation environment. From this figure, it can be seen that all robots have their laser scan topics to perceive environmental information. The dedicated move robot node contains navigation controllers that handle linear and angular velocity. Based on the available

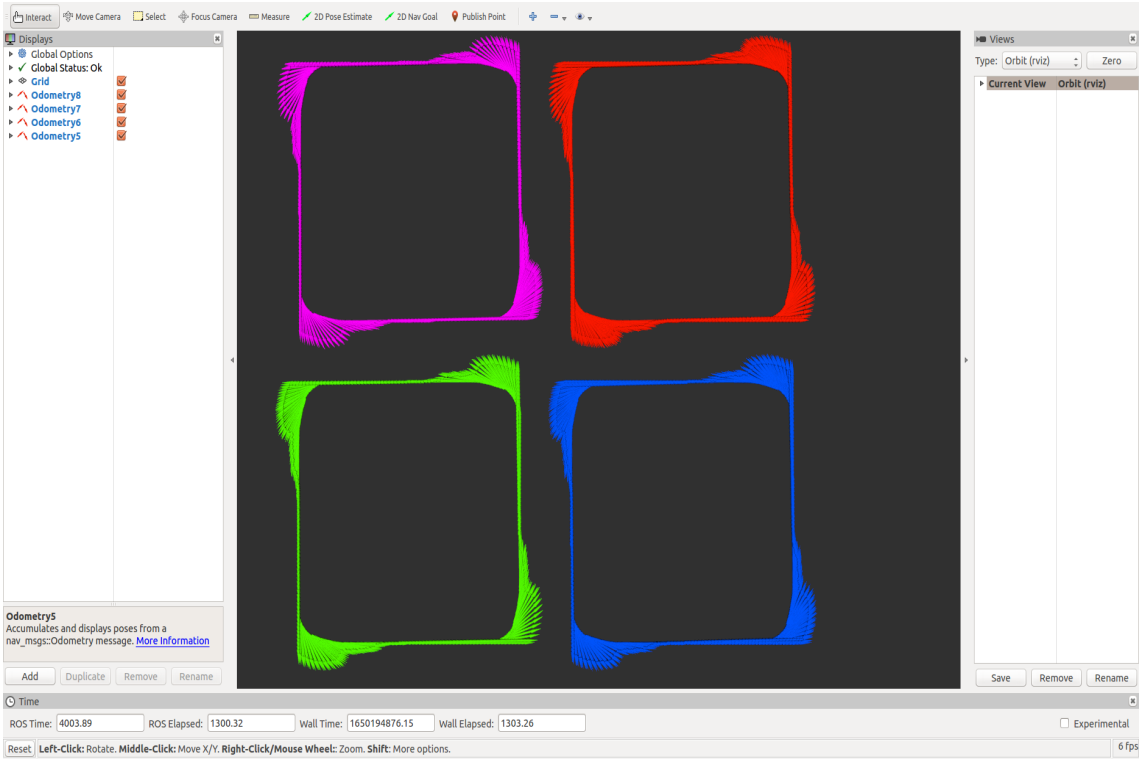

Fig. 5.8 Multi-robot Simulation Trajectory

environment information, move robot nodes issue relevant velocity via command velocity topic. Fig. 5.7 shows a scenario of multi-robot navigation using a laser sensor and proves the possibility of simulating multiple robots in a ROS-Gazebo environment. In Fig. 5.8 and Fig. 5.9, the trajectory of these robots can be seen and captured via RVIZ software. RVIZ is a ROS graphical interface that allows the visualisation of information related to simulation, using plugins for available topics such as odometry, path, and laser scan information.

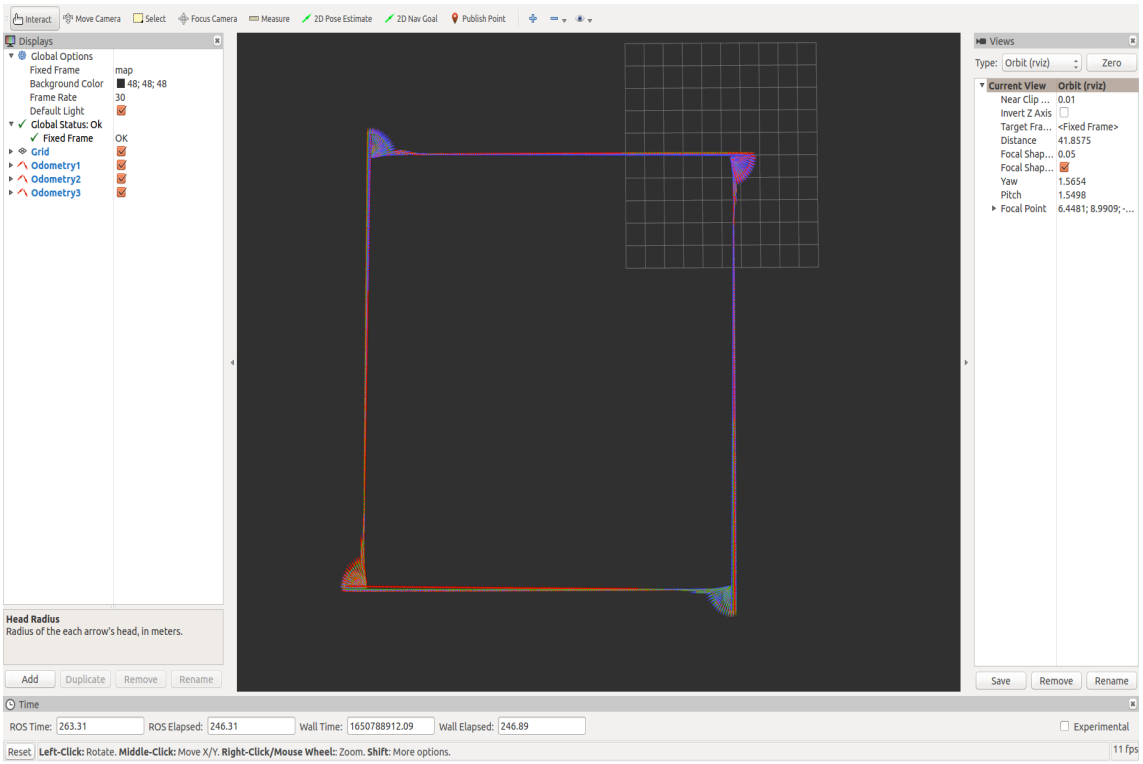

Fig. 5.9 Multi-robot Simulation Trajectory

5.3 Leader-follower Controller

After developing the simulation world and verifying its ability to simulate multiple robots, a platooning experiment was developed by employing a predecessor following topology, as shown in Fig. 2.2. It is a better choice for sensor-based platoon formation than other topologies because each robot's sensory measurement is derived by scanning the preceding robot, as discussed in this approach. Moreover, this form of topology is usually created under communication loss between vehicles. Fig. 5.10 shows a block diagram of a leader-follower controller.

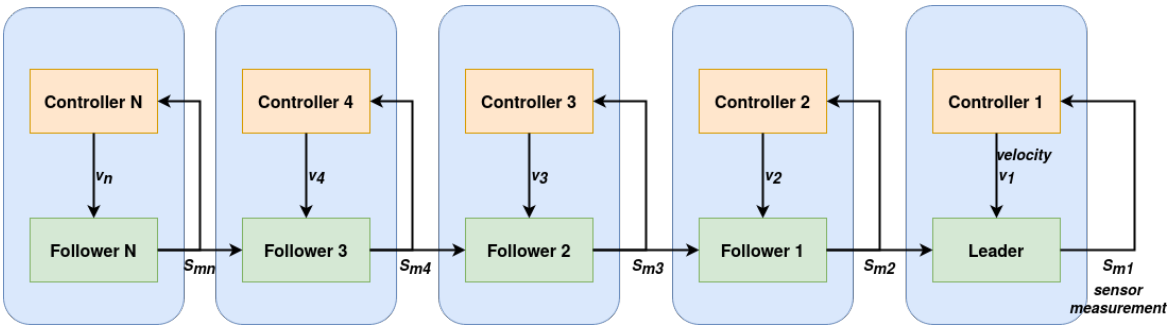

Fig. 5.10 Leader-Follower Controller Diagram

5.3.1 Car-following Theory

A car-following theory explains how one vehicle follows the vehicle in front. The space between vehicles, referred to as longitudinal spacing, is considered essential for cars' safety. This space usually occupies a vehicle's physical dimensions and the gaps between the vehicle. This space is generally measured by distance headway and distance gap. A distance headway is a distance from the front of the leader vehicle to the front of the following vehicle. Therefore, the overall longitudinal space involves the length of the leader vehicle and a gap between the leader and the following vehicle.

General Motors proposes one popular car-following theory model based on the follow-the-leader concept [49, 50]. The theory was developed for human-driven manual vehicles but

can also apply to AGVs. The primary differential-difference equation of the follow-the-leader theory is that each driver of a vehicle responds to a given stimulus according to a relation, such as

$$response = sensitivity * stimulus \tag{5.8}$$

The stimulus could be a function of the positions of a number of cars and their time derivatives, whereas the response has been taken as the vehicle's acceleration. General Motors' follow-the-leader has two assumptions; 1. the spacing between vehicles increases as the speed of the vehicle increases, and 2. the driver must maintain a safe distance to avoid a collision.

Let ΔX^t_{n+1} be the gap available for $(n+1)^{th}$ vehicle, and let ΔX_{safe} is the safe distance, V^t_{n+1} and V^t_n are the velocities, the gap required is given by,

$$\Delta x^t_{n+1} = \Delta x_{safe} + T\,\upsilon^t_{n+1} \tag{5.9}$$

where T is a sensitivity coefficient, The above equation can be written as

$$x_n - x^t_{n+1} = \Delta x_{safe} + T\,\upsilon^t_{n+1} \tag{5.10}$$

Differentiating the above equation with respect to time, we get

$$\upsilon^t_n - \upsilon^t_{n+1} = T a^t_{n+1} \tag{5.11}$$

$$a^t_{n+1} = \frac{1}{T}[\varepsilon^t_n - \varepsilon^t_{n+1}] \tag{5.12}$$

And the most general model has the form,

$$a^t_{n+1} = \left[\frac{\alpha_{l,m}(\upsilon^t_{n+1})^m}{(x^t_n - x^t_{n+1})^l}\right][\upsilon^t_n - \upsilon^t_{n+1}] \tag{5.13}$$

where l is a distance headway exponent, m is a speed exponent, and α is a sensitivity co-efficient.

5.3.2 Leader Robot

A leader robot's navigation algorithm is based on simple if-else conditions. Based on the laser sensor's reading, actuators output relative linear and angular velocity. The leader robot tries to stay in the right lane and turns left when near to obstacle or wall. The laser sensor has a sample range of 720 and is divided into five regions. The sample range between [0:143] is called the right region, [144:287] is called the front right region (fright in the algorithm), [288:431] is called the front region, [432:575] is called the front left region (fleft in the algorithm) and [576:719] is called a left region. Based on these regions, relative linear velocity and angular velocity are applied to the leader.

5.3.3 Follower Robot

The follower robots receive information about preceding robots via a laser sensor. In this algorithm, the scanning range of follower robots is set between [-11.5°, 11.5°]. Therefore they only scan robots in front of them. For this algorithm, ranges are stored for polar coordinate analysis. First, these coordinates are used to calculate the width of the preceding robot. The next step is calculating the distance between the follower and preceding robots for longitudinal control. Finally, if the distance between these robots is sufficient, linear and angular velocities are calculated and applied to follower robots.

5.4 Platoon Simulation Result

The proposed controller is implemented using Python language. As shown in Fig. 5.11, readings from laser sensors drive the robots around the simulation world. For this experiment, five

Algorithm 1: Leader Robot's Navigation

Input : Laser Data in Sample Ranges 0 to 719
Output : Motor Actuation
/ Decide a region and move, Distance/Range is in meter and velocity is in meter/second */*

Determine region in which leader robot is located
if *Front > 1 and Fleft > 1 and Fright > 0.5* **then**
    linearVel = 0.1
    angularVel = 0
end
else if *Front < 2 and Fleft < 3 and Fright > 0.5* **then**
    linearVel = 0.1
    angularVel = 0
end
else if *Front < 1 and Fleft < 1 and Fright < 1* **then**
    linearVel = 0
    angularVel = -0.1
end
else if *Front < 1 and Fleft > 1 and Fright < 1* **then**
    linearVel = 0
    angularVel = -0.1
end
else if *Fright > 0.7 and Front > 1 and Fleft > 1* **then**
    linearVel = 0
    angularVel = 0.1
end
else if *Fright < 0.5 and Front > 1 and Fleft > 1* **then**
    linearVel = 0
    angularVel = -0.1
end
else
    linearVel = 0
    angularVel = 0
end

Algorithm 2: Follower Robots' Navigation

Input : Laser Data in Sample Range 0 to 719
Output : Motor Actuation

```
/* Determine the leader's position                                    */
for i = 0 to 719 do
    if sampleRange[i+1] - sampleRange[i] > 0.5 then
        Store the index i in diff
    end
end
for i = 0 to len(diff) do
    x1Coord = laser(diff)*cos(diff)
    y1Coord = laser(diff)*sin(diff)
    x2Coord = laser(diff+1)*cos(diff+1)
    y2Coord = laser(diff+1)*sin(diff+1)
    dist = d((x1Coord, y1Coord), (x2Coord, y2Coord))
    if dist > 0.5m then
        x1 = x1Coord, x2 = x2Coord
        y1 = y1Coord, y2 = y2Coord
    end
end
xclose = (x1[i+1] + x2[i+2]) / 2
yclose = (y1[i+1] + y2[i+2]) / 2
distClose = d(xclose, yclose)
if distClose > 0.1m then
    theta = atan2(yclose/xclose)
    angvel = theta - 90
    r = distclose / (2 * sin(theta/2))
    linvel = r * theta
end
```

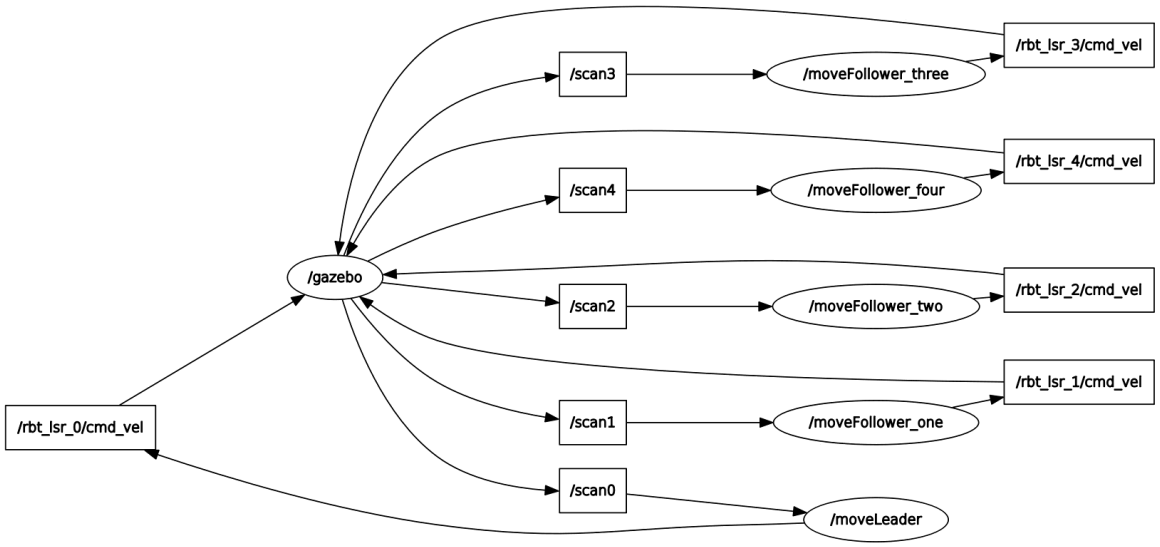

Fig. 5.11 RQT Graph of Leader-follower Navigation

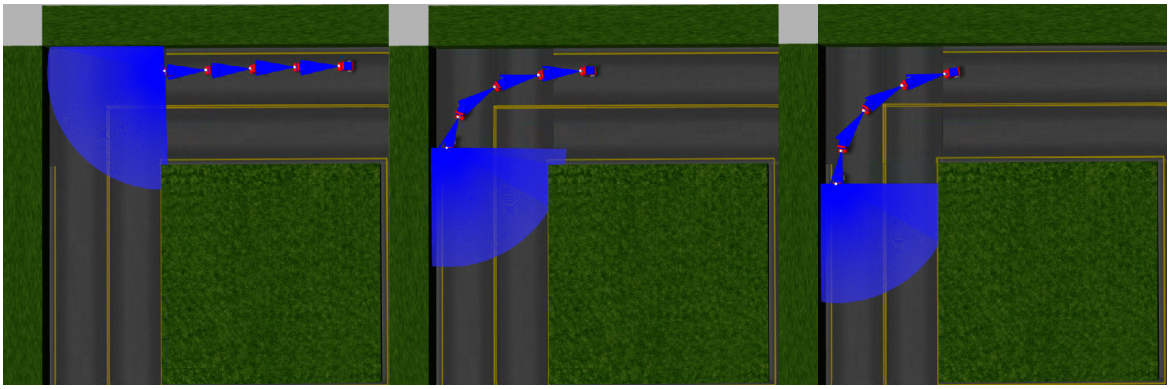

Fig. 5.12 Platoon Navigation

robots were deployed to test the developed controller. A leader robot has a predefined path, and its associated controller is /moveLeader based on the leader robot's algorithm, whereas follower robots' associated controllers are (/moveFollower_one to /moveFollower_four) based on the follower robot's algorithm. All five robots are subscribed to their laser scan topics (/scan0 to /scan4). Here, a simulation world (/gazebo) provides laser readings from robots (/scan0 to /scan4) to the developed robot controllers, and the controllers issue relevant velocity (/rbt_lsr_0/cmd_vel to /rbt_lsr_4/cmd_vel) to the robots in the simulation world (/gazebo).

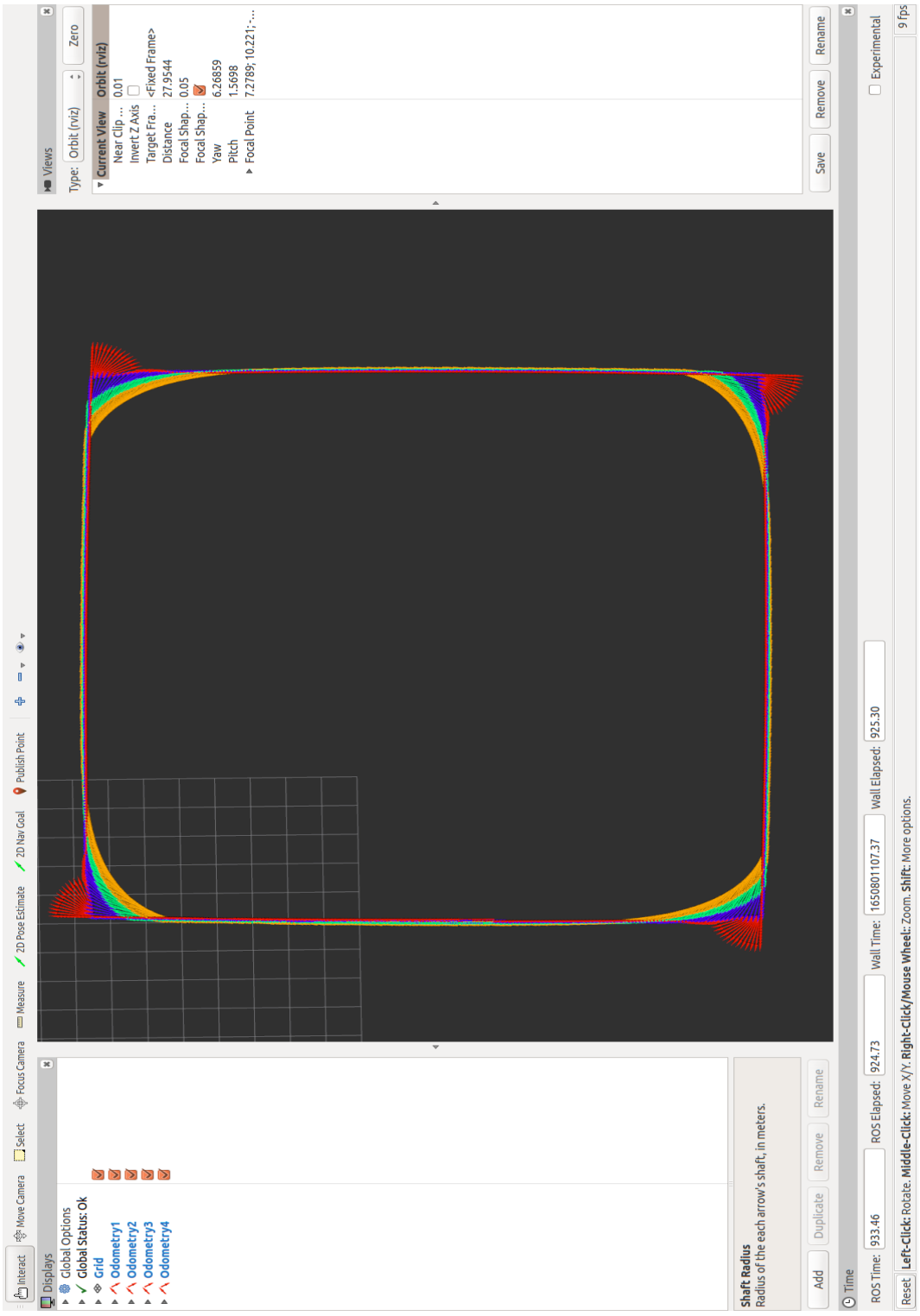

Fig. 5.13 Platoon Navigation Trajectory

Fig. 5.12 shows the simulated scenario containing five mobile robots. While moving through the environment, this platoon stays in the right lane and turns without collision at the end of the lane. Here, the follower robots follow the trajectories of preceding robots, and the leader robot plans the trajectory based on the sensor's reading. Moreover, both linear and angular velocities are calculated and applied. For this experiment, the velocity for a leader robot is set at a minimum to achieve accurate results from the algorithm. While trying the higher velocity, follower robots could not track the leader robot. Fig. 5.13 shows the trajectory generated by the platoon navigation.

Furthermore, having a platoon formation of a maximum of five vehicles is sufficient when considering a real-world scenario. The average length of the vehicle is around 450 centimetres. Now, considering 3 seconds of headway at 20 miles-per-hour speed provides around 2683 centimetres of a gap between each vehicle inside the platoon using the distance formula. This equates to an overall 12982 centimetre or 130 meters long platoon. This gap increases at a higher speed, such as motorway driving at 70 miles-per-hours. Therefore, long platoon sees little benefits in city or town roads as they tend to be smaller with frequent intersections. Thus, a second platoon is recommended for the following five vehicles.

Moreover, city roads are dense, smaller, and narrower and consist of frequent intersections and roundabouts compared to straight and wide motorway roads. Therefore, as an extension to this work, a dynamically reconfigurable platoon can be developed and deployed, which can split at the intersection or roundabouts. In this scenario, the AGVs inside the platoon can act independently based on available local information and split at the intersection based on the AGVs' destination and path. After the intersection or roundabouts, AGVs can form a new platoon. Fig. 5.14 shows different types of intersections and roundabouts that can be useful to simulate a reconfigurable platoon in this situation. Moreover, once a platoon is formed, AGVs within the platoon can record the number of vehicles inside the platoon to decide whether to admit more AGVs to the existing platoon or form a new one.

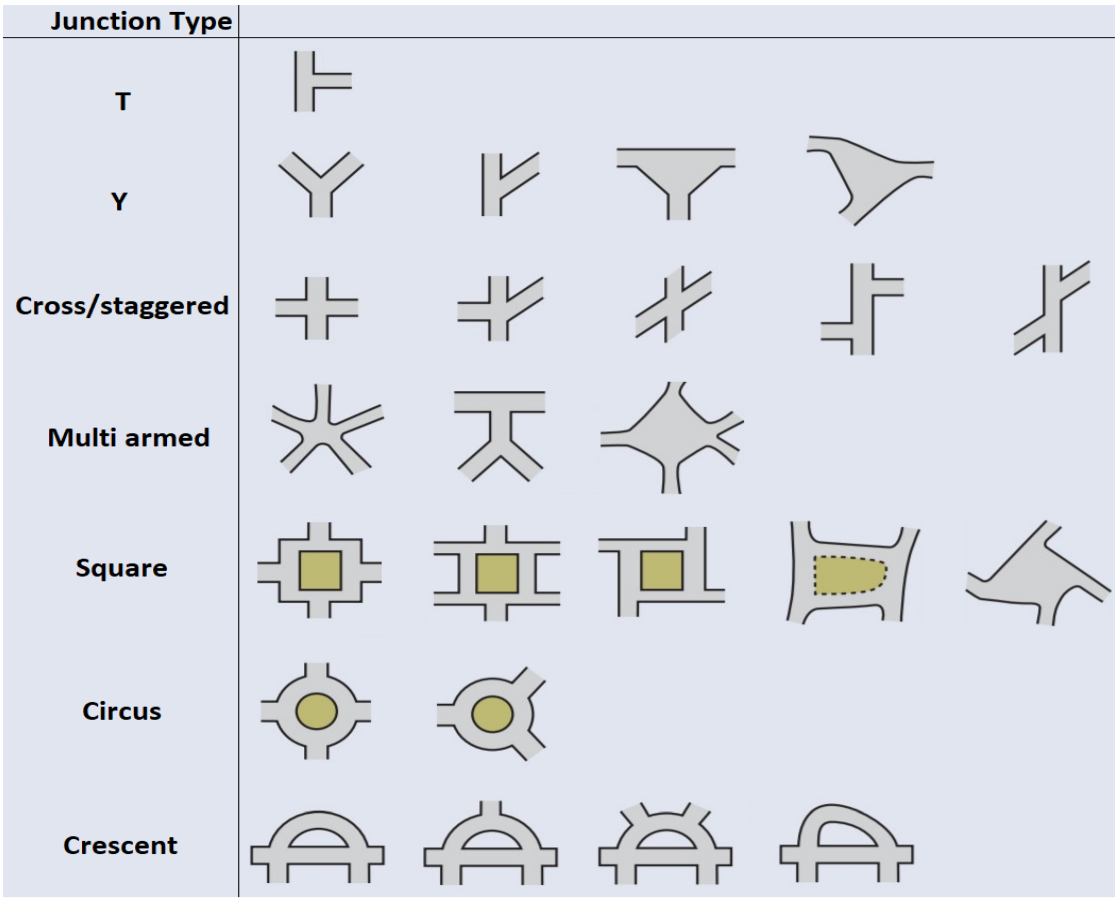

Fig. 5.14 Intersections [147]

5.5 Summary

In this chapter, a multi-robot simulator is developed and used to simulate multiple robots in two scenarios, individual robot navigation and platoon formation navigation. This proposed simulator can be reconfigured to different simulation worlds, and new robots can be added. Much of the work on platoon formation or multi-robot navigation is supported via numerical simulation in literature, which does not provide information on the physical illustration of robot navigation. The benefit of having a simulator is that the behaviours of robots and controllers can be examined. The first scenario proved the feasibility of simulating multiple AGVs under ROS and Gazebo environments. A laser scanner-based platoon formation algorithm is presented and simulated using the predecessor following topology in the second

scenario. The significant outcome of this work is the ability to simulate platoon formation using a laser sensor.

The contribution of this chapter is threefold. First, it presents a multi-robot simulator detailing virtual robots and world development using the ROS-Gazebo framework. Second, it proposes a simple vehicle platoon formation algorithm that handles multiple AGVs based on a laser scanner. Third, the proposed algorithm does not require any communication between AGVs thus, is capable of guiding AGVs in uncertain situations such as sudden loss of communication or time-varying communication delay. Finally, this algorithm's application is not limited to the work discussed here. This algorithm can guide warehouse mobile robots for goods transportation and study the robot behaviour of follower robots in the laboratory-based environment.

One benefit of having AGVs platoon formation is that they are better than mechanically coupled vehicles. Mechanically coupled vehicles tend to be more rigid and longer. Thus, a long platoon of these vehicles is unsuitable for ordinary roads and intersections. Another advantage of vehicle platoons formation is that AGVs have almost instantaneous reaction time, and headway can be significantly reduced, thereby increasing the capacity of existing roads. As currently conceived, the lead vehicle would be driven by a human, but in the future, platoons consisting of AGVs could be a very efficient use of existing roads and significantly increase capacity, lessening the need for expensive new road intersections and bridge infrastructure.

Chapter 6

Detecting Human Emotions

This chapter discusses methods to assess human emotion. Section 6.1 presents the introduction of the chapter. Section 6.2 discusses the materials and methods used to develop this approach. Section 6.3 provides information on feature extraction methods used for this study. Section 6.4 details information on machine learning models and training. Finally, the results are discussed in Section 6.5.

6.1 Introduction

Several techniques have been developed for human emotion recognition over the past decade using various methods such as facial expression, speech, text, and physiological signals [154, 83, 81, 3]. Physiological signals can be obtained using multiple sensors, as explained in Chapter 2. Moreover, these types of signals have several advantages over facial and speech-based methods, such as a human can hide or manipulate facial expression or vocal tone, whereas physiological data are hard to falsify. EEG signals have proven to be accurate and reliable in emotion assessment using physiological signals. As discussed in the literature, most studies have used more than two sensors, including EEG signals. One disadvantage of using an EEG sensor is the ease of use, which requires an EEG device to be worn on the

head. Furthermore, the market for such devices is not yet developed, and these devices can be expensive.

On the other hand, ECG and PPG signals are closely associated with heart activities and monitoring and diagnosing cardiovascular diseases. However, studies discussing the performance of ECG and PPG signals for emotion classification are limited. ECG and PPG sensors can be found in off-the-self smartwatches and fitness bands. Moreover, these types of watches/bands are easy to wear and widely accepted by the consumer market. One advantage of using ECG-PPG features to develop an emotion assessment system is the availability of wearable devices containing these sensors. Such a system can be placed inside wearable devices to assess the emotional state of the user and can enable applications in the automotive industry. Therefore, binary classification is considered to prove the feasibility of using ECG and PPG sensors and the ADM method, as shown in Fig. 1.3.

Here, short signals from ECG and PPG sensor data in the continuously annotated signals of emotion (CASE) dataset [152] are considered for extracting morphology, instantaneous, and spectral entropy features. Based on the current literature, we found no emotion assessment results using these joint features of ECG and PPG sensor and ADM method. The novelty of this work includes three parts. First, this study presents results on combined ECG-PPG features and the ADM method. Second, the approach used in this study is fast, meaning that the emotional state can be derived every 3 seconds. Third, the average classification result of per-subject is derived using SVM, neural network, long short-term memory (LSTM) classifiers, and optimisation techniques.

Morphological features are generally derived from the shape of the signals. These features provide accurate information on signal properties as the signal evolves. Another advantage of using morphological features is obtaining these features at ease because the raw signal is used for extracting information. An instantaneous frequency is a time-varying parameter that

relates to the average frequencies present in the signal as it evolves. On the other hand, the spectral entropy of ECG and PPG signals measures the signal's spectral power distribution.

6.2 Materials and Methods

6.2.1 Dataset

Several dataset are available in the public domain and contain participants' physiological signals and valence-arousal annotations, such as DEAP [82], MAHNOB-HCI [156], AMIGOS [111], RECOLA [141], and DECAF [2]. These dataset primarily focus on EEG signals without ECG and PPG data. As per the authors' knowledge, there is only one public domain dataset, which includes ECG and PPG sensor data and real-time annotation of arousal and valence for given video stimuli. This paper uses the CASE dataset, which contains data from 30 participants, 15 males and 15 females participants.

In CASE, four emotional states were elicited: amusing, boring, relaxing, and scary. Eight video stimuli were selected so that two videos were for each emotional state and were shown to participants to induce these emotions. Moreover, this dataset used three other videos, i.e., the start, end, and interleaving blue-screen videos. A Joystick-based Emotion Reporting Interface (JERI) was used to collect responses from participants, and annotations of arousal and valence were collected simultaneously. This dataset collected data from six physiological measures, i.e., ECG, PPG, GSR, RSP, EMG, and SKT. The data acquisition rate for the physiological data and the annotations was 1000Hz and 20Hz, respectively.

6.2.2 Approach

Features can be extracted from short signals, e.g., a 3-second signal. This study considers this approach to analyse the effect of different emotions on a cardiac cycle. Here, one method extracts a signal's morphological features, such as peak amplitude, valley amplitude,

peak-to-peak amplitude, and inter-beat interval (IBI). The reason behind choosing these features is the ease of finding local maxima and minima and deriving features from them. Hence, a fast approach. However, in some 1-second and 2-second windows, it is not possible to get an IBI as these windows contain only one peak/pulse. Therefore, a 3-second window is deployed in this paper as it provides a minimum of two peaks/pulses of the ECG and PPG waves.

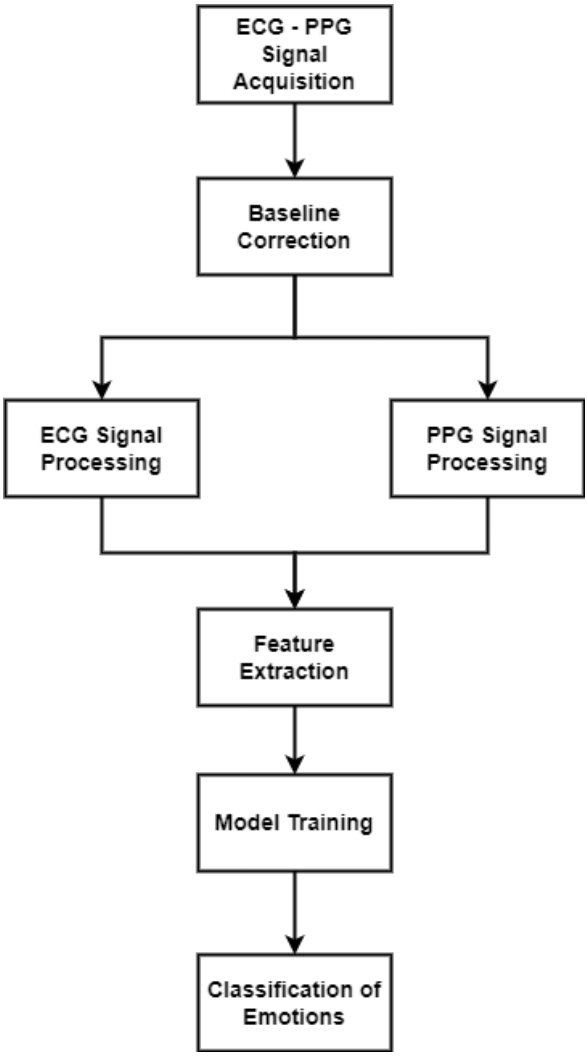

Fig. 6.1 Block Diagram of the Proposed Method

The second method extracts instantaneous frequency and spectral frequency. These two methods are widely applied to study irregularity in heart rhythm. Therefore, these techniques

are used to differentiate heart rhythm between different emotions on a 3-second window. Here, 3 seconds of ECG and PPG signals are extracted and matched with corresponding annotations. As annotations are conducted every 50 milliseconds (20 Hz), a 3-second window provides 60 annotations. Therefore, a mean of 60 annotations is matched with the 3-second signals. Fig. 6.1 shows the block diagram for our proposed method.

6.2.3 Signal Processing

Fig. 6.2 shows two flowcharts for processing ECG and PPG signals. Before extracting features from the signals, it is crucial to remove noise. ECG and PPG are time-resolving signals; therefore, they may contain temporal drift induced by various internal and external sources. A baseline correction was performed to reduce the effect of such drift. In the dataset, before showing a stimulus to participants, the interleaving blue-screen video was shown for 120 seconds, and data recording of this time frame was taken as a baseline period. Here, the mean of the baseline period was subtracted from the stimulus interval. After baseline correction, a band-pass filter was applied to both signals to remove high-frequency noise and low-frequency drifts. The lower cut-off frequencies for ECG and PPG signals were 40Hz and 4Hz, respectively. The higher cut-off frequency for both ECG and PPG signals was 0.5Hz. Only low-pass and high-pass filters are employed to extract the instantaneous frequency and spectral frequency features. For morphological features, the ECG signal used a Pan-Tompkins algorithm [123] and implemented it to derive peaks from the signal. For the PPG signal, peaks were identified by finding local maxima from the 500 sample window size. This window size was determined empirically. Some PPG signals suffer from outliers; therefore, it is crucial to remove them before processing PPG signals. A linear fill method was implemented where these outliers were filled using linear interpolation of neighbouring, non-outliers values to avoid sample loss in the PPG signal. In linear interpolation, two neighbouring samples are averaged, and this value is replaced with an outlier.

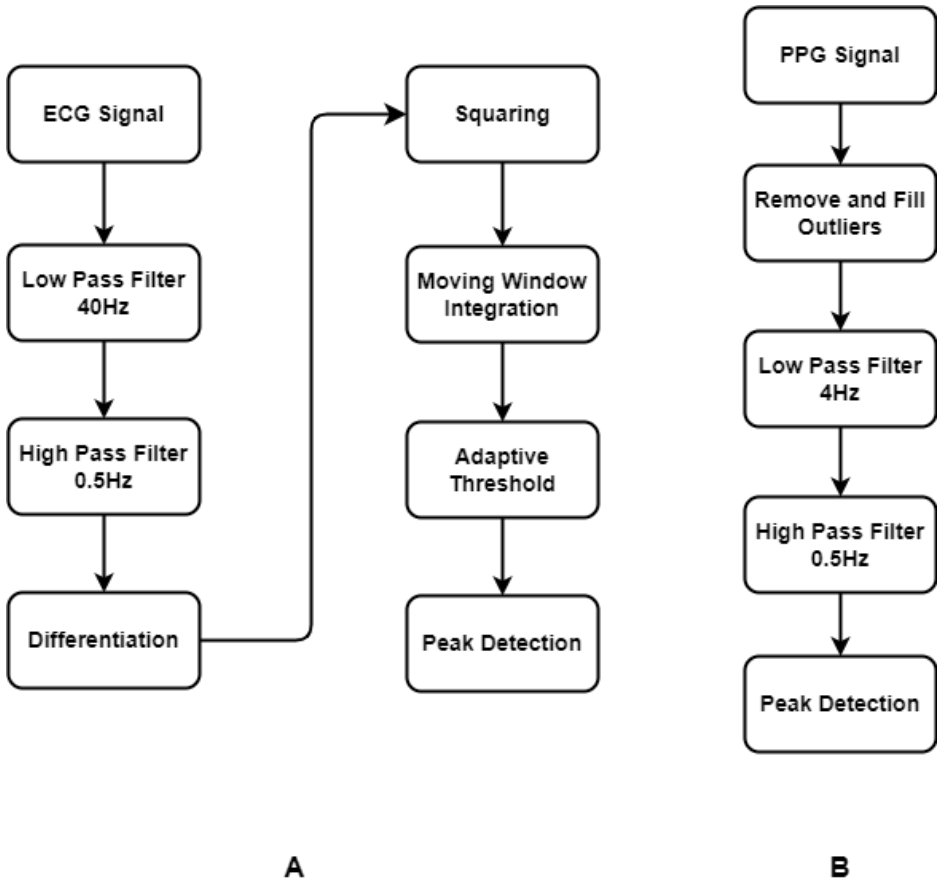

Fig. 6.2 ECG-PPG Signal Processing

6.3 Approach

6.3.1 Morphology Features

In time-domain signals, an ECG beat is composed of four waves: P-wave, QRS complex, T-wave, and U-wave. For PPG beat, these components are the systolic point, diastolic point, dicrotic notch, and second wave. Fig. 6.3 shows a graphical representation of these waves. This work identifies R-wave and S-wave from an ECG signal to obtain four features, as shown in Fig. 6.4. From the PPG signal, the diastolic point and systolic point are identified to obtain four features:

- average peak amplitude of the signal (local maxima)

- average valley amplitude of the signal (local minima)
- peak-to-peak (P2P) amplitude (peak + valley)
- average inter-beat interval (IBI)

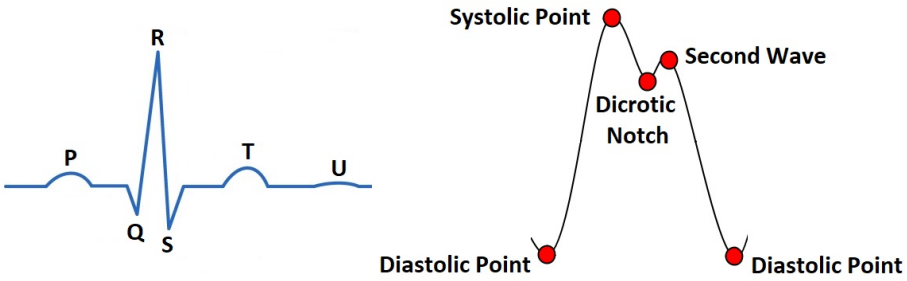

Fig. 6.3 ECG and PPG Signals

More specifically, P-wave represents atrial depolarisation, and T-wave represents ventricular depolarisation. A QRS complex's first negative deflection is called a Q-wave, the first positive deflection in the complex is called R-wave, and a negative deflection after the R-wave is called S-eave. U-wave represents the repolarisation of the Purkinje fibres. The systolic point results from the direct pressure wave travelling from the left ventricle to the periphery of the body, and the diastolic point (or inflection) is a result of reflections of the pressure wave by arteries of the lower body. A dicrotic notch is usually seen in subjects with healthy compliant arteries in the catacrotic phase.

The peaks and valleys of the signal are obtained by finding local maxima and minima. These two features derive the remaining peak-to-peak and IBI features.

6.3.2 Instantaneous frequency

The instantaneous frequency estimates the time-dependent frequency of a signal as the first moment of the power spectrogram and computes the spectrogram using a short-time Fourier transform. ECG and PPG signals are non-stationary. Therefore, the instantaneous frequency

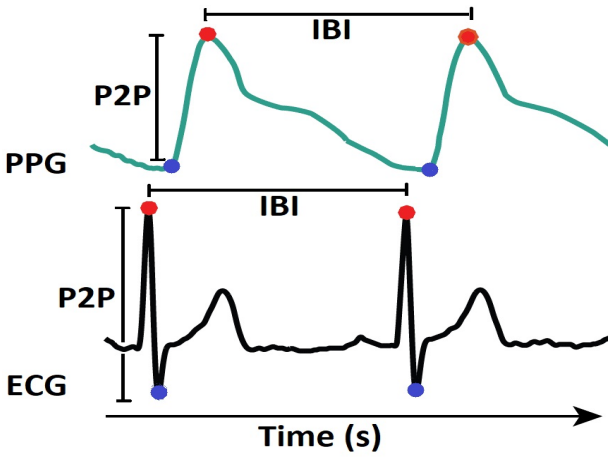

Fig. 6.4 Signal Morphology Features

is an important characteristic which defines the location of the signal's spectral peak as it varies with time [13].

$$f_{inst}(t) = \frac{\int_0^\infty fP(t,f)df}{\int_0^\infty P(t,f)df} \tag{6.1}$$

Equation 5.1 computes the spectrogram power spectrum $P(t,f)$ of the input and uses the spectrum as a time-frequency distribution.

6.3.3 Spectral Entropy

Spectral entropy measures the spikiness and flatness of a signal. A signal with a more spike spectrum has low spectral entropy, whereas a flat spectrum has high spectral entropy. The spectral entropy measures the spectral entropy based on a power spectrogram. The spectral entropy at time t is defined as,

$$H(t) = -\Sigma_{m=1}^{N} P(t,m) log_2 P(t,m) \tag{6.2}$$

Fig. 6.5 shows a typical waveform of instantaneous frequency and spectral entropy from 3-second length ECG and PPG signal.

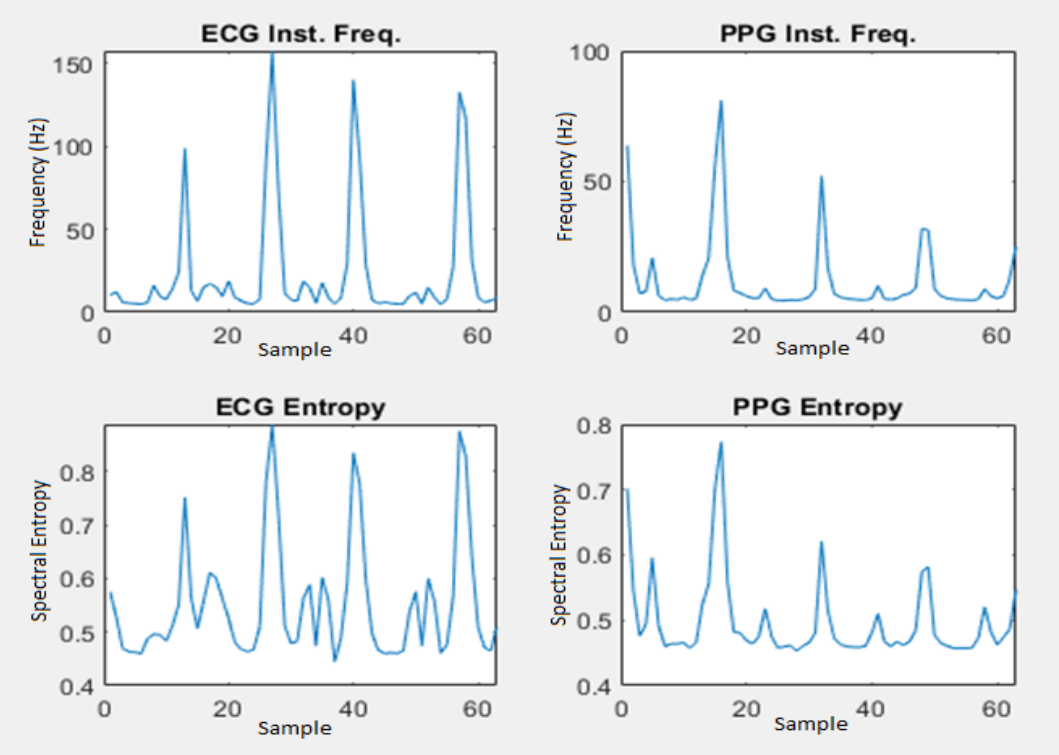

Fig. 6.5 Instantaneous Frequency and Spectral Entropy

6.4 Model Training

For per-subject classification, 418 trials are obtained after extracting features from a 3-seconds window and trained using SVM, neural network, and LSTM classifiers. For results, two separate models are trained for arousal and valence using MATLAB-R2020b. The values for arousal and valence annotations range from 0.5 to 9.5. Thus, a threshold value of 5 is used to create a binary class for binary classification. Any annotation value less than or equal to five is considered a low arousal / negative valence class, whereas an annotation value higher than five is considered a high arousal/ positive valence class. For SVM and LSTM classification, 80% trials are used for training, and 20% trials are used for testing. For NN classification, 70% trials are used for training, 15% trials are used for validation, and 15% trials are used for testing. The number of trials for training and testing varies for each subject as they depend on high/low arousal and positive/negative valence annotations.

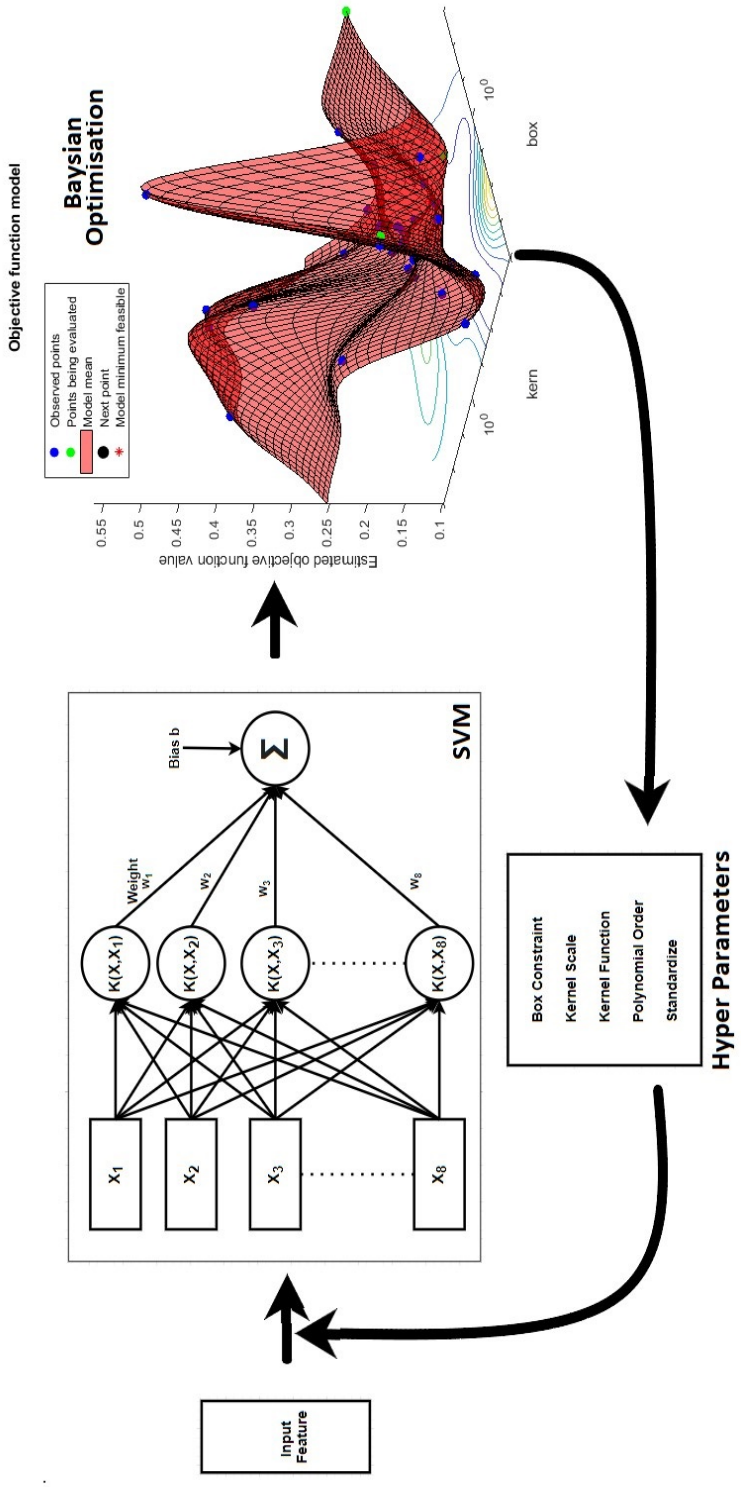

Fig. 6.6 Support Vector Machine and Bayes Optimisation

6.4.1 Support Vector Machine

SVM is a supervised machine learning algorithm for classification, which finds the optimal hyperplane to divide data into two categories at the maximal margin. For SVM classification, Bayesian optimisation [15] is considered for hyperparameter optimisation. This process tries different combinations of hyperparameter values by using an optimisation scheme that seeks to minimise the model classification error and returns a model with the optimised hyperparameters, such as box constraint and kernel scale.

Bayesian optimisation algorithm minimises a scalar objective function f(x) for x. For the same input x, the output differs depending on whether the function is deterministic or stochastic. The minimisation process is comprised of three key elements: a Gaussian process model for the objective function f(x), a Bayesian update process that modifies the Gaussian model after each new evaluation of the objective function, and an acquisition function a(x) which is maximised in order to identify the next evaluation point. In addition, the expected improvement per second plus function is implemented for the optimisation process regarding the acquisition function. The role of this acquisition function is to measure the expected improvement in the objective function while discarding values that would increase it. This function utilises three phrases, expected improvement, per second, plus. Hence, the expected improvement is calculated as:

$$EI(x,Q) = E_Q[max(0, \mu_Q(x_{best}) - f(x))] \tag{6.3}$$

where x_{best} is the location of the lowest posterior mean and $\mu_Q(x_{best})$ is the lowest value of the posterior mean.

Using per second phrase in the acquisition function is to obtain better improvement per second by using time-weighting. During the objective function evaluations, Bayesian optimisation maintains another Bayesian model of objective function evaluation time as a

function of position x. The expected improvement per second that the acquisition function uses is:

$$EIpS(x) = \frac{EI_Q(x)}{\mu_s(x)} \tag{6.4}$$

where $\mu_s(x)$ is the posterior mean of the timing Gaussian process model. The use of the plus phrase is to escape a local objective function minimum by modifying the acquisition function's behaviour when they estimate that they are over-exploiting an area.

6.4.2 Neural Network

A neural network consists of a series of layers. The first layer has a connection from the network input. Each subsequent layer has a connection from the previous layer. The final layer produces the network's output. Adam (adaptive moment estimation) optimiser [79] is considered for hyperparameter optimisation.The algorithm updates exponential moving averages of the gradient (m_t) and the squared gradient (v_t) where the hyper-parameters $\beta_1, \beta_2 \in [0,1)$ control the exponential decay rates of these moving averages.

In Adam, the moving averages of the gradient m_t and the square gradient v_t is computed as:

$$m_t = \beta_1 m_{t-1} + (1-\beta_1) g_t \tag{6.5}$$

$$v_t = \beta_2 v_{t-1} + (1-\beta_2) g_t^2 \tag{6.6}$$

where m_t and v_t are estimates of the first moment (the mean) and the second moment (the uncentered variance) of the gradient, respectively. These moving averages require bias correction and computed as $\hat{m}_t = \frac{m_t}{1-\beta_1^t}$ and $\hat{v}_t = \frac{v_t}{1-\beta_2^t}$.

Finally, the parameters are updated as:

$$\theta_t = \theta_{t-1} - \frac{\alpha \hat{m}_t}{(\sqrt{\hat{v}_t} + \in)} \tag{6.7}$$

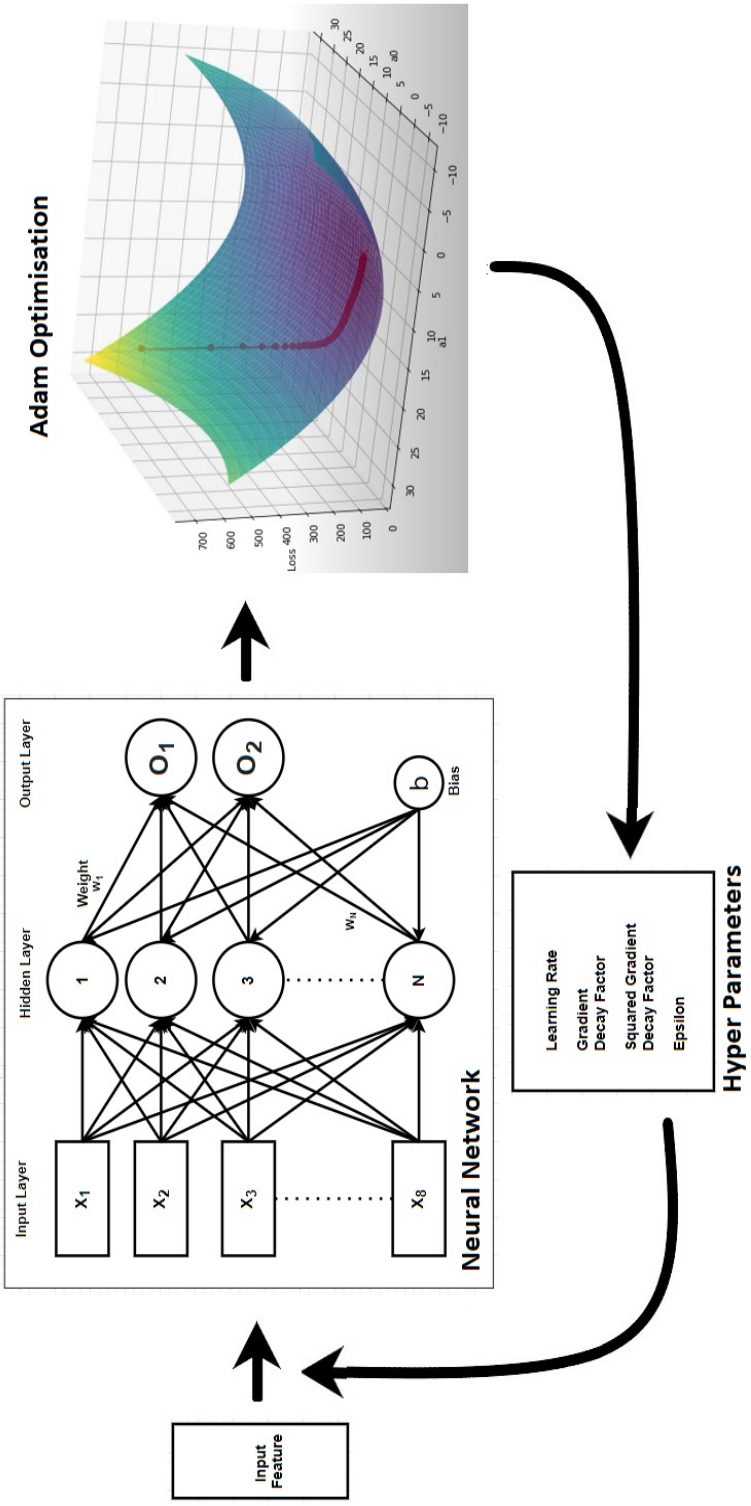

Fig. 6.7 Neural Network and ADAM Optimisation

6.4.3 Long Short-Term Memory

An LSTM layer learns long-term dependencies between time steps in time series and sequence data [61]. Such operations are complemented by employing a variety of memory cells and gating operations. The state of the layer consists of the hidden state and the cell state. The hidden state at time step t contains the output of the LSTM layer for this time step. The cell state contains information learned from the previous time steps. At each time step, the layer adds information to or removes information from the cell state. The layer controls these updates using gates.

The main components of the LSTM layer are the input gate, output gate, forget gate, and cell candidate. The following formulas describe the components at time t.

$$i_t = \sigma_g(W_i x_i + R_i h_{t-1} + b_j) \tag{6.8}$$

$$f_t = \sigma_g(W_f x_t + R_f h_{t-1} + b_f) \tag{6.9}$$

$$g_t = \sigma_c(W_g x_t + R_g h_{t-1} + b_g) \tag{6.10}$$

$$o_t = \sigma_g(W_o x_t + R_o h_{t-1} + b_o) \tag{6.11}$$

These components control the cell state and hidden state of the layer. In these calculations, σ_g denotes the gate activation function and uses the sigmoid function given by $\sigma(x) = (1+e^{-x})^{-1}$ to compute the gate activation function.

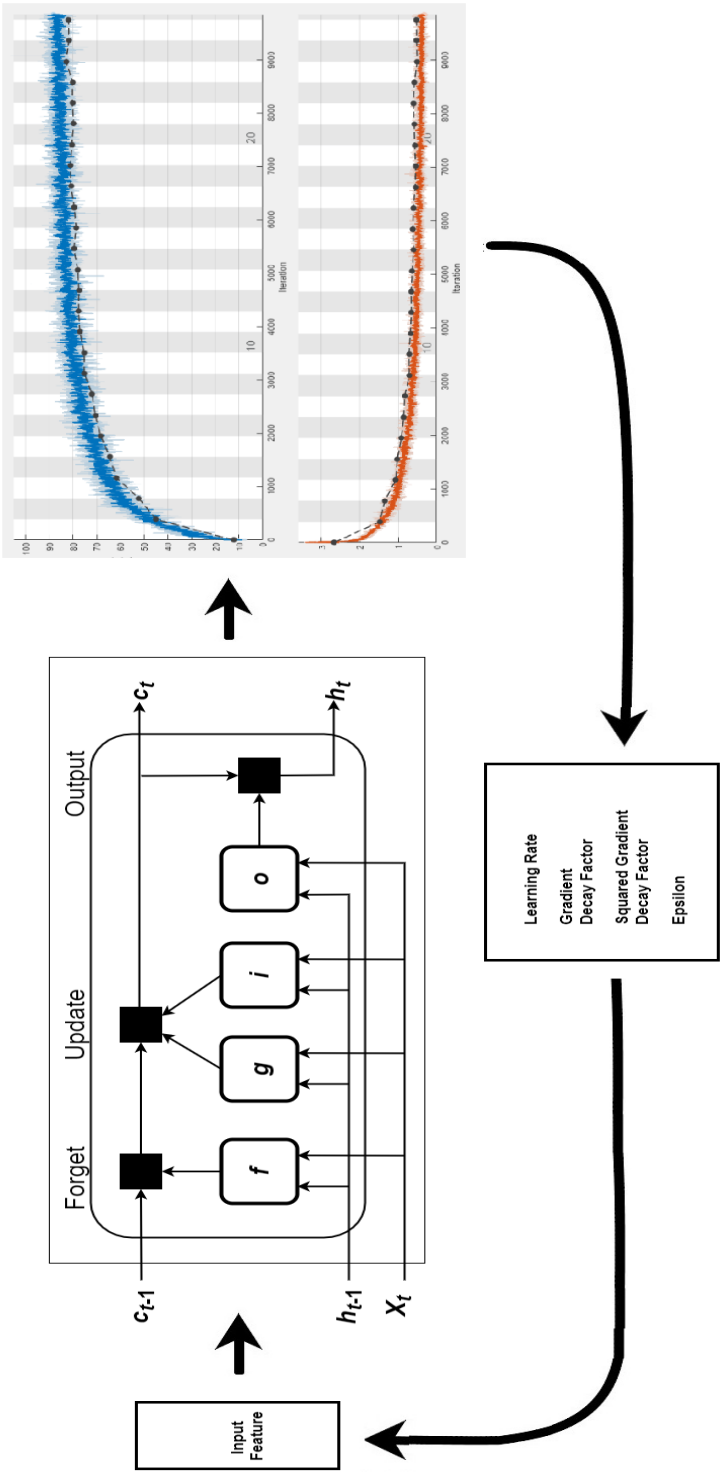

Fig. 6.8 LSTM and ADAM Optimisation

6.5 Results

Table 6.1 and 6.2 present the results from an SVM classifier. As can be seen, the average test accuracy of the SVM classifier is 72.68% and 73.30% for valence and arousal, respectively. Table 6.3 and 6.4 present the results for a neural network classifier. As can be seen, the average test accuracy of the neural network classifier is 72.48% and 73.01% for valence and arousal, respectively. Finally, Table 6.5 and 6.6 present the results for an LSTM classifier. As can be seen, the average test accuracy of the LSTM classifier is 61.53% for valence and 61.87% for arousal, respectively. The statistical significance of the classification accuracy (p-value) and F1 score for both classes are derived alongside the classification result. A neural network and SVM classifiers with relevant optimisation algorithms provide good results, whereas an LSTM classifier does not provide better accuracy than SVM and neural networks. Note that the F1 score computes the average of precision and recall and indicates how accurate a model is on a given dataset. It is high if precision and recall values are high and vice-versa.

For SVM results, except for the arousal accuracy of subject seven and the valence accuracy of subject 10, the results of all subjects prove to be statistically significant as their relative p-values are less than 0.05 ($p \leq 0.05$). Regarding neural network classifier results, except for the valence accuracy of subject ten and subject 28, the results of all subjects prove to be statistically significant. Therefore, it can be said that a $p \leq 0.05$ indicates strong evidence against the null hypothesis. On the other hand, few accuracy results are $p > 0.05$, indicating strong evidence for the null hypothesis. For LSTM results, the valence accuracy of subjects 2, 3, 7, 9, 10, 14, 17, 22, 23, 25, 28, and 30 do not provide statistically significant results. For arousal classification, these subjects are 1, 3, 15, 16, 25, and 30.

Table 6.1 SVM Training Results - Valence

Subject No.	Test Acc. (%)	p-Value	F1-Score (%)	
			PV	NV
1	75.68	3.85×10^{-6}	76.90	74.30
2	77.23	3.64×10^{-6}	78.90	75.40
3	80.00	1.21×10^{-6}	77.80	81.80
4	73.43	7.48×10^{-5}	72.13	74.63
5	79.17	2.45×10^{-7}	78.87	79.45
6	71.73	1.40×10^{-3}	72.34	71.11
7	62.50	2.60×10^{-2}	55.00	67.80
8	66.67	2.50×10^{-3}	57.70	72.50
9	67.19	2.20×10^{-3}	61.82	71.23
10	63.64	7.62×10^{-2}	55.56	69.23
11	82.00	2.23×10^{-6}	82.35	81.63
12	69.23	2.62×10^{-4}	66.67	71.43
13	77.08	8.03×10^{-5}	78.43	75.56
14	76.47	1.10×10^{-3}	75.00	77.78
15	63.51	0.0062	67.47	58.46
16	61.76	1.48×10^{-2}	65.79	56.67
17	71.62	8.02×10^{-5}	72.00	71.23
18	71.67	3.36×10^{-4}	70.17	73.02
19	70.27	1.93×10^{-4}	71.05	69.44
20	83.33	1.34×10^{-6}	84.00	82.61
21	68.96	1.60×10^{-3}	65.38	71.87
22	70.97	4.01×10^{-4}	68.97	72.73
23	71.21	2.34×10^{-4}	70.77	71.64
24	76.67	1.50×10^{-5}	75.00	78.12
25	77.94	1.50×10^{-6}	76.92	78.87
26	72.22	4.80×10^{-4}	75.41	68.08
27	68.06	8.25×10^{-4}	72.94	61.02
28	62.50	1.87×10^{-2}	64.41	60.38
29	98.08	1.15×10^{-14}	98.11	98.04
30	69.56	3.40×10^{-3}	68.18	70.83
Test Accuracy	72.68%			

Table 6.2 SVM Training Results - Arousal

Subject No.	Test Acc. (%)	p-Value	F1-Score (%)	
			HA	LA
1	87.50	8.37×10^{-6}	88.20	86.70
2	61.77	0.0148	59.40	63.90
3	67.14	0.0015	71.60	61.01
4	76.00	1.08×10^{-4}	76.92	75.00
5	64.29	0.0055	71.91	50.98
6	72.22	6.61×10^{-5}	68.75	75.00
7	57.14	0.0604	58.62	55.56
8	78.57	7.75×10^{-6}	80.00	76.92
9	67.19	2.20×10^{-3}	60.38	72.00
10	64.29	1.09×10^{-2}	42.30	50.00
11	74.29	1.96×10^{-5}	75.00	73.53
12	68.18	1.20×10^{-3}	64.41	71.23
13	73.21	2.26×10^{-4}	74.58	71.70
14	58.97	2.59×10^{-2}	60.00	57.90
15	62.50	2.60×10^{-2}	66.67	57.14
16	77.50	2.49×10^{-4}	74.29	80.00
17	79.73	9.66×10^{-8}	76.92	81.93
18	77.94	1.50×10^{-6}	78.26	77.61
19	83.33	6.54×10^{-8}	81.48	84.84
20	80.49	8.63×10^{-9}	80.00	80.95
21	77.42	6.31×10^{-6}	76.67	78.12
22	72.22	6.61×10^{-5}	64.29	77.27
23	77.14	2.10×10^{-6}	75.00	78.95
24	70.00	2.00×10^{-3}	63.41	74.58
25	75.00	7.71×10^{-4}	73.68	76.19
26	72.58	1.60×10^{-4}	72.13	73.02
27	72.97	3.12×10^{-5}	74.36	71.43
28	71.25	5.65×10^{-5}	72.29	70.13
29	82.26	1.10×10^{-7}	81.97	82.54
30	66.00	8.70×10^{-3}	66.67	65.31
Test Accuracy	73.30%			

Table 6.3 NN Training Results - Valence

Subject No.	Test Acc. (%)	p-Value	F1-Score (%)	
			PV	NV
1	72.22	4.80×10^{-4}	73.68	70.59
2	75.00	1.41×10^{-4}	77.19	72.34
3	76.19	3.35×10^{-4}	78.26	73.68
4	80.95	2.68×10^{-5}	80.00	81.82
5	68.00	4.40×10^{-3}	70.37	65.22
6	70.00	5.10×10^{-3}	70.00	70.00
7	61.90	1.97×10^{-2}	66.67	64.86
8	64.29	2.24×10^{-2}	57.14	69.39
9	67.39	7.30×10^{-3}	65.12	69.39
10	62.50	1.22×10^{-1}	66.67	57.14
11	85.29	1.62×10^{-5}	84.85	85.71
12	72.41	2.77×10^{-4}	65.22	77.14
13	75.00	7.71×10^{-4}	72.22	77.27
14	73.08	9.80×10^{-3}	75.86	69.56
15	70.00	8.02×10^{-4}	66.67	72.73
16	63.04	2.49×10^{-2}	69.09	54.05
17	73.21	2.26×10^{-4}	75.41	70.59
18	68.52	2.60×10^{-3}	66.67	70.17
19	74.00	3.15×10^{-4}	64.70	79.36
20	73.33	5.50×10^{-3}	75.00	71.43
21	72.73	1.20×10^{-3}	73.91	71.43
22	76.19	3.35×10^{-4}	76.19	76.19
23	73.08	3.93×10^{-4}	73.08	73.08
24	75.00	4.36×10^{-4}	75.56	74.42
25	70.37	1.20×10^{-3}	71.43	69.23
26	79.17	2.32×10^{-5}	81.48	76.19
27	73.21	2.26×10^{-4}	75.41	70.59
28	58.33	5.95×10^{-2}	47.37	65.52
29	100.00	5.82×10^{-11}	100.00	100.00
30	70.00	1.33×10^{-2}	70.97	68.97
Test Accuracy	72.48%			

Table 6.4 NN Training Results - Arousal

Subject No.	Test Acc. (%)	p-Value	F1-Score (%)	
			HA	LA
1	71.43	1.16×10^{-2}	71.42	71.42
2	65.45	5.40×10^{-3}	66.67	66.67
3	66.67	8.00×10^{-3}	65.22	68.00
4	76.32	5.93×10^{-4}	74.29	78.05
5	69.05	5.80×10^{-3}	66.67	71.11
6	70.83	1.70×10^{-3}	69.56	72.00
7	63.83	3.79×10^{-2}	65.22	57.89
8	82.50	1.70×10^{-5}	82.05	82.93
9	71.43	2.50×10^{-3}	72.73	70.00
10	75.00	7.71×10^{-4}	73.68	76.19
11	73.08	3.93×10^{-4}	74.04	72.00
12	68.00	4.40×10^{-3}	69.23	66.67
13	75.00	1.40×10^{-3}	72.73	76.93
14	58.62	4.45×10^{-2}	60.00	57.14
15	69.05	5.80×10^{-3}	68.29	69.77
16	87.50	1.21×10^{-4}	88.89	85.71
17	73.21	2.26×10^{-4}	68.08	76.92
18	68.97	1.60×10^{-3}	65.38	71.87
19	81.82	1.01×10^{-5}	81.82	81.82
20	81.25	5.96×10^{-6}	79.07	83.02
21	79.17	2.32×10^{-5}	78.26	80.00
22	69.23	2.30×10^{-3}	60.00	75.00
23	75.86	3.52×10^{-5}	74.07	77.42
24	75.00	1.40×10^{-3}	72.73	76.92
25	76.67	1.90×10^{-3}	74.07	78.79
26	81.03	7.90×10^{-7}	80.70	81.36
27	71.15	9.95×10^{-4}	73.68	68.08
28	68.52	2.60×10^{-3}	66.67	70.17
29	72.50	2.10×10^{-3}	68.57	75.56
30	72.22	3.70×10^{-3}	68.75	75.00
Test Accuracy	73.01%			

Table 6.5 LSTM Training Results - Valence

Subject No.	Test Acc. (%)	p-Value	F1-Score (%)	
			PV	NV
1	59.21	0.0254	57.53	60.75
2	47.50	0.0806	52.27	41.67
3	54.69	0.0753	59.15	49.12
4	73.44	7.48×10^{-5}	70.17	76.06
5	63.51	0.0062	59.70	66.67
6	58.62	0.0445	58.62	58.62
7	57.69	0.0601	59.26	56.00
8	70.00	3.26×10^{-4}	67.69	72.00
9	51.43	0.0924	43.33	57.50
10	58.33	0.1169	61.53	54.54
11	61.11	0.0289	64.41	57.14
12	68.75	3.01×10^{-4}	70.59	66.67
13	69.64	0.0014	69.09	70.17
14	47.50	0.1194	48.78	46.15
15	63.41	0.0046	63.41	63.41
16	77.14	2.10×10^{-6}	75.76	78.38
17	50.00	0.0889	52.38	47.39
18	65.28	0.0032	66.67	63.77
19	65.38	0.0022	66.67	0.64
20	77.78	1.90×10^{-5}	78.57	76.92
21	59.38	0.0326	59.37	59.37
22	51.52	0.095	44.83	56.76
23	55.71	0.0605	65.17	39.22
24	73.44	7.48×10^{-5}	73.02	73.85
25	46.05	0.0722	52.87	36.92
26	71.21	2.34×10^{-4}	73.97	67.80
27	60.00	0.0181	56.76	62.79
28	53.03	8.68×10^{-2}	55.07	50.79
29	88.89	1.43×10^{-9}	89.28	88.46
30	46.15	9.47×10^{-2}	46.15	46.15
Test Accuracy	61.53%			

Table 6.6 LSTM Training Results - Arousal

Subject No.	Test Acc. (%)	p-Value	F1-Score (%)	
			HA	LA
1	60.00	0.0572	61.90	57.89
2	64.86	0.0035	66.67	62.86
3	68.57	7.27×10^{-4}	66.67	70.27
4	56.25	0.061	41.67	65.00
5	40.00	0.0237	46.15	32.35
6	72.50	2.24×10^{-5}	67.65	76.10
7	38.71	0.021	42.42	34.48
8	70.69	6.85×10^{-4}	71.19	70.17
9	63.24	0.009	63.77	62.69
10	59.09	3.32×10^{-2}	54.24	63.01
11	68.92	4.37×10^{-4}	67.60	70.13
12	58.82	3.38×10^{-2}	53.33	63.16
13	60.00	3.13×10^{-2}	60.00	60.00
14	70.73	6.74×10^{-5}	72.73	68.42
15	56.90	6.05×10^{-2}	50.98	61.54
16	52.17	1.12×10^{-1}	52.17	52.17
17	60.53	1.71×10^{-2}	58.33	62.50
18	79.76	1.32×10^{-8}	80.00	79.52
19	65.71	3.00×10^{-3}	64.71	66.67
20	60.71	1.27×10^{-2}	61.18	60.24
21	62.86	9.50×10^{-3}	62.86	62.86
22	62.50	7.30×10^{-3}	61.54	63.41
23	61.54	1.14×10^{-2}	57.14	65.12
24	66.07	5.90×10^{-3}	62.74	68.85
25	50.00	1.17×10^{-1}	48.89	51.06
26	63.75	4.30×10^{-3}	64.20	63.29
27	78.21	2.08×10^{-7}	77.33	79.01
28	60.98	1.23×10^{-2}	60.00	61.90
29	68.18	1.20×10^{-3}	67.69	68.66
30	53.70	9.34×10^{-2}	56.14	50.98
Test Accuracy	61.87%			

6.6 Summary

It is crucial to design and develop an accurate emotion recognition system for the application in autonomous vehicles. This chapter presents the proposed SVM, NN, and LSTM schemes' classification performance using ECG and PPG signals from the CASE dataset. Two methods are evaluated, one using morphological features and the second using instantaneous frequency and spectral entropy. The first method provides relatively better accuracy compared to the second method. Moreover, it should be noted that the first method is computationally less demanding than the second. The proposed method of morphological signal improves the classification results of valence and arousal and proves that the 3-second window can provide insight into constantly changing emotional levels.

One study targeted ECG and PPG signals using the DEM method and used the same CASE dataset for reporting arousal and valence accuracy. Statistical features are extracted and trained in this study using an SVM classifier. Regarding results, happiness reached a test accuracy of 44%, relaxation of 67%, boredom of 55%, and fear of 44% [134]. The second paper focused on a similar approach using the DEM method. Here, four emotions, happiness, sadness, fear, and disgust, were elicited by showing videos and used to extract 35 features. Regarding results, the ensemble bagged trees classifier provided an average of 85.7% accuracy over four classes [151]. Contrary to the above two DEM-based studies, this study focused on ADM-based emotion assessment and provided results on per-subject classification.

Chapter 7

Employing Emotion Assessment in Autonomous Navigation

This chapter presents an approach to employing emotions in autonomous driving. First, Section 7.1 introduces this chapter. Then, Section 7.2 discusses the relationship between emotions and driving. Next, Section 7.3 discusses the simulation of controlling AGVs with different felt emotions. Finally, Section 7.4 is the summary of this chapter.

7.1 Introduction

Driving involves a variety of events and activities that stimulate emotional experiences. Emotion recognition applications in AGVs can improve the control and performance of AGVs. Human plays multiple roles when interacting with such vehicles; for example, they can be a driver of an AGV, they can be passenger of an AGV, and they can be bystanders. Emotion assessments can enable multiple applications for humans acting as a driver and passengers of AGVs. For example, AGVs can adapt to different speeds depending on identified emotions, AGV can monitor the human driver to ensure they are awake, observing the road conditions, and are ready to take over a vehicle when needed. On a long journey

and in safe road conditions, AGV can prompt to take over and monitor human emotions over time to get a reliable assessment of emotion. Moreover, AGVs can offer better multimedia choices depending on the driver's or passenger's felt emotions.

There are multiple definitions of the term 'emotion'. One study proposed a formal definition considering all traditionally significant aspects of emotion while attempting to differentiate it from other psychological processes. That is: "Emotion is a complex set of interactions among subjective and objective factors, mediated by neural hormonal systems, which can (a) give rise to affective experiences such as feelings of arousal, pleasure/displeasure; (b) generate cognitive processes such as emotionally relevant perceptual effects, appraisals, labelling processes; (c) activate widespread physiological adjustments to the arousing conditions; and (d) lead to behaviour that is often, but not always, expressive, goal-directed, and adaptive" [80].

To answer the question of why a driver feels particular emotion, one should consider that human emotion can be part of the following components: (a) a cognitive component; (b) a feeling component, referring to emotional experience; (c) a motivational component, consisting of action tendencies or states of action readiness (e.g., tendencies to flee or fight); (d) a somatic component, consisting of central and peripheral physiological responses; and (e) a motor component, consisting of expressive behaviour (e.g., fight and flight and facial and vocal expressions) [113]. In addition, the cause of the emotion is based on what is happening between the stimulus (the present scenario (stimulus) or input) and the emotion (the driver's response to that scenario or output). Moreover, a varied level of quality and quantity of present stimulus determines felt emotion.

Fig. 7.1 provides an overview of a possible implementation of such technology. For example, a driver can wear a wearable device consisting of ECG and PPG sensors. This wearable device continuously collects the driver's heart rate data and extracts meaningful features. These features are then sent to AGV's control unit to assess the emotional state

in which a machine-learning model can be employed. Then, the emotional state of a driver is derived. Finally, the vehicle controller takes this identified emotion as one of the tuning parameters to deliver a safe driving experience while enhancing trust between human and autonomous driving.

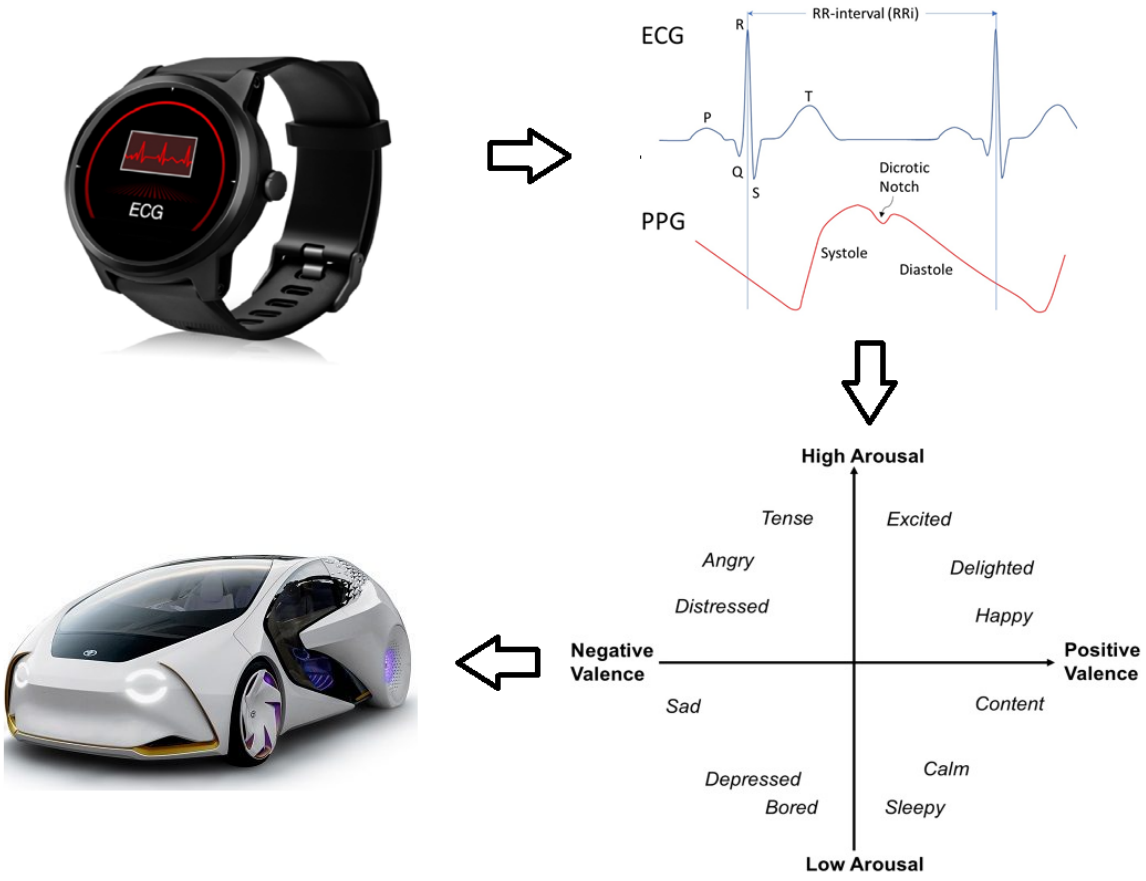

Fig. 7.1 Emotion Assessment for Autonomous Vehicles

7.2 Emotions and Driving Behaviour

Several emotions can influence driving behaviour. The aim of emotion recognition should be to support the driver in performing primary, secondary, and tertiary driving tasks. The primary driving task includes steering, accelerating, braking, and choosing the correct lane, speed,

route, and distance to other vehicles. The secondary driving task includes dimming, operating windscreen wipers, coupling, changing gears, and blinking, which can be considered safety-related. The tertiary driving task includes operating an air conditioner, seat heater, radio, and phone, mainly concerning comfort.

One of the primary psychological elements that affect driving is the driver's emotion, which can occasionally be uncontrolled by cognition and have an unplanned impact on driving habits. Emotion is a brief, readily influenced, and quickly alterable mental state that appears when something significant to us is at stake. It triggers a coordinated collection of behavioural, experiential, and physiological response patterns that affect how we react to perceived challenges and opportunities. Drivers are frequently impacted by their experiences while driving, particularly those that are emotionally upsetting. Consequently, researchers have become interested in the link between unfavourable emotions and driving behaviour. Table 7.1 presents the effects of negative emotions during driving tasks.

Table 7.1 Emotional States and Their Effect on Driving [65]

Emotions	**Impact on Driving**
Angry	Can contribute to road rage and accidents
Drowsiness	Can contribute to reduced judgement and alertness
Sadness	Can contribute to reduced reaction time
Confusion	Can contribute to reduced self-control and traffic violations
Nervous	Can contribute to reduced decision-making and concentration
Stressed	Can contribute to poor driving performance
Happiness	Very high level can contribute to negative performance

Effects of several emotions on driving tasks are studied and investigated [42].

- Aggressiveness and anger emotions can influence driving behaviour which often results in road rage and accidents. Moreover, low levels of such emotions are also linked with disrupting the driver's attention and concentration.

- Emotions like fatigue and drowsiness can be responsible for a low level of activation which causes sleepiness, thus impacting the ability to drive safely. In addition, as fatigue drops alertness and judgement, drivers are prone to accidents and their response time towards hazards is also slowed.

- Stress is another common emotion experienced by drivers. Driver's stress is the process of facing a situation where the perceived demand, primarily based on previous experiences, internal body sensations, and external stimuli, is higher than the available resources [48]. Stress can be acute or chronic and usually results in poor drive performance.

- Confusion during a driving task can result in reduced self-control and lead to traffic violations and accidents in some cases. A driver's confusion can arise from the defective in-car system or external situations such as complicated routes and diversions.

- Nervousness is an affective state that implies a level of arousal above the degree of activation best suited for the driving task. For example, a driver with nervousness can affect decision-making and concentration and is one of the most dangerous states during automobile driving.

- Sadness has a strong negative influence on driving performance. Sadness is associated with low arousal, which can significantly decrease the attention level. This emotion can have a negative impact on the driver's reaction time.

- Happiness has been reported to produce fewer accidents. Positive emotions, in general, were stated to have diverse impacts on numerous cognitive aspects. While a very high level of happiness might have a negative impact on the driver's performance, a moderate level could lead to ideal performance.

Therefore, AGVs should be able to monitor the driver's emotional state and take corresponding actions to ensure that the driver and surrounding AGVs and pedestrians can have a better experience with such technologies. Generally, humans/drivers exist in a state of equilibrium, neither too excited nor not excited enough. Therefore, for optimal performance, moderate stimulation is enough to be attentive to driving tasks and surroundings.

7.3 Emotions and their Effect on AGV

Different driving control and in-car experience can be provided to drivers or passengers, as discussed previously. This research considers the velocity control of an AGV resulting from identified emotions. Several emotions can be identified from a proposed approach in Chapter 6. This simulation considers one emotion from each quadrant of the circumplex model of affect and applies control law accordingly.

Fig. 7.2 shows four overall emotions resulting from the varied arousal and valence levels. In the circumplex model of affect, higher arousal activation (or positive arousal) and pleasant valence (or positive valence) are associated with emotions reflecting happiness. This quadrant includes emotions such as amused, delighted, excited, and astonished. Then, positive valence and negative arousal are associated with relaxed emotions. This quadrant covers emotions such as calm, satisfaction, serenity, and gladness. Next, negative arousal and negative valence are associated with emotions reflecting sadness. In this quadrant, emotions such as bored, depression, gloom, and misery are included. Finally, negative valence and positive arousal are associated with angry emotions. This quadrant has annoyed, scared, frustrated, and

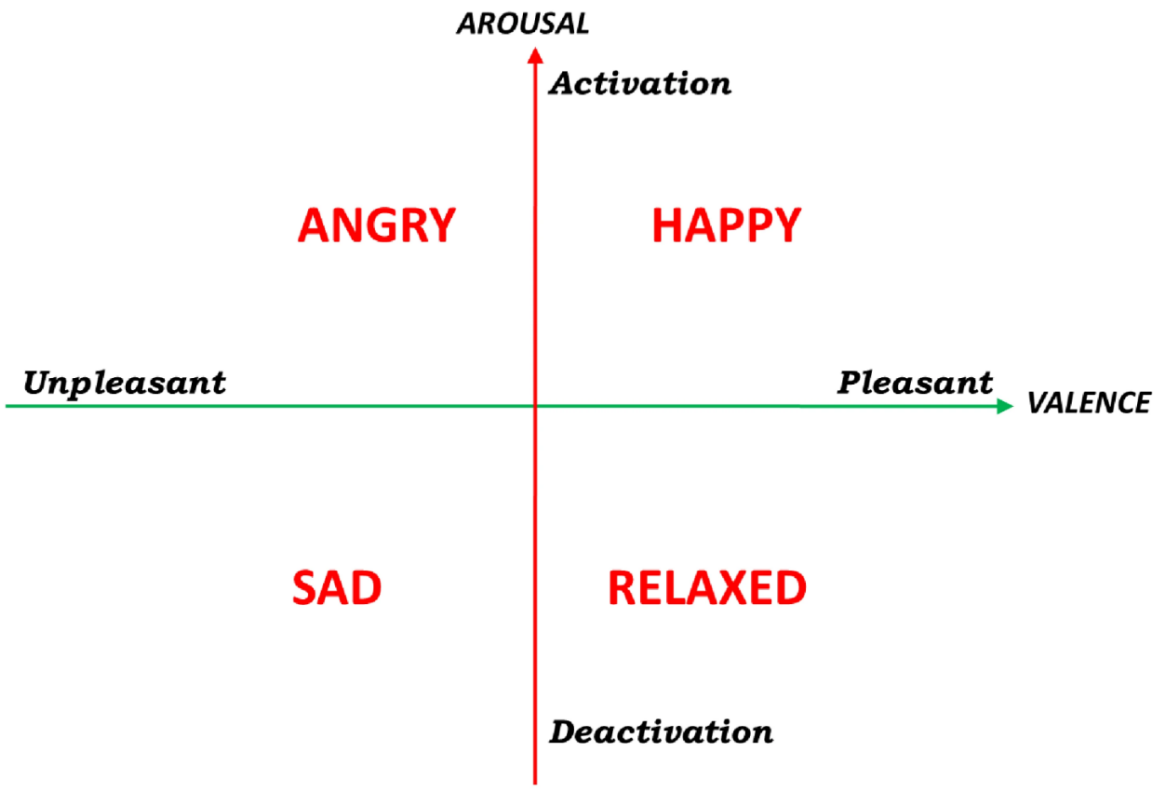

Fig. 7.2 Averaged Emotion in each Quadrant

tense emotions. In Chapter 6, four emotions were assessed, and they were amused, scared, relaxed, and bored. Therefore, the simulation in this study considers these four emotions. For simulation purposes, a driver feeling amused is considered the default emotion, and the transition between amused and the other three emotions is then simulated.

7.3.1 Transition between Amused and Relaxed Emotions

At first, a simulation of one AGV is carried out using a controller developed in Chapter 5. Then, a velocity versus time graph is provided to see the result of each emotion in controlling an AGV. It should be noted that an odometry graph will not provide the effect of velocity control; therefore, these trajectory graphs are not included. Here, the velocity for a driver feeling amused emotion is taken as 1 metre per second, and for a driver feeling relaxed emotion is 0.8 metre per second. Fig. 7.3 shows the velocity control of a vehicle. First, a

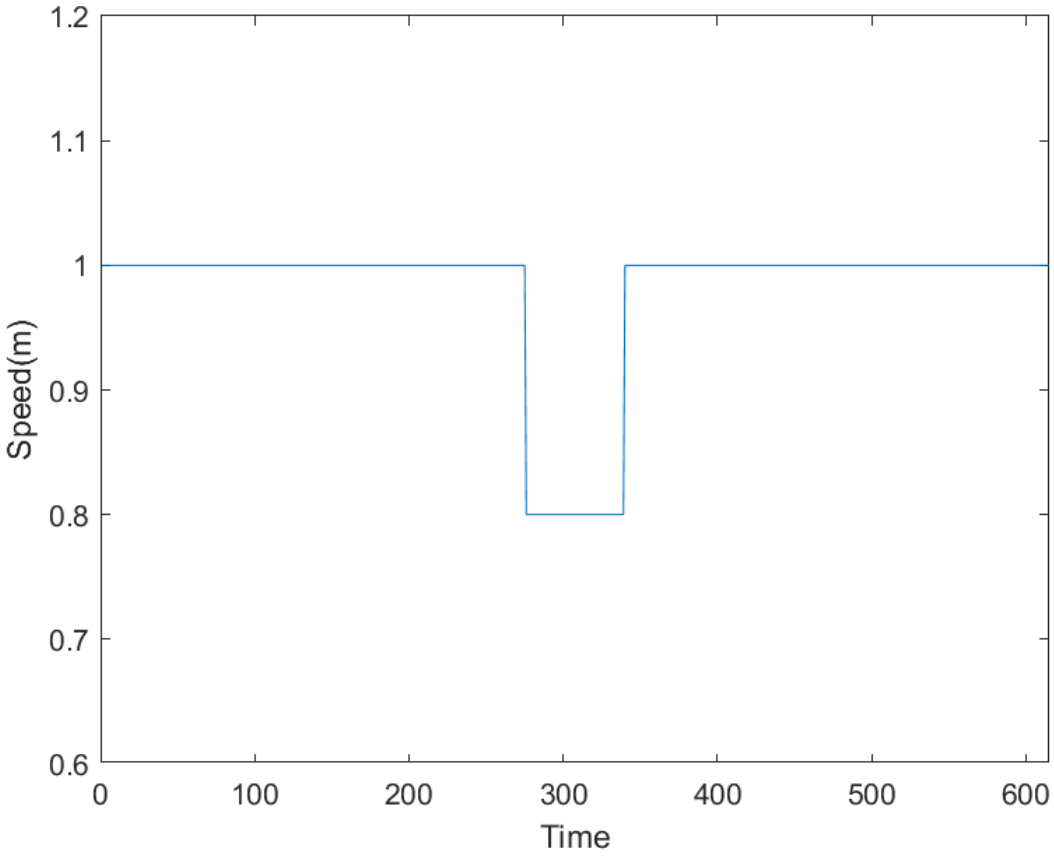

Fig. 7.3 Transition between Amused and Relaxed Emotions

driver feels amused; therefore, AGV produces relevant velocity. Once a driver feels relaxed, a vehicle can drive a little slower to improve the driving experience. Other controls can include changing an in-car ambient light and suggesting emotion-dependent music. As well as, a vehicle can prompt the driver to take control of the AGV.

7.3.2 Transition between Amused and Boring Emotions

The second scenario considers an emotional transition between amused and boring emotions. Lone and long driving can contribute to the driver feeling bored. Here, the velocity for a driver feeling amused emotion is 1 metre per second, and for a driver feeling bored is 0.5 metre per second. Fig. 7.4 shows the velocity control of a vehicle. First, a driver feels amused, and the vehicle produces relevant velocity. Once a driver starts feeling bored, a

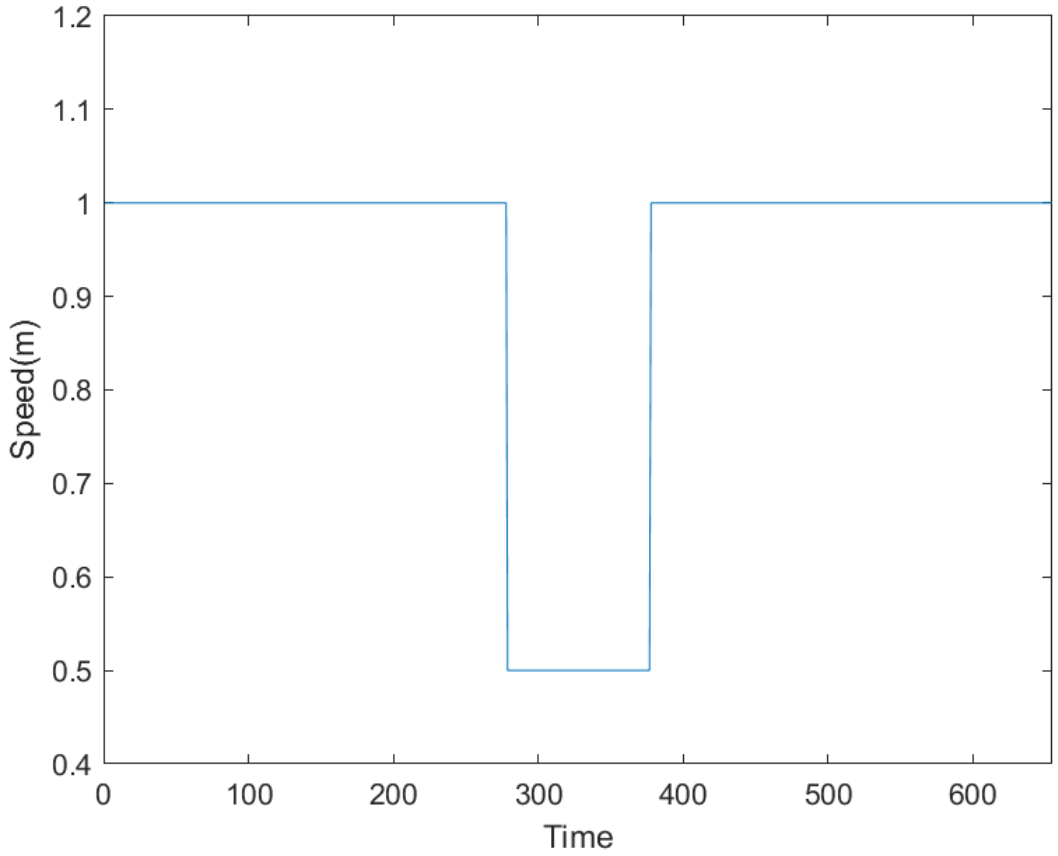

Fig. 7.4 Transition between Amused and Boring Emotions

vehicle can cut the speed by half to improve the driving experience. Other controls can include providing in-car voice assistance to improve the driver's alertness. As well as, a vehicle can take over control of an AGV if a driver is riding a vehicle. After restoring the driver's emotion to feeling amused, AGV can drive at a normal speed.

7.3.3 Transition between Amused and Scared Emotions

The third scenario considers an emotional transition between amused and scary emotions. Here, the velocity for a driver feeling amused emotion is 1 metre per second, and for a driver feeling scared is 0.1 metre per second. Fig. 7.5 shows the velocity control of a vehicle. First, a driver feels amused, and the vehicle produces relevant velocity. Once a driver feels scared, a vehicle can reduce speed significantly to improve the driving experience. As well as, a

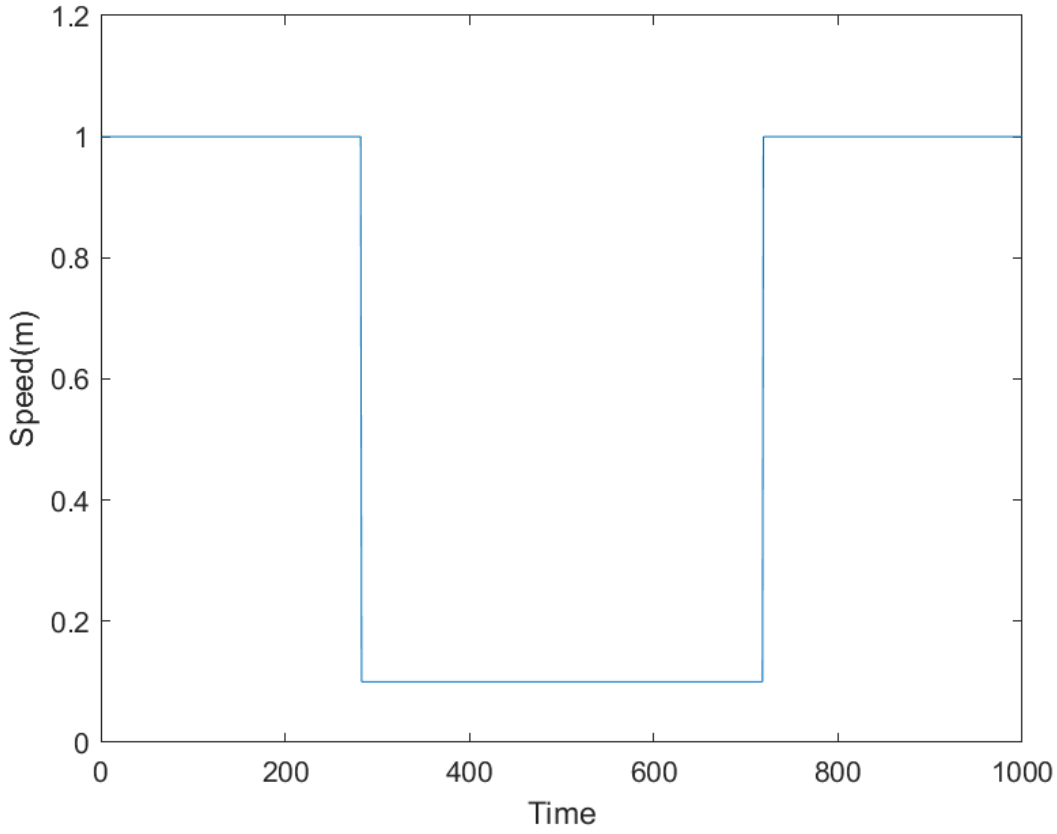

Fig. 7.5 Transition between Amused and Scary Emotions

vehicle can take over the control of an AGV if a driver is riding a vehicle. Other controls can include providing in-car voice assistance to improve the driver's alertness, stopping an AGV at a safe place, and calling for emergency assistance if needed. Once a driver's emotion is restored to default emotion, a vehicle will drive at normal speed. Overall, three scenarios are considered and simulated using a single AGV. The next study considers a response to platoon formation to these four emotions.

7.3.4 Emotions and their Effect on Platoon Formation

After simulating a single AGV and analysing the effect of velocity control using identified emotions, multiple AGVs are simulated. This simulation uses a controller developed in chapter 5 and introduces one variable for emotion to control the velocity. The same emotions

are considered as used for a single AGV simulation. Once autonomous vehicles are made available to consumers, a significant amount of such vehicles will drive on the road. Once a platoon is formed, other vehicles will have to change their control input depending on the vehicle in front of them in a formation.

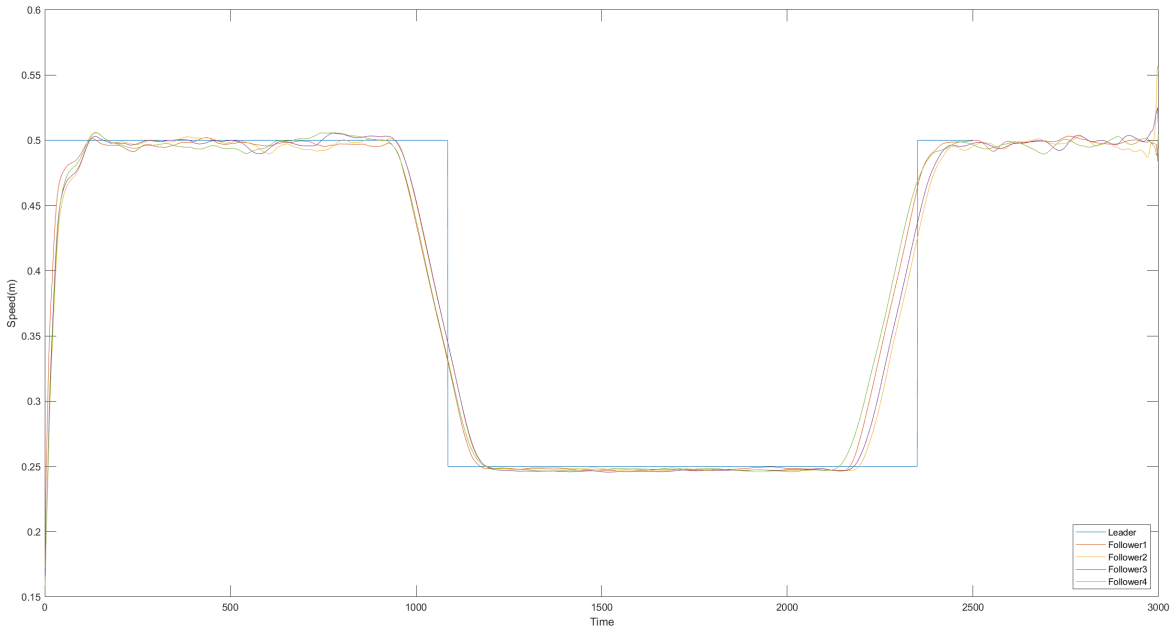

Fig. 7.6 Amused and Boring Emotions Transition - Platoon Formation

Fig. 7.6 shows the result of platoon formation under amused and boring emotions. Here, a leader vehicle's velocity during amused emotion is 0.5 meters per second and drops to 0.25 meters per second once boring emotion is identified. During this process, all follower vehicles adapt to the leader vehicle's velocity to maintain platoon formation. After transitioning from boring to amused emotion, all vehicles in platoon formation drive at a normal speed.

Fig. 7.7 shows the result of platoon formation under amused and relaxed emotions. Here, a leader vehicle's velocity during amused emotion is o.5 meters per second. Once a driver feels relaxed or relaxed emotion is identified, AGVs velocity is reduced to 0.4 meters per second. During this transition, all follower vehicles adapt to the leader vehicles' velocity to maintain platoon formation. After transitioning from relaxed to amused emotion, all vehicles

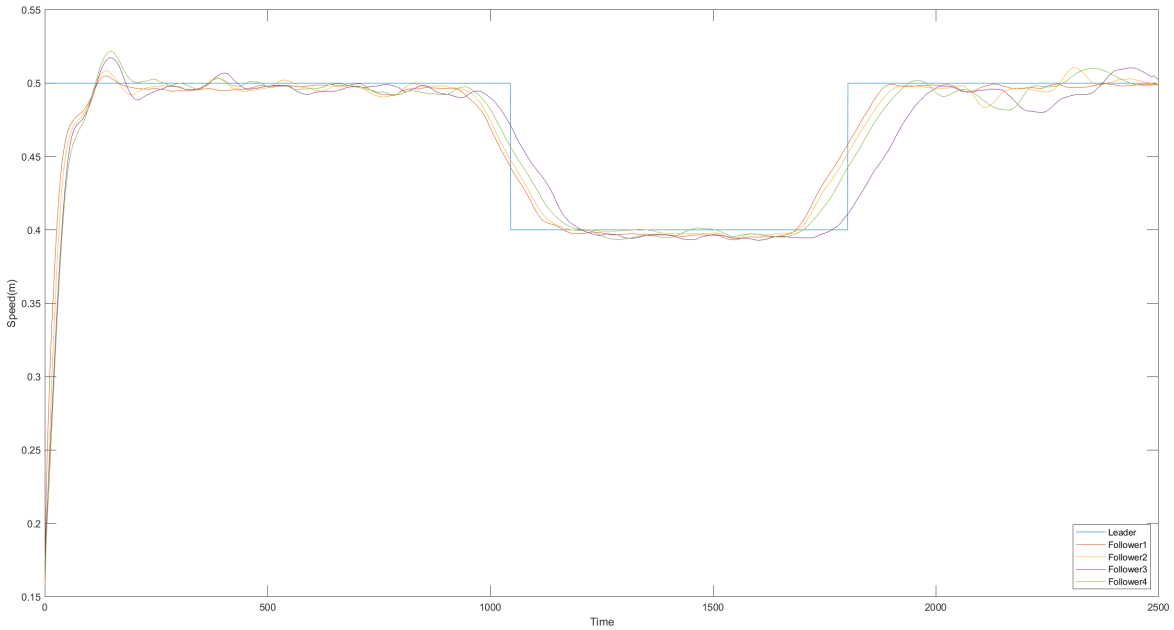

Fig. 7.7 Amused and Relaxed Emotions Transition - Platoon Formation

in platoon formation drive at a normal speed. Furthermore, a relaxed emotion can last for a prolonged amount of time. In this case, AGVs will continue to drive at the relevant velocity.

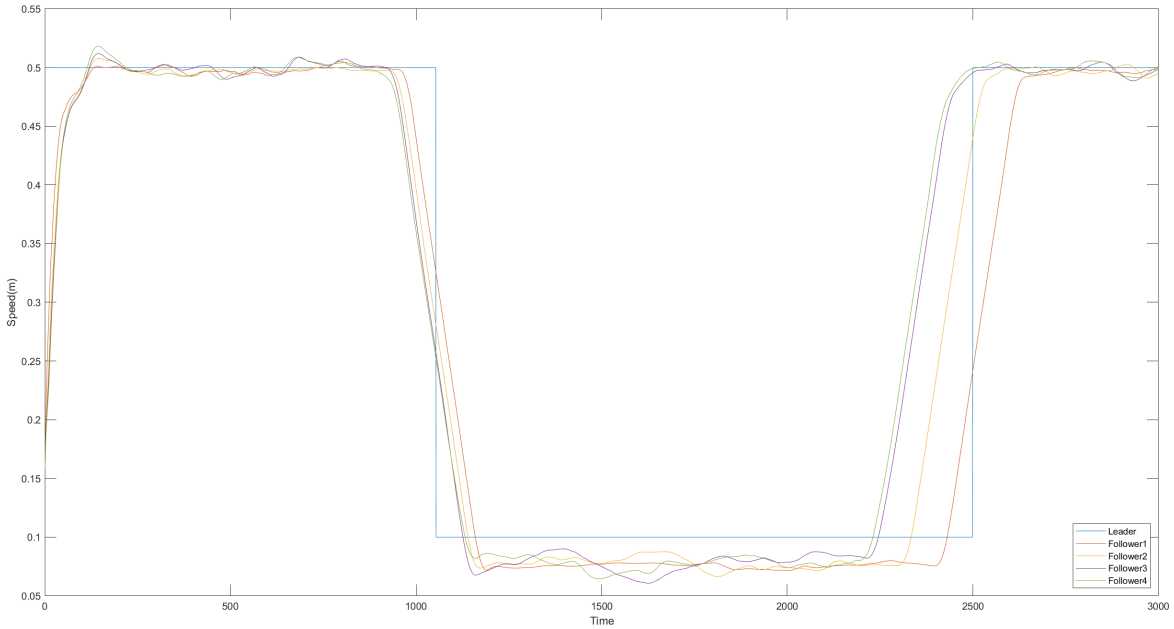

Fig. 7.8 Amused and Scary Emotions Transition - Platoon Formation

Fig. 7.8 shows the performance of platoon formation under amused and scary emotions. Here, a leader vehicle's velocity during amused emotion is 0.5 meters per second. Once a scary emotion is identified, AGV's velocity is reduced to 0.1 meters per second. During this transition, all follower vehicles adapt to the leader vehicle's velocity to maintain platoon formation. After transitioning from scary to amused emotion, all vehicles in platoon formation drive at a normal speed.

7.4 Summary

This chapter presented an understanding of emotions, why humans/drivers feel different emotions, and their impact on driving tasks. A couple of simulations are considered to see the effect of emotion on driving tasks. In the first scenario, one AGV is simulated with four emotions. In the second scenario, a platoon formation is simulated with four emotions. A velocity graph is considered to see the effect of control applied to vehicles. The limitation of this simulation study is that only linear velocity is considered for controlling AGVs using emotions. In a real-life scenario, non-linear conditions can be seen; thus AGVs should be able to control both linear and angular velocities. Moreover, this study targets the leader vehicle's emotion, and the resultant control commands are applied to all follower vehicles. There may be a scenario where the driver of a vehicle within a platoon experience different emotions than the leader vehicle. Therefore, a platoon formation should adjust depending on each driver's emotional state.

Chapter 8

Conclusion

This chapter presents the summary of this thesis. First, Section 8.1 summarises the research work. Then, Section 8.2 provides a summary of the achievements. Finally, Section 8.3 proposes future work to be conducted.

8.1 Research Summary

This thesis presents an approach to the formation control of AGVs, human emotion assessment using physiological sensors, and integration of human emotions to control the AGVs. The evolution of technology, such as AGVs and wearable technology, has tremendous exposure to human lives. Moreover, every day people are getting closure to these types of technologies. Therefore, finding a novel way to bring these technologies together and developing applications to improve the performance of these technologies could enhance the human experience. Furthermore, most research on developing controllers for AGVs considers feedback from sensors, actuators, and machines. However, human feedback is equally important; therefore, emotion assessment for AGVs could play a vital role in the overall operation of such vehicles. Four research questions are proposed to carry out this

study. First, RQ1 and RQ2 are answered in Chapters 4 and 5. Next, RQ3 is answered in Chapter 6. Finally, RQ4 is answered in Chapter 7.

Firstly, a literature review on developing multi-robot navigation controllers is presented, as covered in Chapter 2. The advantages and disadvantages of each method are discussed. Afterwards, several publications are discussed targeting multi-robot navigation, mainly using leader-follower, behaviour-based, and virtual structure approaches. Moreover, many academic publications are reviewed to understand the current developments in AGV technology, including controller design. Many researchers use the leader-follower approach for the vehicle platooning problem. A behaviour-based control has the advantage of being highly autonomous and having the ability to work in a distributed way. Then, literature on human emotion assessment methods is presented. Four commonly used methods are described, and they are vision-based, speech-based, text-based, and physiological sensor-based emotion recognition. A physiological sensor-based method is selected, and an understanding of ECG and PPG sensors is established. Finally, a review of the use of emotion assessment in autonomous driving is discussed.

A couple of controllers are implemented: MPC and leader-follower controllers, as covered in Chapters 4 and 5. MPC is one of the widely used advanced control algorithms. One advantage of using MPC is the ability to handle multiple inputs and constraints. However, this benefit comes at the cost of computational load as MPC needs to perform control computation at every iteration. Therefore, an MPC is implemented for multiple AGVs and shows the feasibility of simulating multiple AGVs in a Stage simulator. Afterwards, a multi-robot simulation based on ROS and Gazebo is presented by developing a leader-follower controller. Once the AGVs are deployed in the real world, these vehicles will follow the platoon formation. A leader-follower approach is a highly adaptable approach in this scenario. This approach can be implemented by establishing communication between vehicles. However, during the loss of communications, these vehicles depend on available sensor data. Therefore,

during the development of such a controller, the focus is placed on AGV navigation under the loss of communication. Finally, platoon formation control is enabled using only the laser scanner sensor and validated via a simulation study, as discussed in Chapter 5.

A novel emotion assessment method is developed to measure emotion using heart signals, as covered in Chapter 6. Most recent studies target EEG-based (brain signal) human emotions assessment and provide good results. However, from a practical point of view, such sensors are challenging to use daily or when driving an AGV. On the other hand, users widely accept a smartwatch, and significant advances are made in developing these watches. Moreover, several smartwatches are currently equipped with physiological sensors. Therefore, two methods are developed to measure emotions using ECG and PPG sensors. A morphological feature method offers better accuracy and is considered a fast approach than the second method, which extracts instantaneous frequency and spectral entropy. The classification accuracy is derived via three different classifiers, and it found that the results of morphological features are statistically significant.

Finally, an approach is presented that shows how emotions can be integrated to control AGVs, as covered in Chapter 7. This approach shows how emotions can be utilised to deliver a safe and comfortable driving experience while improving trust between such AGVs and humans. A simulation of AGVs' control is carried out using four different emotions and their effect on AGVs. In this approach, a specific emotion has a specific control of the speed for AGVs. Other applications, such as in-car multimedia assistance, voice assistance, and take-over and hand-over controls, are challenging to simulate. Therefore, these applications are not considered in this approach. Two studies were conducted to analyse the proposed approach. In the first study, a single AGV is simulated. Then, a platoon formation is simulated.

8.2 Thesis Contributions

This research study contributed to bringing together the field of AGV's control and measuring human emotions. Furthermore, the research work presented in this thesis contributed to several new solutions. The following list highlights the most significant contribution:

A non-linear model predictive controller is developed to study the behaviour of multi-robot navigation. The robot model is based on a bicycle model, and a simulation of one robot and multiple robots' navigation is proposed. A discussion about creating a simulation environment for multi-robot simulation is presented. After that, steps taken to develop a differential drive mobile robot and simulation world are presented. A laser sensor-based control algorithm is proposed and implemented on multiple robots for navigation. Finally, a rule-based algorithm is proposed capable of driving multiple robots in platoon formation using a laser sensor.

Novel emotion assessment methods are proposed by classifying felt valence and arousal levels. These methods use morphological features, instantaneous frequency, and spectral entropy of ECG and PPG signals. Compared with the current work mainly using EEG sensors, the proposed method is easy to implement in everyday life and can enhance the relationship between AGVs and humans. Furthermore, this method can easily be implemented on existing smartwatches consisting of ECG and PPG sensors.

Finally, the effect of human emotions on AGVs is simulated. Then, different scenarios based on emotions are considered and implemented. The overall benefit of this approach is that autonomous driving can be made safer. At present, automobile companies are working towards achieving the fifth level of autonomy, which is heavily focused on controlling AGVs using sensors and actuators. The result of this research can be used to propose the sixth level of autonomy, which includes human interaction with AGVs and assessing several human parameters to improve the driving experience.

The following journal and conference papers have been published during research:

- A. Soni and H. Hu (2018). Formation Control for a Fleet of Autonomous Ground Vehicles: A Survey. MDPI Robotics, 7(4):67.

- A. Soni and H. Hu, "A multi-robot simulator for the evaluation of formation control algorithms," The Proceedings of the 11th Computer Science and Electronic Engineering (CEEC), Colchester, United Kingdom, 2019, pp. 79-84.

The following emotions assessment patent is under consideration:

- K. Zhou and A. Soni (2020), "Improvements in or Relating to Wearable Sensor Apparatus (GB Patent No. GB2016726.8)", UK Intellectual Patent Office.

The following papers have been planned for potential publication:

- A. Soni, I. Daly, H. Zhang, H. Hu, D. Gu, and K. Zhou (2023), "Using Electrocardiogram and Photoplethysmography Data to Assess Human Emotions", to be submitted to IEEE Sensors for review.

- A. Soni and H. Hu (2023), "Using Human Emotions to Optimise a Control of Autonomous Ground Vehicles", to be submitted to IEEE Conference for review.

8.3 Future Work

This thesis presents novel methods for formation control under communication loss and human emotion assessment. Some challenges have been addressed, yet several problems remain and can be summarised as follows.

- A dynamic role-changing leader should be targeted in a leader-follower approach. Platoon formation is temporary; some vehicles may join and leave the platoon. Therefore, the platoon formation controller should adapt to these challenges. Considering the swarm intelligence-based algorithms, it can be observed that they can handle a

population of AGVs, but they do not offer formation control ability. Therefore, new parameters or another algorithm should be implemented along with these algorithms.

- A couple of implementation challenges require solutions to deploy AGVs successfully. One is the lane merging and changing of the vehicles, which requires cooperation between vehicles and platoons in an uncoordinated traffic environment. Estimating other vehicles' intentions and information sharing between vehicles is vital in these operations. The second is the response to emergency vehicles. Giving way to emergency vehicles such as ambulances and police vehicles is another challenge that requires developing specific controllers for AGVs. If these vehicles encounter existing vehicle formations, what should be the behaviour of the formation and vehicles inside the formations?

- For emotion assessment, two features are considered in this thesis. However, it should be noted that other features can be extracted, particularly in physiological signals. Therefore, more methods can be derived to extract features to check whether it improves the accuracy of the classifier.

- Implementation of emotion assessment via wearable technology and deriving subsequent control based on a human's present emotion still need to be explored from a practical implementation point of view. This thesis provides an approach to how this can be made possible. A feasibility study should be conducted on integrating and realising these approaches in a practical scenario. Several smartwatches are already equipped with ECG and PPG sensors. However, fully autonomous vehicles are yet to be available to consumers.

References

[1] Ab Wahab, M. N., Nefti-Meziani, S., and Atyabi, A. (2015). A comprehensive review of swarm optimization algorithms. *PLOS ONE*, 10.

[2] Abadi, M., Subramanian, R., Kia, S., Avesani, P., Patras, I., and Sebe, N. (2015). Decaf: Meg-based multimodal database for decoding affective physiological responses. *IEEE Transactions on Affective Computing*, 6:209–222.

[3] Acheampong, F., Wenyu, C., and Nunoo-Mensah, H. (2020). Text-based emotion detection: Advances, challenges, and opportunities. *Engineering Reports*, 2.

[4] Affanni, A., Najafi, T. A., and Guerci, S. (2022). Development of an eeg headband for stress measurement on driving simulators. *MDPI - Sensors*, 22:1785.

[5] Agrafioti, F., Hatzinakos, D., and Anderson, A. (2012). Ecg pattern analysis for emotion detection. *IEEE Transactions on Affective Computing*, 3:102–115.

[6] Amoozadeh, M., Deng, H., Chuah, C.-N., Zhang, H. M., and Ghosal, D. (2015). Platoon management with cooperative adaptive cruise control enabled by vanet. *Vehicular Communications*, 2:110–123.

[7] Arkin, R. C. (1998). *Behavior-based robotics*. Mit Press.

[8] Balch, T. and Arkin, R. (1998). Behavior-based formation control for multirobot teams. *IEEE Transactions on Robotics and Automation*, 14:926–939.

[9] Bang, S. and Ahn, S. (2017). Platooning strategy for connected and autonomous vehicles: Transition from light traffic. *Transportation Research Record: Journal of the Transportation Research Board*, 2623:73–81.

[10] Bernardo, M. d., Salvi, A., Santini, S., and Valente, A. S. (2015). Third-order consensus in vehicles platoon with heterogeneous time-varying delays. *IFAC-PapersOnLine*, 48:358–363.

[11] BioSec.Lab PPG Dataset (Biosec1) - Benchmark Dataset for PPG Biometrics (2022). Photoplethysmograph (ppg) based biometric recognition. [online] https://www.comm.utoronto.ca/~biometrics/PPG_Dataset/index.html.

[12] Birk, A. (1998). Behavior-based robotics, its scope and its prospects. *IECON '98. proceedings of the 24th Annual Conference of the IEEE Industrial Electronics Society (Cat. No.98CH36200)*, Aachen, Germany.

[13] Boashash, B. (1992). Estimating and interpreting the instantaneous frequency of a signal, part-1: Fundamentals. *Proceedings of the IEEE*, 80:520–538.

[14] Bradley, M., Greenwald, M., Petry, M., and Lang, P. (1992). Remembering pictures: Pleasure and arousal in memory. *Journal of Experimental Psychology: Learning, Memory, and Cognition*, 18:379–390.

[15] Bull, A. (2011). Convergence rates of efficient global optimization algorithms. *arXiv - stat.ML*.

[16] Chan, L. and Baoli, M. (2015). A nonlinear formation control of wheeled mobile robots with virtual structure approach. *2015 34th Chinese Control Conference (CCC)*, Hangzhou, China.

[17] Chandra Mohan, B. and Baskaran, R. (2012). A survey: Ant colony optimization based recent research and implementation on several engineering domain. *Expert Systems with Applications*, 39:4618–4627.

[18] Chawla, M. and Duhan, M. (2015). Bat algorithm: A survey of the state-of-the-art. *Applied Artificial Intelligence*, 29:617–634.

[19] Chehardoli, H. and Homaeinezhad, M. (2017a). Stable control of a heterogeneous platoon of vehicles with switched interaction topology, time-varying communication delay and lag of actuator. *proceedings of the Institution of Mechanical Engineers, Part C: Journal of Mechanical Engineering Science*, 231:4197–4208.

[20] Chehardoli, H. and Homaeinezhad, M. (2018). Third-order leader-following consensus protocol of traffic flow formed by cooperative vehicular platoons by considering time delay: constant spacing strategy. *proceedings of of the Institution of Mechanical Engineers, Part I: Journal of Systems and Control Engineering*, 232:285–298.

[21] Chehardoli, H. and Homaeinezhad, M. R. (2017b). Third-order safe consensus of heterogeneous vehicular platoons with mpf network topology: Constant time headway strategy. *proceedings of the Institution of Mechanical Engineers, Part D: Journal of Automobile Engineering*, 232:1402–1413.

[22] Chen, G. and Lewis, F. L. (2010). Leader-following control for multiple inertial agents. *International Journal of Robust and Nonlinear Control*, 21:925–942.

[23] Chen, X. and Jia, Y. (2015). Adaptive leader-follower formation control of non-holonomic mobile robots using active vision. *IET Control Theory and Applications*, 9:1302–1311.

[24] Chen, Y. Q. and Wang, Z. (2005). Formation control: a review and a new consideration. *IEEE/RSJ International Conference on Intelligent Robots and Systems*, Edmonton, AB, Canada:3181–3186.

[25] Christi, D., Koymans, A., Chanard, T., Lasgouttes, J., and Kaufmann, V. (2016). Pioneering driverless electric vehicles in europe: The city automated transport system (cats). *Transportation Research Procedia*, 13:30–39.

[26] Chunyu, J., Qu, Z., Pollak, E., and Falash, M. (2009). *A New Multi-objective Control Design for Autonomous Vehicles*, pages 81–102. Optimization and Cooperative Control Strategies. Springer.

[27] Cook, D., Vardy, A., and Lewis, R. (2014). A survey of auv and robot simulators for multi-vehicle operations. *2014 IEEE/OES Autonomous Underwater Vehicles (AUV)*, Oxford, MS, USA.

[28] Darwin, C. (1872). *The Expression of the Emotions in Man and Animals.* John Murray.

[29] di Bernardo, M., Falcone, P., Salvi, A., and Santini, S. (2015a). Design, analysis, and experimental validation of a distributed protocol for platooning in the presence of time-varying heterogeneous delays. *IEEE Transactions on Control Systems Technology*, 24.

[30] di Bernardo, M., Salvi, A., and Santini, S. (2015b). Distributed consensus strategy for platooning of vehicles in the presence of time-varying heterogeneous communication delays. *IEEE Transactions on Intelligent Transportation Systems*, 16:102–112.

[31] Dimarogonas, D. and Kyriakopoulos, K. (2006). A connection between formation control and flocking behavior in nonholonomic multiagent systems. *2006 IEEE International Conference on Robotics and Automation, 2006. ICRA 2006.*, Orlando, FL, USA.

[32] Do, K. (2008). Formation tracking control of unicycle-type mobile robots with limited sensing ranges. *IEEE Transactions on Control Systems Technology*, 16:527–538.

[33] Dong, J., Chen, H. T., and Liu, S. (2012). A behavior-based policy for multirobot formation control. *Applied Mechanics and Materials*, 220-223:1181–1185.

[34] Dong, L., Chen, Y., and Qu, X. (2016). Formation control strategy for nonholonomic intelligent vehicles based on virtual structure and consensus approach. *Procedia Engineering*, 137:415–424.

[35] Dorigo, M., Caro, G. D., and Gambardella, L. M. (1999). Ant algorithms for discrete optimization. *Artificial Life*, 5:137–172.

[36] Du, N., Zhou, F., Pulver, E. M., Tilbury, D. M., Robert, L. P., Pradhan, A. K., and Yang, X. J. (2020). Examining the effects of emotional valence and arousal on takeover performance in conditionally automated driving. *Transportation Research Part C*, 112:78–87.

[37] Dzedzickis, A., A., K., and V., B. (2020). Human emotion recognition: Review of sensors and methods. *MDPI Robotics*, 20:592.

[38] Egger, M., Ley, M., and Hanke, S. (2019). Emotion recognition from physiological signal analysis: A review. *Electronic Notes in Theoretical Computer Science*, 343:35–55.

[39] Ekman, P. (2009). Darwin's contributions to our understanding of emotional expressions. *Philos Trans R Soc Lond B Biol Sci.*, 364:3449–3451.

[40] Elkilany, B. G., Abouelsoud, A. A., and Fathelbab, A. M. (2017). Adaptive formation control of robot swarms using optimized potential field method. *2017 IEEE International Conference on Industrial Technology (ICIT)*, Toronto, ON, Canada.

[41] Essghaier, A., Beji, L., Kamel, M. E., Abichou, A., and Lerbet, J. (2011). Co-leaders and a flexible virtual structure based formation motion control. *International Journal of Vehicle Autonomous Systems*, 9:108.

[42] Eyben, F., Wollmer, M., Poitschke, T., Schuller, B., Blaschke, C., Farber, B., and Nguyen-Thien, N. (2010). Emotion on the road—necessity, acceptance, and feasibility of affective computing in the car. *Advances in Human-Computer Interaction*, 2010:17.

[43] Faisal, A., Kamruzzaman, M., Yigitcanlar, T., and Currie, G. (2019). Understanding autonomous vehicles: A systematic literature review on capability, impact, planning and policy. *Journal of Transport and Land Use*, 12:45–72.

[44] Faris, H., Aljarah, I., Al-Betar, M. A., and Mirjalili, S. (2017). Grey wolf optimizer: a review of recent variants and applications. *Neural Computing and Applications*, 30:413–435.

[45] Fernandes, P. and Nunes, U. (2010). Platooning of autonomous vehicles with intervehicle communications in sumo traffic simulator. *13th International IEEE Conference on Intelligent Transportation Systems*, Funchal, Portugal.

[46] Fernandes, P. and Nunes, U. (2015). Multiplatooning leaders positioning and cooperative behavior algorithms of communicant automated vehicles for high traffic capacity. *IEEE Transactions on Intelligent Transportation Systems*, 16:1172–1187.

[47] Foote, T. (2013). tf: The transform library. *IEEE Conference on Technologies for Practical Robot Applications (TePRA)*, Woburn, MA, USA:1–6.

[48] Francis, A. (2018). The embodied theory of stress: A constructionist perspective on the experience of stress. *Review of General Psychology*, 22:398–405.

[49] Gazis, D. C., Herman, R., and Potts, R. B. (1959). Car-following theory of steady-state traffic flow. *Operations Research*, 7:499–505.

[50] Gazis, D. C., Herman, R., and Potts, R. B. (1961). Nonlinear follow-the-leader models of traffic flow. *Operations Research*, 9:545–567.

[51] Goshvarpour, A. and Goshvarpour, A. (2018). Poincaré's section analysis for ppg-based automatic emotion recognition. *Chaos, Solitons & Fractals*, 114:400–407.

[52] GOV.UK (2020). Centre for connected and autonomous vehicles. [online] https://www.gov.uk/government/organisations/centre-for-connected-and-autonomous-vehicles.

[53] Grandi, R., Falconi, R., and Melchiorri, C. (2013). Coordination and control of autonomous mobile robot groups using a hybrid technique based on particle swarm optimization and consensus. *2013 IEEE International Conference on Robotics and Biomimetics (ROBIO)*, Shenzhen, China.

[54] Guo, H.-W., Huang, Y.-S., Lin, C.-H., Chien, J.-C., Haraikawa, K., and Shieh, J.-S. (2016). Heart rate variability signal features for emotion recognition by using principal component analysis and support vectors machine. *2016 IEEE 16th International Conference on Bioinformatics and Bioengineering (BIBE)*, Taichung, Taiwan:274–277.

[55] Haag, A., Goronzy, S., Schaich, P., and Williams, J. (2004). *Emotion Recognition Using Bio-sensors: First Steps towards an Automatic System*, pages 36–48. Affective Dialogue Systems. Berlin, Heidelberg: Springer.

[56] Han, G., Fu, W., and Wang, W. (2016). The study of intelligent vehicle navigation path based on behavior coordination of particle swarm. *Computational Intelligence and Neuroscience*, 2016:1–10.

[57] Handayani, A. S., Husni, N. L., Nurmaini, S., and Yani, I. (2017). Formation control design for real swarm robot using fuzzy logic. *2017 International Conference on Electrical Engineering and Computer Science (ICECOS)*, Palembang, Indonesia.

[58] Harris, A. and Conrad, J. M. (2011). Survey of popular robotics simulators, frameworks, and toolkits. *2011 proceedings of IEEE Southeastcon*, Nashville, TN, USA.

[59] Hayashi, Y. and Namerikawa, T. (2016). Flocking algorithm for multiple nonholonomic cars. *2016 55th Annual Conference of the Society of Instrument and Control Engineers of Japan (SICE)*, Tsukuba, Japan.

[60] Hentout, A., Maoudj, A., and Bouzouia, B. (2016). A survey of development frameworks for robotics. *2016 8th International Conference on Modelling, Identification and Control (ICMIC)*, Algiers, Algeria.

[61] Hochreiter, S. and Schmidhuber, J. (1997). Long short-term memory. *Neural Computation*, 9:1735–1780.

[62] Huang, Z., Chu, D., Wu, C., and He, Y. (2019). Path planning and cooperative control for automated vehicle platoon using hybrid automata. *IEEE Transactions on Intelligent Transportation Systems*, 20:959–974.

[63] Izquierdo-Reyes, J., Ramirez-Mendoza, R. A., Bustamante-Bello, M. R., Pons-Rovira, J. L., and Gonzalez-Vargas, J. E. (2018). Emotion recognition for semi-autonomous vehicles framework. *International Journal on Interactive Design and Manufacturing (IJIDeM)*, 12:1447–1454.

[64] J3016-202104 (2021). Taxonomy and definitions for terms related to driving automation systems for on-road motor vehicles. [online] https://www.sae.org/standards/content/j3016_202104.

[65] Jeon, M. (2015). Towards affect-integrated driving behaviour research. *Theoretical Issues in Ergonomics Science*, 16:553 – 585.

[66] Jia, D. and Ngoduy, D. (2016a). Enhanced cooperative car-following traffic model with the combination of v2v and v2i communication. *Transportation Research Part B: Methodological*, 90:172–191.

[67] Jia, D. and Ngoduy, D. (2016b). Platoon based cooperative driving model with consideration of realistic inter-vehicle communication. *Transportation Research Part C: Emerging Technologies*, 68:245–264.

[68] Jia, D., Ngoduy, D., and Vu, H. L. (2018). A multiclass microscopic model for heterogeneous platoon with vehicle-to-vehicle communication. *Transportmetrica B: Transport Dynamics*, 7:311–335.

[69] Kamel, M. A., Yu, X., and Zhang, Y. (2016). Real-time optimal formation reconfiguration of multiple wheeled mobile robots based on particle swarm optimization. *2016 12th World Congress on Intelligent Control and Automation (WCICA)*, Guilin, China.

[70] Karaboga, D. and Basturk, B. (2007). A powerful and efficient algorithm for numerical function optimization: artificial bee colony (abc) algorithm. *Journal of Global Optimization*, 39:459–471.

[71] Karaboga, D. and Basturk, B. (2008). On the performance of artificial bee colony (abc) algorithm. *Applied Soft Computing*, 8:687–697.

[72] Karaboga, D., Gorkemli, B., Ozturk, C., and Karaboga, N. (2012). A comprehensive survey: artificial bee colony (abc) algorithm and applications. *Artificial Intelligence Review*, 42:21–57.

[73] Karegowda, A. and Prasad, M. (2013). A survey of applications of glowworm swarm optimization algorithm. *proceedings of the 2013 IJCA International Conference on Computing and Information Technology*.

[74] Katsis, C. D., Katertsidis, N., Ganiatsas, G., and Fotiadis, D. I. (2008). Toward emotion recognition in car-racing drivers: A biosignal processing approach. *IEEE Transactions on Systems, Man, and Cybernetics - Part A: Systems and Humans*, 38:502–512.

[75] Kavathekar, P. and Chen, Y. (2012). Vehicle platooning: A brief survey and categorization. *2011 ASME/IEEE International Conference on Mechatronic and Embedded Systems and Applications, Parts A and B*, Washington, DC, USA.

[76] Kennedy, J. and Eberhart, R. (1995). Particle swarm optimization. *ICNN'95 - International Conference on Neural Networks*, Perth, WA, Australia.

[77] Keren, G., Kirschstein, T., Marchi, E., F., R., and Schuller, B. (2017). End-to-end learning for dimensional emotion recognition from physiological signals. *2017 IEEE International Conference on Multimedia and Expo (ICME)*, Hong Kong, China:985–990.

[78] Kim, K., Bang, S., and Kim, S. (2004). Emotion recognition system using short-term monitoring of physiological signals. *Medical & Biological Engineering & Computing*, 42:419–427.

[79] Kingma, D. and Ba, J. (2017). Adam: A method for stochastic optimization. *arXiv - cs.LG*.

[80] Kleinginna, P. and Kleinginna, A. (1981). A categorized list of emotion definitions, with suggestions for a consensual definition. *Motivation and Emotion*, 5:345–379.

[81] Ko, B. (2018). A brief review of facial emotion recognition based on visual information. *MDPI Sensors*, 18:401.

[82] Koelstra, S., Muehl, C., Soleymani, M., Lee, J.-S., Yazdani, A., Ebrahimi, T., Pun, T., Nijholt, A., and Patras, I. (2012). Deap: A database for emotion analysis using physiological signals. *IEEE Transactions on Affective Computing*, 3:18–31.

[83] Koolagudi, S. and Rao, K. (2012). Emotion recognition from speech: a review. *International Journal of Speech Technology*, 15:99–117.

[84] Krishnanand, K. and Ghose, D. (2005). Detection of multiple source locations using a glowworm metaphor with applications to collective robotics. *Proceedings 2005 IEEE Swarm Intelligence Symposium, 2005. SIS 2005*, Pasadena, CA, USA.

[85] Kuhn, T. S. (1962). *The structure of scientific revolutions*. Chicago: University of Chicago Press.

[86] Kuppan Chetty, R., Singaperumal, M., and Nagarajan, T. (2012). Behavior based multi robot formations with active obstacle avoidance based on switching control strategy. *Advanced Materials Research*, 433-440:6630–6635.

[87] Kusal, S., Patil, S., Choudrie, J., Kotecha, K., Vora, D., and Pappas, I. (2022). A review on text-based emotion detection – techniques, applications, datasets, and future directions. *ARXIV - CS*, page 74.

[88] Lawton, J., Beard, R., and Young, B. (2003). A decentralized approach to formation maneuvers. *IEEE Transactions on Robotics and Automation*, 19:933–941.

[89] Lee, G. and Chwa, D. (2017). Decentralized behavior-based formation control of multiple robots considering obstacle avoidance. *Intelligent Service Robotics*, 11:127–138.

[90] Lee, H.-G., Kang, D.-H., and Kim, D.-H. (2021). Human–machine interaction in driving assistant systems for semi-autonomous driving vehicles. *MDPI - Electronics*, 10:2405.

[91] Lee, M., Lee, Y., Pae, D., Lim, M., Kim, D., and Kang, T. (2019). Fast emotion recognition based on single pulse ppg signal with convolutional neural network. *Applied Sciences*, 9:3355.

[92] Lee, S.-M. and Myung, H. (2012). Particle swarm optimization-based receding horizon control for multi-robot formation. *2012 9th International Conference on Ubiquitous Robots and Ambient Intelligence (URAI)*, Daejeon, Korea.

[93] Lee, S.-M. and Myung, H. (2013). *Cooperative Particle Swarm Optimization-Based Predictive Controller for Multi-robot Formation*, pages 533–541. Intelligent Autonomous Systems 12. Springer.

[94] Lei, B. and Li, W. (2008). *Formation Control for Multi-robots Based on Flocking Algorithm*, pages 1238–1247. Intelligent Robotics and Applications. Springer.

[95] Li, G., Xu, H., and Lin, Y. (2018a). Application of bat algorithm based time optimal control in multi-robots formation reconfiguration. *Journal of Bionic Engineering*, 15:126–138.

[96] Li, R., Zhang, L., Han, L., and Wang, J. (2017). Multiple vehicle formation control based on robust adaptive control algorithm. *IEEE Intelligent Transportation Systems Magazine*, 9:41–51.

[97] Li, S. E., Zheng, Y., Li, K., and Wang, J. (2015). An overview of vehicular platoon control under the four-component framework. *2015 IEEE Intelligent Vehicles Symposium (IV)*.

[98] Li, Y., Li, K., Zheng, T., Hu, X., Feng, H., and Li, Y. (2016). Evaluating the performance of vehicular platoon control under different network topologies of initial states. *Physica A: Statistical Mechanics and its Applications*, 450:359–368.

[99] Li, Z., Yuan, W., Chen, Y., Ke, F., Chu, X., and Chen, C. L. P. (2018b). Neural-dynamic optimization-based model predictive control for tracking and formation of nonholonomic multirobot systems. *IEEE Transactions on Neural Networks and Learning Systems*, 29:6113–6122.

[100] Liu, B. and El Kamel, A. (2016). V2x-based decentralized cooperative adaptive cruise control in the vicinity of intersections. *IEEE Transactions on Intelligent Transportation Systems*, 17:644–658.

[101] Lorente, M. P. S., Lopez, E. M., Florez, L. A., Espino, A. L., Martínez, J. A. I., and Sanchis de Miguel, A. (2021). Explaining deep learning-based driver models. *MDPI - Applied Sciences*, 11:3321.

[102] Loria, A., Dasdemir, J., and Alvarez Jarquin, N. (2016). Leader–follower formation and tracking control of mobile robots along straight paths. *IEEE Transactions on Control Systems Technology*, 24:727–732.

[103] Low, C. B. (2015). Adaptable virtual structure formation tracking control design for nonholonomic tracked mobile robots, with experiments. *2015 IEEE 18th International Conference on Intelligent Transportation Systems*, Gran Canaria, Spain.

[104] Maei, H. R. and Sutton, R. S. (2010). Gq( ): A general gradient algorithm for temporal-difference prediction learning with eligibility traces. *3d Conference on Artificial General Intelligence (AGI-10)*.

[105] Maghenem, M., Loria, A., and Panteley, E. (2018). A robust delta-persistently exciting controller for leader-follower tracking-agreement of multiple vehicles. *European Journal of Control*, 40:1–12.

[106] Mariottini, G., Morbidi, F., Prattichizzo, D., Vander Valk, N., Michael, N., Pappas, G., and Daniilidis, K. (2009). Vision-based localization for leader–follower formation control. *IEEE Transactions on Robotics*, 25:1431–1438.

[107] Marjovi, A., Vasic, M., Lemaitre, J., and Martinoli, A. (2015). Distributed graph-based convoy control for networked intelligent vehicles. *2015 IEEE Intelligent Vehicles Symposium (IV)*, Seoul, Korea.

[108] Mataric, M. and Michaud, F. (2008). *Behavior-Based Systems - Handbook 0f Robotics*, pages 891–909. Springer, Heidelberg.

[109] Mehrabian, A. (1996). Pleasure-arousal-dominance: A general framework for describing and measuring individual differences in temperament. *Current Psychology*, 14:261–292.

[110] Meza-García, B. and Rodríguez-Ibáñez, N. (2021). Driver's emotions detection with automotive systems in connected and autonomous vehicles (cavs). *Proceedings of the 5th International Conference on Computer-Human Interaction Research and Applications - SUaaVE*, pages 258–265.

[111] Miranda-Correa, J., Abadi, M., Sebe, N., and Patras, I. (2018). Amigos: A dataset for affect, personality and mood research on individuals and groups. *IEEE Transactions on Affective Computing*, 12:479–493.

[112] Mirjalili, S., Mirjalili, S. M., and Lewis, A. (2014). Grey wolf optimizer. *Advances in Engineering Software*, 69:46–61.

[113] Moors, A. (2009). Theories of emotion causation: A review. *Cognition and Emotion*, 23:625–662.

[114] Moraes, J. L., Rocha, M. X., Vasconcelos, G. G., Vasconcelos Filho, J. E., De Albuquerque, V. H. C., and Alexandria, A. R. (2018). Advances in photopletysmography signal analysis for biomedical applications. *MDPI - Sensors*, 18:1894.

[115] Murugappan, M., Murugappan, S., and Zheng, B. (2013). Frequency band analysis of electrocardiogram (ecg) signals for human emotional state classification using discrete wavelet transform (dwt). *Journal of Physical Therapy Science*, 25:753–759.

[116] Navarro, I., Zimmermann, F., Vasic, M., and Martinoli, A. (2016). Distributed graph-based control of convoys of heterogeneous vehicles using curvilinear road coordinates. *2016 IEEE 19th International Conference on Intelligent Transportation Systems (ITSC)*, Rio de Janeiro, Brazil.

[117] Neshat, M., Sepidnam, G., Sargolzaei, M., and Toosi, A. N. (2012). Artificial fish swarm algorithm: a survey of the state-of-the-art, hybridization, combinatorial and indicative applications. *Artificial Intelligence Review*, 42:965–997.

[118] Oehl, M., Siebert, F. W., Tews, T.-K., Höger, R., and Pfister, H.-R. (2011). Improving human-machine interaction – a non invasive approach to detect emotions in car drivers. *International Conference on Human-Computer Interaction*, 6763:577–585.

[119] Oikawa, R., Takimoto, M., and Kambayashi, Y. (2015). Distributed formation control for swarm robots using mobile agents. *2015 IEEE 10th Jubilee International Symposium on Applied Computational Intelligence and Informatics*, Timisoara, Romania.

[120] Oikawa, R., Takimoto, M., and Kambayashi, Y. (2016). *Composing Swarm Robot Formations Based on Their Distributions Using Mobile Agents*, pages 108–120. Multi-Agent Systems and Agreement Technologies. Springer.

[121] Oncu, S., Ploeg, J., van de Wouw, N., and Nijmeijer, H. (2014). Cooperative adaptive cruise control: Network-aware analysis of string stability. *IEEE Transactions on Intelligent Transportation Systems*, 15:1527–1537.

[122] Oncu, S., van de Wouw, N., Heemels, W. P. M. H., and Nijmeijer, H. (2013). String stability of interconnected vehicles under communication constraints. *51st IEEE Conference on Decision and Control (CDC)*, Maui, HI, USA.

[123] Pan, J. and Tompkins, W. (1985). A real-time qrs detection algorithm. *IEEE Transactions on Biomedical Engineering*, BME-32:209–222.

[124] Parker, L. (2008). *Multiple Mobile Robot Systems - Handbook of Robotics*, pages 921–941. Springer, Heidelberg.

[125] Parker, L., Rus, D., and Sukhatme, G. (2016). Multiple mobile robot systems. *Springer Handbook of Robotics*, page 1335–1384.

[126] Passino, K. (2002). Biomimicry of bacterial foraging for distributed optimization and control. *IEEE Control Systems*, 22:52–67.

[127] Pendleton, S., Andersen, H., Du, X., Shen, X., Meghjani, M., Eng, Y., Rus, D., and Ang, M. (2017). Formation control for a fleet of autonomous ground vehicles: A survey. *Machines*, 5:6.

[128] Peng, Z., Yang, S., Wen, G., Rahmani, A., and Yu, Y. (2016). Adaptive distributed formation control for multiple nonholonomic wheeled mobile robots. *Neurocomputing*, 173:1485–1494.

[129] Pessin, G., Osório, F. S., and Wolf, D. F. (2010). Particle swarm optimization applied to intelligent vehicles squad coordination. *IFAC article Volumes*, 43:401–406.

[130] Picard, R. (1997). *Affective Computing*. MIT Press.

[131] Pickard, A. J. (2013). *Research Methods in Information*. Facet.

[132] Plutchik, R. (1991). *The emotions*. Lanham, Md.: University Press of America.

[133] Poli, R., Kennedy, J., and Blackwell, T. (2007). Particle swarm optimization: an overview. *Swarm Intelligence*, 1:33–57.

[134] Polo, E. M., Mollura, M., Zanet, M., Lenatti, M., Paglialonga, A., and Barbieri, R. (2021). Analysis of the effect of emotion elicitation on the cardiovascular system. *Computing in Cardiology (CinC)*, Brno, Czech Republic:1–4.

[135] Qian, X., de La Fortelle, A., and Moutarde, F. (2016). A hierarchical model predictive control framework for on-road formation control of autonomous vehicles. *2016 IEEE Intelligent Vehicles Symposium (IV)*, Gothenburg, Sweden.

[136] Rani, B. and Kumar, A. (2015). *A Comprehensive Review on Bacteria Foraging Optimization Technique.*, pages 1–25. Multi-Objective Swarm Intelligence. Springer.

[137] Reisenzein, R. (2000). *Wundt's three-dimensional theory of emotion*, pages 219–250. Structuralist Knowledge Representation: Paradigmatic Examples. Rodopi.

[138] Ren, W. (2007). Consensus strategies for cooperative control of vehicle formations. *IET Control Theory and Applications*, 1:505–512.

[139] Ren, W. and Beard, R. W. (2004). Decentralized scheme for spacecraft formation flying via the virtual structure approach. *Journal of Guidance, Control, and Dynamics*, 27:73–82.

[140] Reynolds, C. W. (1987). Flocks, herds and schools: A distributed behavioral model. *ACM SIGGRAPH Computer Graphics*, 21:25–34.

[141] Ringeval, F., Sonderegger, A., Sauer, J., and Lalanne, D. (2013). Introducing the recola multimodal corpus of remote collaborative and affective interactions. *10th IEEE International Conference and Workshops on Automatic Face and Gesture Recognition (FG)*, Shanghai, China:1–8.

[142] Roy, D., Maitra, M., and Bhattacharya, S. (2016). Study of formation control and obstacle avoidance of swarm robots using evolutionary algorithms. *2016 IEEE International Conference on Systems, Man, and Cybernetics (SMC)*, Budapest, Hungary.

[143] Russell, J. (1980). A circumplex model of affect. *Journal of Personality and Social Psychology*, 39:1161–1178.

[144] Salvi, A., Santini, S., and Valente, A. S. (2017). Design, analysis and performance evaluation of a third order distributed protocol for platooning in the presence of time-varying delays and switching topologies. *Transportation Research Part C: Emerging Technologies*, 80:360–383.

[145] Santini, S., Salvi, A., Valente, A. S., Pescape, A., Segata, M., and Lo Cigno, R. (2017). A consensus-based approach for platooning with intervehicular communications and its validation in realistic scenarios. *IEEE Transactions on Vehicular Technology*, 66:1985–1999.

[146] Savkin, A. V., Wang, C., Baranzadeh, A., Xi, Z., and Nguyen, H. T. (2016). Distributed formation building algorithms for groups of wheeled mobile robots. *Robotics and Autonomous Systems*, 75:463–474.

[147] Scottish Government (2010). Designing streets: A policy statement for scotland. [online] https://beta.gov.scot/publications/designing-streets-policy-statement-scotland/pages/6/.

[148] Selvaraj, J., Murugappan, M., Wan, K., and Yaacob, S. (2013). Classification of emotional states from electrocardiogram signals: a non-linear approach based on hurst. *BioMedical Engineering OnLine*, 12:44.

[149] Semsar-Kazerooni, E., Elferink, K., Ploeg, J., and Nijmeijer, H. (2017). Multi-objective platoon maneuvering using artificial potential fields. *IFAC-PapersOnLine*, 50:15006–15011.

[150] Sengupta, S., Basak, S., and Peters, R. (2018). Particle swarm optimization: A survey of historical and recent developments with hybridization perspectives. *Machine Learning and Knowledge Extraction*, 1:157–191.

[151] Shahid, H., Butt, A., Aziz, S., Khan, M., and Hassan Naqvi, S. (2020). Emotion recognition system featuring a fusion of electrocardiogram and photoplethysmogram features. *14th International Conference on Open Source Systems and Technologies (ICOSST)*, Lahore, Pakistan:1–6.

[152] Sharma, K., Castellini, C., van den Broek, E., Albu-Schaeffer, A., and Schwenker, F. (2019). A dataset of continuous affect annotations and physiological signals for emotion analysis. *Nature: Scientific Data - Dataset*.

[153] Shi, Y. and Eberhart, R. (1998). A modified particle swarm optimizer. *1998 IEEE International Conference on Evolutionary Computation article. IEEE World Congress on Computational Intelligence (Cat. No.98TH8360)*, Anchorage, AK, USA.

[154] Shu, L., Xie, J., Li, Z., Li, Z., Liao, D., Xu, X., and Yang, X. (2018). A review of emotion recognition using physiological signals. *MDPI Sensors*, 18:2074.

[155] Sini, J., Marceddu, A. C., and Violante, M. (2020). Automatic emotion recognition for the calibration of autonomous driving functions. *MDPI - Electronics*, 9:518.

[156] Soleymani, M., Lichtenauer, J., Pun, T., and Pantic, M. (2012). A multimodal database for affect recognition and implicit tagging. *IEEE Transactions on Affective Computing*, 3:42–55.

[157] sourceforge.net (2009). The stage robot simulator. [online] https://playerstage.sourceforge.net/doc/Stage-3.2.1/.

[158] Staranowicz, A. and Mariottini, G. L. (2011). A survey and comparison of commercial and open-source robotic simulator software. *proceedings of the 4th International Conference on PErvasive Technologies Related to Assistive Environments - PETRA '11*, Heraklion, Crete, Greece.

[159] Tamura, T., Maeda, Y., Sekine, M., and Yoshida, M. (2014). Wearable photoplethysmographic sensors—past and present. *MDPI - Electronics*, 3:282–302.

[160] Tan, K.-H. and Lewis, M. (1996). Virtual structures for high-precision cooperative mobile robotic control. *proceedings of IEEE/RSJ International Conference on Intelligent Robots and Systems. IROS '96*, Osaka, Japan.

[161] Thakur, A. and Dhull, S. (2021). Speech emotion recognition: A review. *Advances in Communication and Computational Technology*, 668:815–827.

[162] The National Law Review (2021). The dangers of driverless cars. [online] https://www.natlawreview.com/article/dangers-driverless-cars.

[163] Tilahun, S. L. and Ngnotchouye, J. M. T. (2017). Firefly algorithm for discrete optimization problems: A survey. *KSCE Journal of Civil Engineering*, 21:535–545.

[164] U.S. Department of Transportation Volpe Center (2017). How an automated car platoon works. [online] https://www.volpe.dot.gov/news/how-automated-car-platoon-works.

[165] Valbuena Reyes, L. A. and Tanner, H. G. (2015). Flocking, formation control, and path following for a group of mobile robots. *IEEE Transactions on Control Systems Technology*, 23:1268–1282.

[166] Wan, S., Lu, J., and Fan, P. (2018). Semi-centralized control for multi robot formation. *2nd International Conference on Robotics and Automation Engineering (ICRAE)*, Shanghai, China.

[167] Wani, T. M., Gunawan, T. S., Qadri, S. A. A., Kartiwi, M., and Ambikairajah, E. (2021). A comprehensive review of speech emotion recognition systems. *IEEE Access*, 9:47795–47814.

[168] Watson, D. and Tellegen, A. (1985). Toward a consensual structure of mood. *Psychological Bulletin*, 98:219–235.

[169] Wikipedia (2022). Electrocardiography. [online] https://en.wikipedia.org/wiki/Electrocardiography.

[170] Xiao, L. and Gao, F. (2011). Practical string stability of platoon of adaptive cruise control vehicles. *IEEE Transactions on Intelligent Transportation Systems*, 12:1184–1194.

[171] Xu, D., Zhang, X., Zhu, Z., Chen, C., and Yang, P. (2014). Behavior-based formation control of swarm robots. *Mathematical Problems in Engineering*, 2014:1–13.

[172] Yajima, H., Oikawa, R., Takimoto, M., and Kambayashi, Y. (2017). Practical formation control of swarm robots using mobile agents. *2017 Intelligent Systems Conference (IntelliSys)*, London, UK.

[173] Yang, L., Gongyou, T., and Peidong, W. (2012). Formation distance problem in multi-agents control. *2012 Fifth International Conference on Intelligent Computation Technology and Automation*, Zhangjiajie, China.

[174] Yang, X.-S. (2009). Firefly algorithms for multimodal optimization. *Stochastic Algorithms: Foundations and Applications*, 5792:169–178.

[175] Yang, X.-S. (2010). A new metaheuristic bat-inspired algorithm. *Nature Inspired Cooperative Strategies for Optimization (NICSO 2010)*, 284:65–74.

[176] Yang, X.-S. (2013). Swarm intelligence based algorithms: a critical analysis. *Evolutionary Intelligence*, 7:17–28.

[177] Yoo, G., Seo, S., Hong, S., and Kim, H. (2016). Emotion extraction based on multi bio-signal using back-propagation neural network. *Multimedia Tools and Applications*, 77:4925–4937.

[178] Zepf, S., Hernandez, J., Schmitt, A., Minker, W., and Picard, R. W. (2021). Driver emotion recognition for intelligent vehicles: A survey. *ACM Computing Surveys*, 53:1–30.

[179] Zhang, C., Zhang, F.-m., Li, F., and Wu, H.-s. (2014a). Improved artificial fish swarm algorithm. *2014 9th IEEE Conference on Industrial Electronics and Applications*, Tianjian, China.

[180] Zhang, Y., Song, G., Qiao, G., Zhang, J., and Peng, J. (2014b). Consensus and obstacle avoidance for multi-robot systems with fixed and switching topologies. *2014 IEEE International Conference on Robotics and Biomimetics (ROBIO 2014)*, Bali, Indonesia.

[181] Zhao, D., Sun, Y., Wan, S., and Wang, F. (2017). Sfst: A robust framework for heart rate monitoring from photoplethysmography signals during physical activities. *Biomedical Signal Processing and Control*, 33:316–324.

[182] Zheng, Y., Eben Li, S., Wang, J., Cao, D., and Li, K. (2016). Stability and scalability of homogeneous vehicular platoon: Study on the influence of information flow topologies. *IEEE Transactions on Intelligent Transportation Systems*, 17:14–26.

[183] Zhu, Q., Huang, Z., Sun, Z., Liu, D., and Dai, B. (2018). Reinforcement learning based throttle and brake control for autonomous vehicle following. *2017 Chinese Automation Congress (CAC)*, Jinan, China.

[184] Zlot, R., Stentz, A., Dias, M., and Thayer, S. (2002). Multi-robot exploration controlled by a market economy. *IEEE International Conference on Robotics and Automation*, Washington, DC, USA, 3:3016–3023.